Numerical and experimental analysis of the vertical dynamic behaviour of a railway track

Measurement of the vertical displacements and assessment of ProRail norms

A. Ortega García

Master of Science Thesis

Delft University of Technology

Numerical and experimental analysis of the vertical dynamic behaviour of a railway track

Measurement of the vertical displacements and assessment of ProRail norms

Master of Science Thesis

For the degree of Master of Science in Structural Engineering at Delft University of Technology

A. Ortega García

24 April 2014

Faculty of Civil Engineering and Geosciences (CEG) · Delft University of Technology

The work in this thesis was supported by ProRail. Their cooperation is hereby gratefully acknowledged.

Abstract

An assessment of the ProRail norm that standardises the vertical displacement of the track was done. The research explored the relation *Displacement - Velocity - Safety of the track*. Three research questions were drawn: 1) How to measure vertical displacement of the track? 2) Can the limits of the norm be modified? 3) What parameter is a good indicator of the track condition? Numerical and experimental analyses were designed to answer the research questions.

The approach of the research related the vibration frequencies of the track, defined by track quality condition, to the frequency of the load, defined by axle distance and velocity of the train. Safety is ensured if the frequency of the load does not match the characteristic vibration frequency of the track. The vibration frequency of the track is dependent on the vertical displacement.

The numerical analysis was divided in two stages. First, the development of a computational model of a railway track using FEM software. Modal, harmonic and transient analyses were performed to verify the accuracy of the model. The second stage involved a sensitivity analysis to examine the safety of the track for different vertical displacement and vehicle velocity combinations. Large vertical displacement of the track is generated by modelling a void under the sleeper.

The analysis showed that the displacement of the track is directly proportional to the size of the void under the sleeper. In addition, the presence of voids in the structure shift the FRF of the track into the low frequency region. Due to limitation of the computational model, the research could not give a conclusive answer to the second research question.

The experimental analysis consisted on recollection of field data using the ESAH-M system. In the field, vertical displacement of the sleeper was measured; the information was post-processed using numerical software. The performance of the instrument was evaluated using the results from transient analysis. The ESAH-M system demonstrated to be a suitable instrument to measure displacements and accelerations of the track.

Table of Contents

Acknowledgements

I would like to thank my dissertation committee for their time and help during the completion of this thesis. Their supervision and kind consideration is greatly appreciate.

To V.L. Markine and I. Shevtsov I extend a kind gratitude for being my mentors in the railway engineering field. I appreciate the guidance provided while working in and out of the track.

From the R&RE department, I want to thank L.J.M. Houben and A.P.M. Barnhoorn for their tremendous help during my time in the faculty.

I want to acknowledge S. Martínez, J. Alonso, A. Alonso and F. Rivero for inspire and helping me in completing a Master's degree.

A heartfelt thank to P.F. Carrion-Gordon, K.O. Karsen, I.E. Monster, P.S.C. van't Zand and J.B.A. Stals. Their professionalism and good advising in critical moments of my studies allowed me to complete this Master's degree.

I would like to thank my family and friends, specially Mari la Ardilla, Gato Vampiro, Huey, Brendolee, Los Doctores, Los Knights, Delft Monsters, Los Civiles, Las Papayas, Los Becarios and La Banda. Thank you for your support, the motivation, the *occasional* beer and the good times.

To my parents, Concepción and Agustín, for preparing me to face and overcome any challenge in my life, no matter the size of it.

And to Mónica, for being by my side all this time and support me unconditionally. Thank you for believing in me.

Delft, University of Technology — A. Ortega García
24 April 2014

"An expert is a person who has made all the mistakes that can be made in a very narrow field."

— *Niels Bohr*

"Start by doing what is necessary, then what is possible. And suddenly you will be surprised to do the impossible."

— *Francesco d'Assisi*

Chapter 1

Introduction

1-1 Infrastructure management

ProRail Ltd. is the governmental organisation that owns and manages the Dutch national railway infrastructure. Their main responsibilities are to maintain and extend the network, as well as regulate the state and quality of the railway track.

ProRail is interested in knowing the state of the track to guarantee that the quality of the rail fulfils the safety standards.

The topic of the research studies the vertical displacement of the rail generated by a vertical (static or dynamic) load, i.e. the weight of a train, and the effect that such displacement has in the superstructure. The research focuses on assessing the current Dutch standard that limits the maximum allowable vertical displacement of the rail under the action of a moving vehicle.

1-2 ProRail norm for vertical displacement of the track

Specification *OHD00033-1-V005* with title *Instandhoudingspecificaties Spoorinfra - Deel 1 - Baan en Overwegen* is the standard studied and assessed in this research. The norm specifies the condition of all the elements in the track structure in order to be accepted for service.

Subsection *1114.OK.01* of the specification focuses in the quality of the ballast layer. Table 1-1 (extracted from the norm) presents the maximum vertical deflection under SLS and ULS (BW and VW respectively) that the track must not exceed. The measurement of the deflection is relative to a maximum length of 4 meters. The magnitude of such displacement is dependent of the velocity of the moving vehicle, as well.

Maximum verticale beweging (invering) onder belasting*	BW	VW
Bij snelheid $\leq$ 40km/u	20mm	30mm
Bij snelheid $>$ 40km/u	10mm	20mm

*(maximale lengte afwijking is 4 meter)

Table 1-1: Maximum vertical displacement of the track

1-3 Research questions

The principal objective of the research project is to assess the current ProRail specification and contribute with a critical revision of it. This project may provide ProRail a reliable scientific document to revise the norm. Three research questions are answered in order to accomplish the main goal of the project.

1-3-1 Condition of the track: how to measure the actual displacement?

It is important to assure that the condition of the track in the field obeys the ProRail Specification *OHD00033-1-V005* subsection *1114.OK.01*. Diverse methods exist to measure displacement of the rail, directly or indirectly. For the purpose of this research, a number of measuring systems are reviewed, compared and discussed. The goal is to define what is the most suitable method to measure rail displacements in the field.

1-3-2 Evaluation of the norm: shall the limits be modified?

The question analyses the ProRail specification. The evaluation of the norm consists in understanding where do these limits come from, what is the background calculation and the reasoning that defines the existing norm. The goal is to perform a revision of the norm and define if the limits of the regulation shall be modified or they are in acceptance with the quality requirements.

1-3-3 Track condition indicator: shall the norm limit the vertical displacement of the rail?

The goal of the question is to revise the convenience of measuring the displacement of the rail to describe the condition of the track. Is this the most suitable indicator to define the quality of the track? Should another parameter be considered instead?

1-4 Domain and scope

The limitations in time and funding of the research forces the project to scale the data recollection and simulations to specific cases.

The research domain is limited to the railway network in The Netherlands. Although different track designs exist, the research focuses only in the ballasted track (Classical track).

For the interest of the research, the calculations and measurements performed are limited to the vertical direction of the track (negative in the direction of gravity). The longitudinal or lateral response of the track is not included.

Chapter 2

Research approach

Three parameters are considered in the ProRail norm definition (Table 1-1):

- Velocity of the vehicle running over the track.
- Maximum vertical displacement of the rail.
- Safety of the structure.

The first two elements are simple parameters that can be measured and simulated with easiness. The third element, safety of the structure, is an implicit element of the norm. The norm limits the displacement according to the velocity of the train, if the condition of the track does not meet the requirements, risk of structural flaw exists.

Safety of the structure cannot be measured directly; it is not a quantifiable parameter. Safety of the structure is a desired condition of the track. For practical purposes, the research proposes to redefine the norm in the next visual relation:

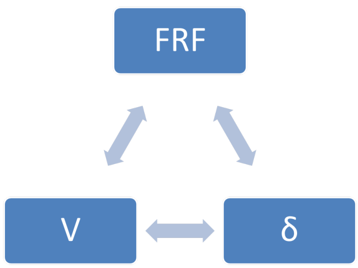

Figure 2-1: Relation between velocity (V), displacement (δ) and Frequency Response Function (FRF) of the track

Velocity and displacement remain the same as the norm. The safety of the structure is redefine in the next concept:

> Safety of the structure is ensured if the frequency of the load (given the combination of velocity and displacement of the rail) does not match the vibration frequency of the track.

If the frequency of the load is close to the characteristic vibration frequencies of the track, large deformations and stresses in the track may occur. Therefore, in this research the definition of *safety* is translated to dynamic forces and displacements.

In the research, the relation between the three parameters is analysed. This approach, along with the methodology described in following paragraphs, are the selected course of action to answer the research questions.

2-1 Methodology

The selected methodology to follow in the research consists of six main stages. Each stage is properly developed and reported in this document.

- Computational model
- Model verification
- Transient analysis
- Field tests
- Sensitivity analysis
- Conclusions

2-1-1 Computational model

The first action is to propose a computational model of the track that behaves and responds as the actual track in the field. Literature review from Chapter 3 is used in this stage to design the model. The model is built using the CAE software ANSYS *Structural Mechanics*.

2-1-2 Model verification

By performing modal and harmonic analysis, it is possible to evaluate the accuracy of the model. If the model does not behave like the real track, the analysis and results generated through simulations are meaningless.

2-1-3 Transient analysis

Once the model has been verified, the subsequent action is to run a transient analysis. The analysis is designed to observe the response of the model under different structural conditions. The simulations will provide meaningful results that must be validated using field data.

2-1-4 Field tests

In Section 3-5, a list of available instruments to measure rail displacement is given. For this task, the ESAH-M equipment is proposed as the measuring instrument to be used in the field. The results obtained from previous analysis are corroborated with field data.

The results generated in this stage are used to answer the first research question. The performance of the ESAH-M instrument for measuring displacements and accelerations in the field determines the eligibility of the system for further tests.

2-1-5 Sensitivity analysis

The validated model from the first two stages has been revised using data from field tests. The model is used to complete a sensitivity analysis and understand the consequences of having large vertical displacements during service life of the track.

After this analysis, the second research question can be answered. The results show the effect of allowing larger displacements in the rail and therefore a critical conclusion can be done to the current ProRail specification.

2-1-6 Conclusions

General overview of the work done during the research can be found in this stage. The answers for the research questions are revisited. Conjectures outlined during earlier stages of the research are validated or debunked.

Chapter 3

Background and literature review

General railway design concepts are reviewed in this chapter in order to introduce the reader to the research topic. The state-of-the-art of specific subjects are included as well according to their relevance in the project.

3-1 Railway track structure

Ballasted track is the most common design of a railway track used nowadays. The principal advantages over other track designs are the relative low construction cost, larger elasticity and drainage [8].

The structure of the track consists of two parts: the *Superstructure* and the *Substructure*. The first one includes the rail, fastening system and sleepers; the second one is composed of granular materials placed by layers according to their mechanical properties. Figure 3-1 [8] illustrates the elements that form the ballasted track.

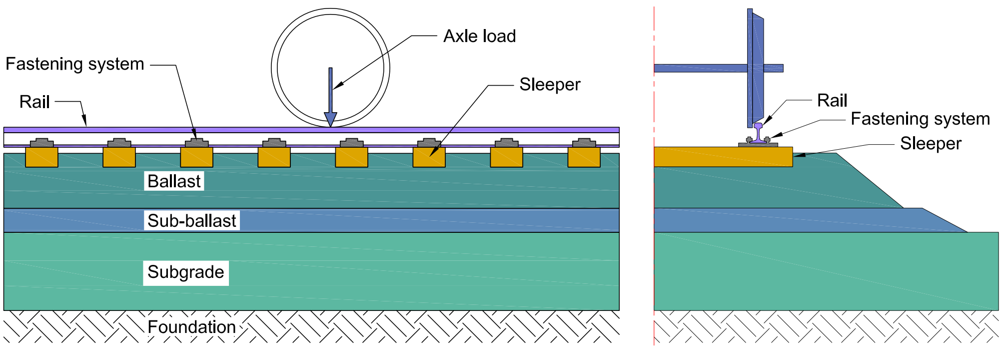

(a) Lateral view (b) Half cross-section

Figure 3-1: Ballasted track

The axle load is transferred from the top to the bottom of the structure. Each element of the track reduces the vertical stresses that the underneath element must resist. Consequently, the geometry of the structure and the mechanical properties of each element are the basis of the structural design of the railway track.

3-1-1 Rail

The rail is the element in contact with the wheel and thus the most important part of the track structure. This element is expected to withstand the larger vertical stresses and deformations.

Different materials and profiles of the rail are commercially available (Figure 3-2(a)). The International Union of Railways (UIC) standards are the governing design guidelines for the rail profiles used in The Netherlands.

3-1-2 Fastening system

The fastening system transfers the forces between the rail and the sleeper. In addition, the system ensures the horizontal alignment of the track (gauge between rails).

The fastening is a complex system that includes a number of elements. Among these elements, the *rail pad* is the component that filters out the high frequency forces coming from the rail into the sleeper. For the interest of the research, this is the most relevant element of the system.

3-1-3 Sleeper

The sleeper is the component of the superstructure that transfers the forces coming from the rail into the ballast bed. The geometry and material of the sleeper define the rail support and how uniformly the stresses are passed to layers beneath. The interaction between the sleeper and the ballast layer is of interest in the research.

Sleepers can be manufactured using different materials: timber, reinforced concrete or steel. Also, sleepers can be fabricated in different geometries: twin-block, monoblock, wide and double-H. In The Netherlands, the monoblock concrete sleeper is the most common presentation of this element. The mass of a single sleeper can vary from 200 to 300kg.

3-1-4 Ballast

The granular layer under the sleepers are the first component of the substructure of the railway track. The ballast consist of coarse material with grading 20/50mm, generally. The internal friction between grains resists the compressive stresses transmitted from the superstructure. It also provides lateral stability to the track and ensures a good drainage.

Differential settlements of the whole track structure are mainly produced by the deterioration of the ballast. A review of the degradation process is included in further sections of this chapter.

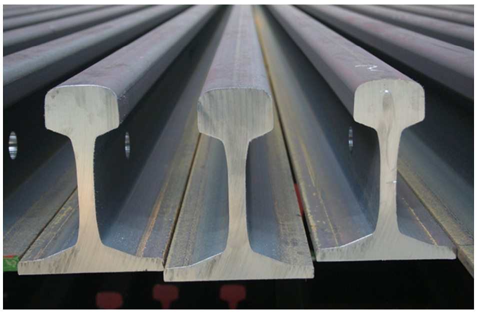

(a) UIC rail profiles

(b) Fastening system

(c) Monoblock concrete sleepers

(d) Ballast

Figure 3-2: Ballasted track elements

3-2 Track dynamics

3-2-1 Model of the track

The mass-spring system is a well-known and largely used mathematical model in the dynamics field. This system is the basis to model the ballasted railway track (Figure 3-3). The structure is represented using discrete elements such as masses for the rail and sleeper, and spring-dashpot combinations for the rail pad and ballast bed.

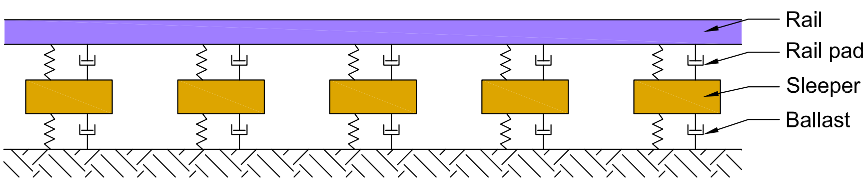

Figure 3-3: Dynamic model for ballasted track

The vehicle moving over the track can also be modelled using a mass-spring system. The interaction of the track with the vehicle is represented using the Hertzian-spring principle.

The scope of the research limits the study to the response of the track only. Therefore, the effects and dynamic behaviour of the vehicle is reduced to concentrated external forces applied on the track. The author refers the reader to [8] for further information about the vehicle-track dynamic interaction.

3-2-2 Vibration modes

The model of the track vibrates in different shapes according to the excitation given. The vibration modes are related to resonant frequencies; these frequencies are characteristic of the system.

In [6], the vibration of the railway track structure is divided into three groups according to the vibration frequency of the mode (Table 3-1). The mid and high frequency regions are revised in the following paragraphs.

Range	Frequency [Hz]
Low	0 - 40
Mid	40 - 400
High	400 - 1500

Table 3-1: Frequency ranges for railway track vibration

Vibration of track

The vibration of the track corresponds to the mid frequency range (40Hz to 400Hz). Two vibration modes are observed in this group.

In the first one, called full-track vibration, all the elements of the track vibrate and the structure bends as a whole (Figure 3-4(a)). The mode is observed when the system vibrates at frequencies between 40Hz and 140Hz.

The second vibration mode of the classification is the anti-resonant vibration (Figure 3-4(b)). In this mode, the sleepers in the structure show a large vertical movement while the rail appears to be almost static. The anti-resonant vibration is found in the frequency range of 80Hz to 300Hz.

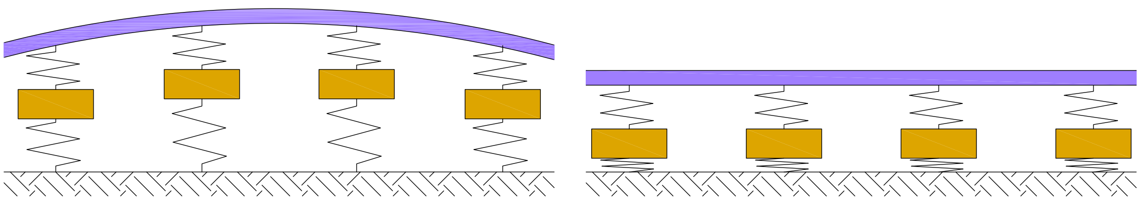

(a) Full-track vibration (b) Anti-resonant vibration

Figure 3-4: Full track vibration modes for ballasted track

Vibration of rail

In the high frequency range (400Hz to 1500Hz), only the rail vibrates. Two characteristic vibration modes are known for the rail in this frequency range.

The first high frequency vibration mode is the rail vibration. In this mode, the rail vibrates relative to the supports; the other elements of the track show little to no movement. An example of this mode is shown in Figure 3-5(a); it can be found in the frequency range between 250Hz and 1500Hz.

The second mode of the rail vibration is known as pin-pin vibration. When this vibration mode occurs, the rail bends like a beam supported by its ends (Figure 3-5(b)); the length of the beam is determined by the distance between sleepers. First order pin-pin vibration generally occurs in the frequency range of 500Hz to 1200Hz.

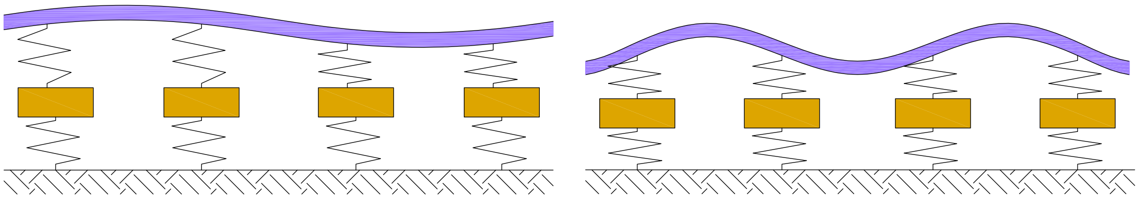

(a) Rail vibration (b) Pin-pin vibration

Figure 3-5: Rail vibration modes for ballasted track

3-3 Discontinuity in the track

The vertical geometry of the track alignment is not constant along the length of the structure. Multiple discontinuities can be found in the track. These interruptions in the rail exist due to geometrical or material requirements.

Examples of track discontinuities are a common crossing in the geometrical design of a turnout (Figure 3-6(a)), an expansion joint to allow enlargement of the rail due to temperature changes (Figure 3-6(b)), an Insulated Rail Joint (IRJ) to connect two rail pieces (Figure 3-6(c)), and a welded joint to build a Continuous Welded Rail (CWR) (Figure 3-6(d)).

3-3-1 Dynamic force amplification

Several studies and mathematical models have been developed to describe the effect of a discontinuity in the vertical geometry of the track alignment of the track. When the wheel of a vehicle crosses through one of these irregularities, the vertical load is amplified. This impact load is called dynamic force amplification F_{dyn}).

The dynamic force amplification has been studied by several researchers. For instance, Jenkins [11] presents a model generated by the passing of a load over an IRJ. Figure 3-7 shows the time dependent behaviour of F_{dyn} as the wheel of the train crosses over the joint.

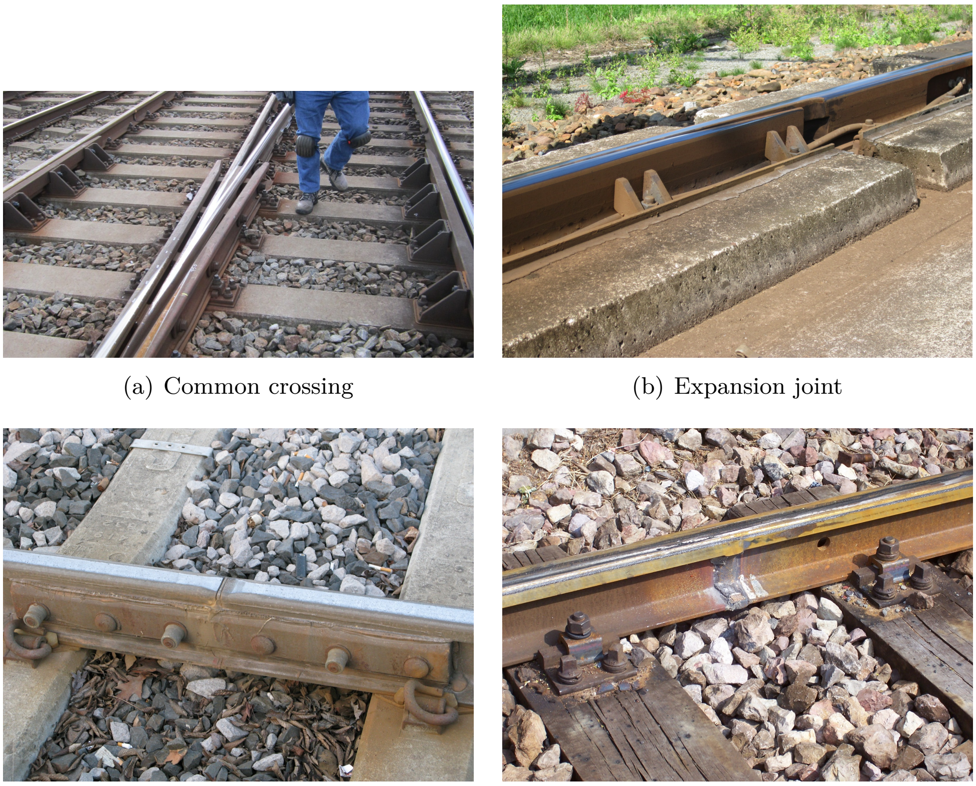

(a) Common crossing

(b) Expansion joint

(c) Insulated Rail Joint

(d) Welded joint

Figure 3-6: Examples of track discontinuities

Eq. (3-1) and Eq. (3-2) are given to calculate the peak values P_1 and P_2 of the moving load over an IRJ.

$$P_1 = P_0 + 2\alpha\, v \sqrt{\frac{k_H\, m_{T1}}{1 + \dfrac{m_{T1}}{m_u}}} \tag{3-1}$$

$$P_2 = P_0 + 2\alpha\, v \sqrt{\frac{m_u}{m_u + m_{T2}}} \left[1 - \frac{c_T\, \pi}{\sqrt{k_{T2}\,(m_u + m_{T2})}} \right] \sqrt{k_{T2}\, m_u} \tag{3-2}$$

The model is dependent of the axle load, train velocity, mass and stiffness of the system, and the geometry of the irregularity (dip angle of the joint).

Although the model is specific for IRJ, the general idea of the dynamic force amplification (and the peak values P_1 and P_2) is valid for other short wave irregularities in the track.

3-3-2 Welds

In CWR tracks, the rail is formed by different pieces of rail connected to each other through welds. Welding of the rail can be done using flash-butt weld or thermite weld (exothermic

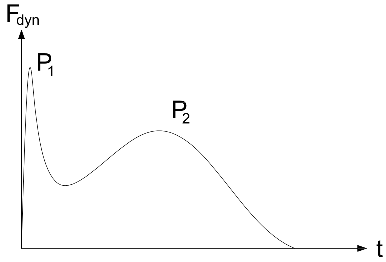

Figure 3-7: Dynamic force amplification in the case of **IRJ!**

welding). After the rail pieces are connected, the head of the rail is ground to eliminate residual material from the rolling surface (Figure 3-8). Nowadays, thermite welding is the most common method to construct a CWR.

The insertion of weld to the rail produces several local effects in the geometry and the material of the element [8]. One of the most significant is the modification of the rail profile (rolling surface). The renewal process (welding and grinding) leaves the profile of the rail with short-wave irregularities [23]. As discussed in previous sections, such irregularities amplify the dynamic forces in the wheel-rail interface.

(a) Welding

(b) Grinding

Figure 3-8: Thermite welding for construction of a CWR

In [23], a model is developed to determine the amplification of the force when a vehicle crosses a weld imperfection (Eq. (3-3)). The model is dependent of the equivalent track mass, the vehicle velocity and the geometry of the weld imperfection.

$$F_{dyn,max} = \gamma M_{track} V^2 \frac{1}{d} \left| \frac{dz}{dx} \right|_{max} \tag{3-3}$$

The model is calibrated using field measurements and FEM modelling. The final approximate equation is a linear relation between the force, the velocity and the gradient of the weld (Eq. (3-4)).

$$F_{dyn,max} = 0.22V \tan(\alpha) \tag{3-4}$$

3-4 Foundation modulus

Foundation modulus (C), sometimes referred to as track modulus, relates the local compressive stresses on the track (σ) with the local vertical subsidence (w) [8] (Eq. (3-5)).

$$\sigma = C\,w \tag{3-5}$$

When discrete and continuous support models are considered, the foundation modulus is transformed into spring constant k_d (Eq. (3-6)).

$$k_d = C\,A_{rs} \tag{3-6}$$

In continuous models, the spring constant k_d relates the vertical displacement of the rail w_{max} to the vertical load on the structure Q using Eq. (3-7).

$$k_d = \frac{a}{4}\sqrt[3]{\frac{Q^4}{EIw_{max}^4}} \tag{3-7}$$

Considering the previous mathematical description, foundation modulus can be defined as the capacity of the structure to withstand the stresses and deformations generated by the service loads. Hence, the quality of a railway track is closely related to this modulus [17] [14].

Loss of track geometry (vertical displacement of the rail) is mainly caused by the degradation of the ballast layer under the passage of traffic [5]. This infers that the element in the track structure that governs the vertical displacement of the rail is the ballast.

Since the ballast layer is the main responsible of the loss in track geometry, the research revises the interaction of this layer with the surrounding elements (sleepers) and the mechanical behaviour under service loads.

3-5 Measurement of rail displacement

The real magnitude of the vertical displacement w at the top of the rail is difficult to determine. It can be measured from outside or inside the track by means of different methods and devices.

- Imetrum Video gauge [27]
- High speed deflectograph [8] [10]

- Non-contact laser and camera system [17]
- Sleeper displacements (ESAH-M)

These methods offer results of local vertical displacement of the rail but require the presence of working teams in the track. This situation translates into financial costs and time consumption for ProRail. More important, it is desired to reduce the risk that working inside or next to the track always entails for the workers and the passing vehicle.

In order to avoid incursion of personal and equipment to the track, a device capable of performing vertical displacement measurements from a moving vehicle is preferred. However, such device is not commercially available yet [8].

3-6 Sleeper-Ballast interface

3-6-1 Ballast degradation

Track geometry maintenance is one of the principal activities performed after the construction of a track. Maintenance of track geometry includes tamping, stone blowing, ballast cleaning and ballast profiling. All of these activities involve the renewal or modification of the ballast layer after the degradation of the granular material.

Degradation of the material takes place when high frequency loads occur on the track. These loading conditions are common when a discontinuity of the rolling surface exist, e.g. a wheel passing over a crossing nose in a turnout. These conditions produce a high impact load that is transmitted from the top of the rail into the ballast layer. Crushing of the granular material is expected in the vicinity of the discontinuity.

In [13], computational simulations are designed and tested in order to emulate the plastic deformation of the ballast under cyclic loading. The results show that before crushing, the ballast has a permanent settlement. This deformation occurs in the first few cycles of loading where the granular material compacts and consolidates.

If impact load occurs after the grains have reached a natural accommodation, plastic deformation of the ballast is expected. Crushing is concentrated underneath the sleepers and mostly takes place during the early load cycles [13].

A number of authors had studied the phenomenon of ballast crushing and present theoretical and empirical models to describe it [25]. However, this phenomenon remains an extremely complex mechanism and, according to [3], it is unlikely that any theoretical or empirical equation will be able to accurately predict the settlement pattern with time.

3-6-2 Under-Sleeper Pad

The use of rail pads in the boundary between rail and sleeper is meant to reduce the high frequency forces transmitted from one element to the other. In a similar way, a boundary element can be used to control the forces that the sleeper transmits to the ballast bed. This element is known as Under-Sleeper Pad (USP) and is a topic that has being subject of a number of studies [1].

For instance, a number of advantages and disadvantages are mentioned by the UIC in [26] about the use of this element in the structure of the track:

Advantages of USP

- Reduction of long pitch corrugation in tight radius curves
- Substitution for Under-Ballast Mat (UBM) to reduce noise and vibrations
- Less maintenance, stretching of tamping intervention periods
- Reduction of ballast depth
- Reduction of rail and sleeper stresses, better load distribution
- Improvement of track geometry
- Improvement of track stability
- Reduction in whole life costs, especially with heavier loading of tracks

Disadvantages of USP

- USP lead to higher deflection, velocity and acceleration of the rail and sleeper.
- The additional elasticity of USP is a disadvantage in particular frequency ranges. The significant range is between 200 and 300 Hz, depending on the combined stiffness of the rail pad and the USP. These frequencies are typical of out of round wheels on high speed lines.

Experimental stiffness and damping properties of USP are reported in [12] and summarised in Table 3-2.

USP model	k_u [kN/m]	c_u [kNs/m]
Soft	34.3×10^3	2.5
Medium	72.7×10^3	6.9
Hard	108.9×10^3	10.5

Table 3-2: Stiffness and damping values for USP

Chapter 4

Computational model

4-1 Modelling software

ANSYS *Structural Mechanics* is a CAE software used for the linear or non-linear, static or dynamic analysis of structures (Figure 4-1).

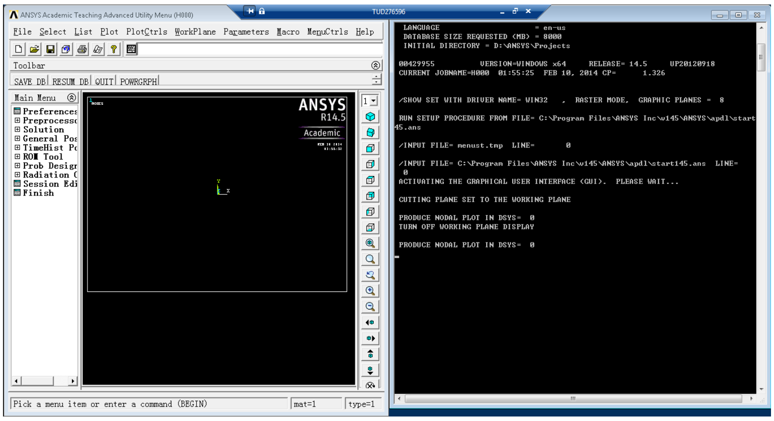

Figure 4-1: GUI of ANSYS

The software performs the FEM analysis using the input data provided by the user. The development of the model and the definition of the simulation parameters are done using ANSYS Parametric Design Language (APDL). A description of this programming language and the command files used during the research are included in Appendix B.

The program includes a post-process tool capable to generate time dependent results for displacements, accelerations and forces of any element in the model. The results are saved as a CSV file that can be loaded in MATLAB for further revision and analysis. The MATLAB functions developed for these analyses are included in Appendix G.

4-2 Definition of the model

A section of a ballasted track (Figure 4-2) is modelled using the mass-spring system described in Section 3-2-1. The reduced number of elements in the model allow to simplify the numerical work perform by the computational tool.

The model described in this chapter is later used for the different analyses included in the research.

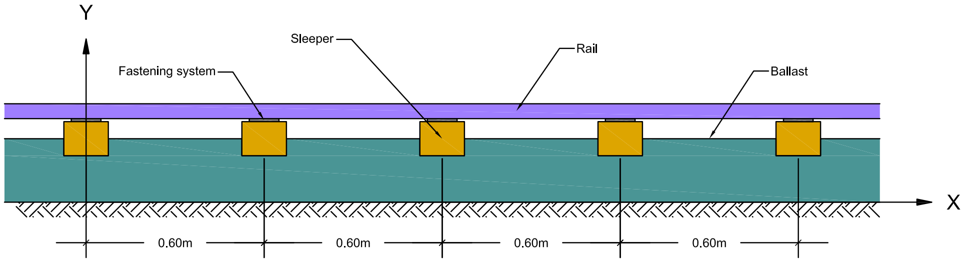

Figure 4-2: Ballasted railway track

4-2-1 Units

Declaration of units for the model is not required in ANSYS. However, consistency must remain for all the data input during the pre-process. The units used for the simulations are presented in Table 4-1.

Dimension	Unit	Symbol
Length	metre	[m]
Force	kilonewton	[kN]
Mass	tonne	[ton]

Table 4-1: Model units

4-2-2 Geometry

The model consists of 2.40 metres of a classic ballasted railway track represented with diverse structural elements in the X-Y plane (2-D model). The structure consist of a discrete system of springs, dampers and masses (Figure 4-3).

Taking into account symmetry of the structure in the longitudinal direction (X-axis), only half of the track is modelled. Each element has material and geometrical properties according to their function in the superstructure. Simple elements used in the definition of the model are:

- 2-D beam

- Lumped mass
- Spring-damper system
- Spring-damper system with gap

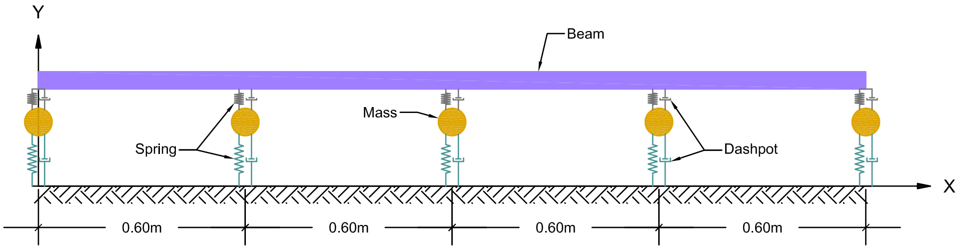

Figure 4-3: Model elements

4-2-3 Elements

Description of the elements that conform the model is given in the next subsections. Further explanation and characteristics of the elements are included in Appendix A. The numerical information is recollected from [8] and [6].

Rail

The rail is modelled as a beam using the structural element BEAM188. The geometrical and mechanical properties of the standard UIC-60 rail profile define the behaviour of the element during simulations.

ANSYS can import and mesh an IGES file that contains the profile to be attached to the beam definition. The cross-section for UIC-60 is drawn in AutoCAD and exported as an IGES extension file (Figure 4-4).

ANSYS uses the file to calculate the geometrical properties of the profile. However, the mechanical properties of the material must be determined by the user. Density and elasticity properties (ρ, E and ν) for the rail are inserted separately.

The rail is meshed in small element pieces of longitude dx (Figure 4-5). The distance between nodes defines the detail of the model and thus the quality of the results. Nevertheless, a large number of nodes produces large output file size. The time to complete a simulation increases if the element is meshed into shorter pieces as well.

Rail pad

Rail pads are modelled using the combination of a spring and a damper (COMBIN14). The combination system has stiffness k_p and damping c_p.

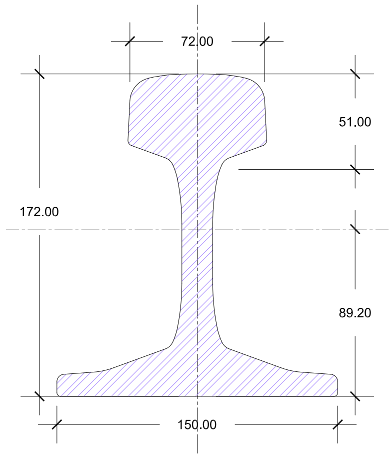

Figure 4-4: UIC-60 cross section

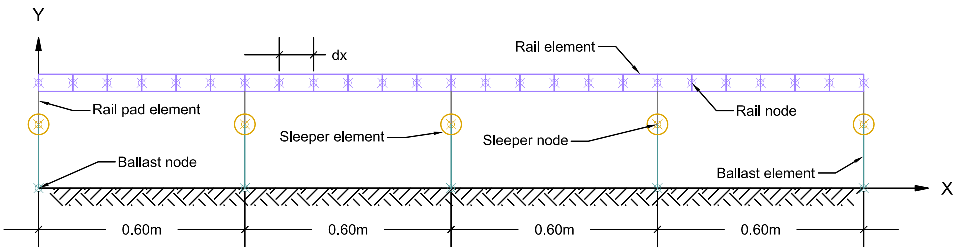

Figure 4-5: Rail element definition

Sleeper

The geometry of the sleeper is neglected for the sake of simplicity. The sleeper is modelled as a lumped mass with no rotational properties (MASS21). Only the mass of the element is taken into account during the simulation which translates into inertial forces. Half of the track is considered through the research, therefore, half of the sleeper mass is input in the model.

Ballast

The granular material under the sleeper is modelled as a spring-damper system. Two conditions are considered during the modelling that will be used in later simulations.

Good ballast The sleeper is well supported on the ballast; any vertical force coming from the sleeper is directly transferred to the granular material. Ballast is represented using a spring-damper element (COMBIN14) with stiffness and damping properties k_b and c_b respectively.

Degraded ballast Contact between the sleeper and the ballast is not constant in arbitrary elements. The sleeper has no perfect support on the ballast and a gap has developed between the two elements (Figure 4-6).

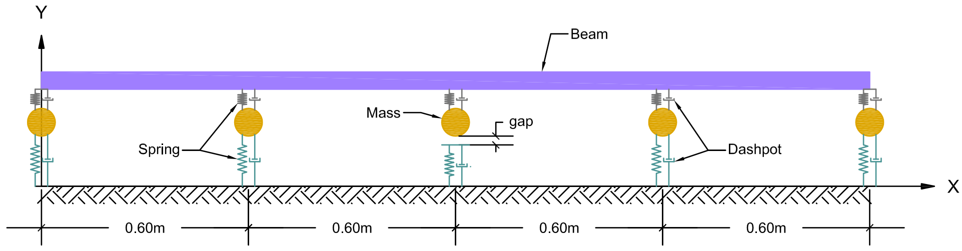

Figure 4-6: Modelling of degraded ballast

The spring-damper system reacts to external forces when the gap is closed. The ballast under the sleeper has a non-linear behaviour as presented in Figure 4-7. When the gap is open, the system is not active and the sleeper has no support from the ballast. The unsupported sleeper condition is described using the non-linear spring-damper element COMBIN40.

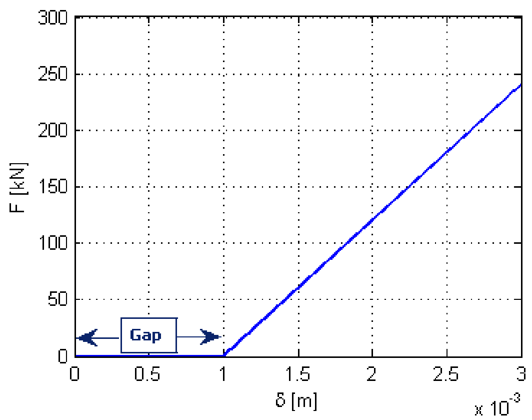

Figure 4-7: Bi-linear behaviour of ballast

Numerical information used to construct the model in the software is summarised in Table 4-2. The selected data is based on information from [8], [6] and [28].

4-2-4 Boundary conditions

The research is focused in the behaviour of the track elements along the vertical direction (Y-axis). Since the model is generated in a 2-D plane, it is not expected to have mechanical response of the elements in the third axis (Z-axis).

The nodes located at $x = 0.00m$ and $x = 2.40m$ are free to rotate in the X-Y plane and displace in the Y-axis. Under this condition, wave reflection at the ends of the rail are avoided.

Element	Parameter	Value	Unit
Rail	ρ	7.85	ton/m^3
	E	210×10^6	kN/m^2
	ν	0.30	–
Rail pad	k_p	100×10^3	kN/m
	c_p	15	kNs/m
Sleeper	m	0.150	ton
Ballast	k_b	27×10^3	kN/m
	c_b	12.30	kNs/m

Table 4-2: Numerical data for model parameters

4-2-5 Constrains

The ballast elements are fixed at their lower nodes ($y = 0.00m$), no displacement or rotation is allowed at these points.

Figure 4-8 shows the lateral view of the model. Elements, boundary conditions and constrains are present as previously defined.

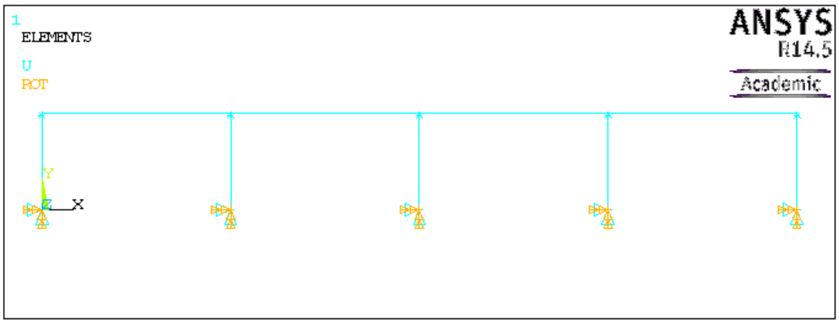

Figure 4-8: Model in ANSYS GUI

Chapter 5

Modal and harmonic analysis

Two analyses are run in order to study the structural behaviour of the model described in Chapter 4. The objective is to verify that the response of the model is similar to that of a ballasted railway track.

The analyses presented in this chapter remain a linear analysis. Both analyses are completed using two conditions of the model:

- Supported sleeper
- Unsupported sleeper

In the first condition, all the sleepers are fully supported; connectivity between elements is complete and constant over time. In the second condition, the sleeper located at $x = 1.20m$ is unsupported. The ballast element is removed from the model and the sleeper is *hanging* from the rail. The goal is to observe the changes in the structure response when the supporting condition changes.

5-1 Modal analysis

Firstly, a modal analysis is run to observe the vibration modes of the structure. The vibration frequencies of these modes are compared to the ones reported in [6], previously studied in Section 3-2-2.

ANSYS contains a feature to calculate the vertical vibration modes of a structure. The user defines the maximum number of modes to extract or the range of vibration frequencies to be considered in the analysis. According to [6], vibration of the rail can reach high frequencies up to 1500Hz. Hence, the analysis is limited to maximum vibration frequency of 1500Hz or 1000 vibration modes.

5-1-1 Track vibration modes

In Figure 5-1, the vibration corresponding to the whole track are presented; vibration modes for both ballast conditions are included. The corresponding frequency for each vibration mode is reported in Table 5-1.

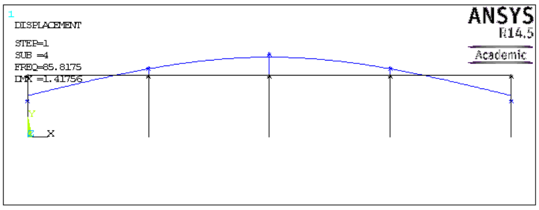

(a) Supported, Full track mode

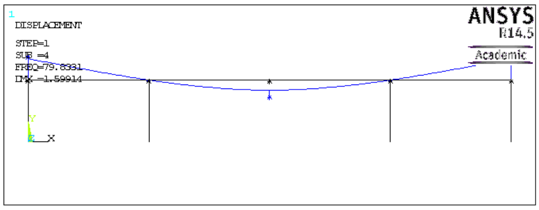

(b) Unsupported, full track mode

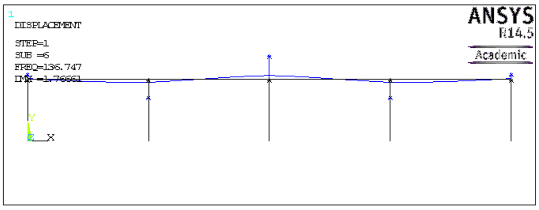

(c) Supported, Anti-resonant mode

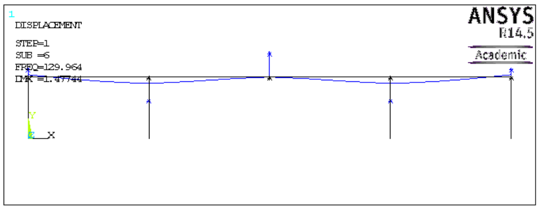

(d) Unsupported, Anti-resonant mode

Figure 5-1: Track vibration modes

Track mode	Frequency [Hz]	
	Supported	Unsupported
Full track	61.47	49.22
Anti-resonant	136.75	129.96

Table 5-1: Vibration frequencies for track vibration modes

The track vibration (full track and anti-resonant) occurs in the mid frequency region (40Hz to 140Hz) as expected. The shape of the vibrations remains the same despite of having one unsupported sleeper. However, the frequency corresponding to each vibration mode reduces.

5-1-2 Rail vibration modes

The rail vibration modes (rail and pin-pin vibration) are shown in Figure 5-2; the related frequencies for each mode are listed in Table 5-2. Both support conditions are reported.

The modes for rail vibrations are located in the high frequency range; this is in concordance with the literature reviewed in Chapter 3 [6].

The shape of the rail vibrations does not change for different support conditions; neither does the vibration frequencies for those modes. Amplitudes of high frequency vibrations are

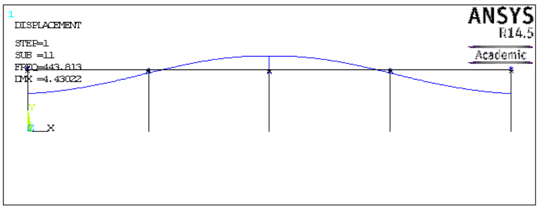

(a) Supported, rail vibration mode

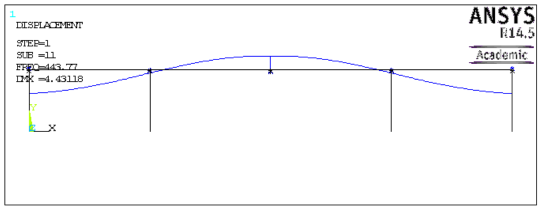

(b) Unsupported, rail vibration mode

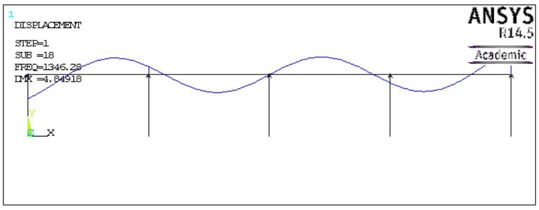

(c) Supported, pin-pin vibration mode

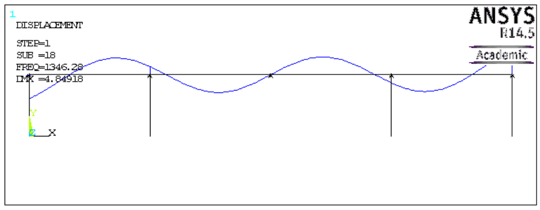

(d) Unsupported, pin-pin vibration mode

Figure 5-2: Rail vibration modes

considerably lower than the ones observed in the track vibration section.

Rail mode	Frequency [Hz]	
	Supported	Unsupported
Rail	443.81	443.77
Pin-pin	1346.28	1346.28

Table 5-2: Vibration frequencies for rail vibration modes

5-2 Harmonic analysis

In the harmonic analysis, the model response to an impact load is studied. By applying an impact load, the structure will vibrate in all its vibration frequencies. From this simulation, it is possible to analyse the response of each element in the frequency domain.

The impact load is constructed using load steps (Figure 5-4). The first step (LS_1) defines the beginning of the analysis at $t = 0.00s$. Second step (LS_2) occurs after a small amount of time δt. In this step, the impact load F_0 is applied to the structure. The third step (LS_3) allows the structure to vibrate freely for a period of time t.

The APDL files for each load step are included in Appendix C. The parameters to be used in the analysis are presented in Table 5-3.

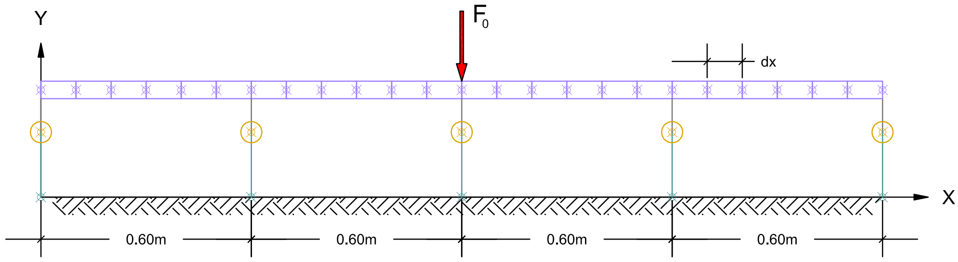

Figure 5-3: Impulse load applied to model

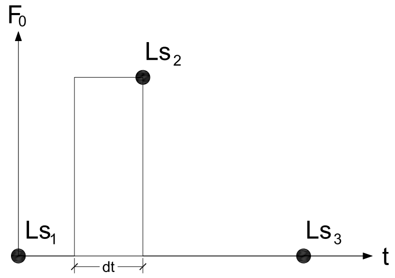

Figure 5-4: Load step for harmonic analysis

The frequency range of the results is obtained from the time step previously defined.

$$F_s = \frac{1}{2\,\delta t} \tag{5-1}$$

$$F_s = \frac{1}{2(0.00025)} \tag{5-2}$$

$$F_s = 2000Hz \tag{5-3}$$

5-2-1 Rail response

In this subsection, the response of the rail from the harmonic analysis will be revised. The analysis is done at the central rail node, the node where the impulse load was applied. The response for supported and unsupported conditions are included for each plot.

In Figure 5-5, histories of rail displacement are reported; the response is presented in time and frequency domain .

Parameter	Value	Unit
δx	0.01	m
F_0	100	kN
δt	0.00025	s
t	2.00	s

Table 5-3: Parameters for harmonic analysis

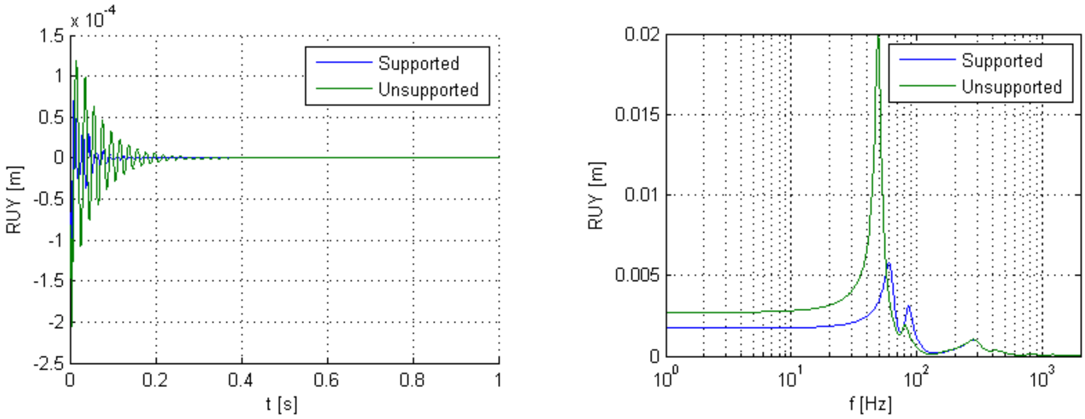

(a) Time domain (b) Frequency domain

Figure 5-5: Rail displacement

Firstly, attention is paid to the response for good ballast condition. In Figure 5-5(b), two peaks are easily identified in the Frequency Response Function (FRF): one at f=60Hz, the other at f=85Hz. According to the modal analysis performed in previous sections, these peaks correspond to the full-track vibration mode (Table 5-1).

The same peaks are recognised in the FRF plot for degraded ballast condition. However, the peaks are located at lower frequencies than in the previous ballast condition: f=50Hz and f=80Hz. In addition, the presence of an unsupported sleeper increases the amplitude of the response considerably.

In the high frequency range (f≤400Hz), the response of the rail is practically equal for both conditions of the ballast. This behaviour was previously observed in the modal analysis for rail vibrations (Table 5-2 and Figure 5-2). The rail displacement for high frequency vibration has a lower amplitude than for low and mid frequency ranges.

5-2-2 Sleeper response

The sleeper analysed is located at $x = 1.20m$, below the point where the impulse load was applied. Both support conditions are considered in the figures presented.

Figure 5-6 shows the time and frequency domain response for displacement of the sleeper. The peaks previously identified in the displacement of the rail are observed in Figure 5-6(b) as well. The peaks correspond to the full-track vibration mode studied during the modal analysis.

For frequencies larger than 400Hz (high frequency range), the displacement of the sleeper is virtually non-existent. Therefore, the response of the sleeper is limited to the low and mid frequency ranges.

In Figure 5-7, the histories and FRF for sleeper acceleration are plotted. The acceleration of the sleeper is limited to the mid frequency vibration range (40Hz to 400Hz).

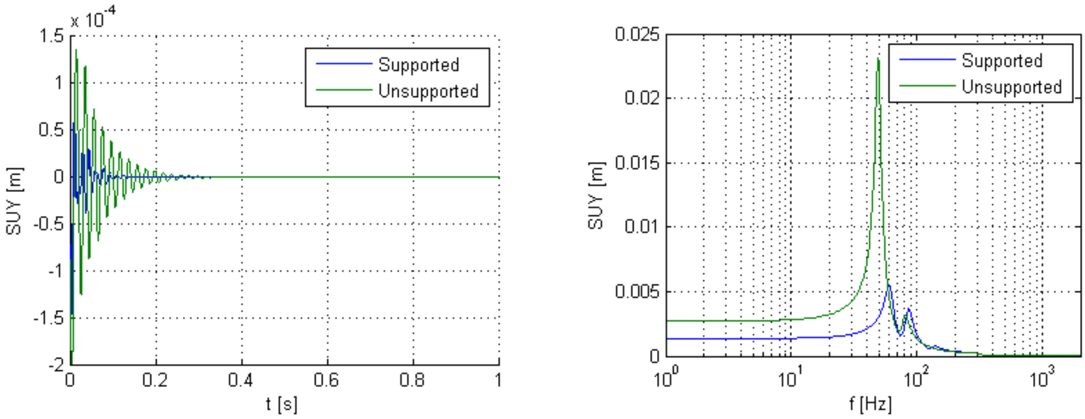

(a) Time domain (b) Frequency domain

Figure 5-6: Sleeper displacement

Four peaks are observed in Figure 5-7(b) at frequencies 60Hz, 87Hz, 147Hz and 282Hz for the supported sleeper condition plot. The plot for the unsupported condition shows a shift into lower frequencies for the first three peaks (50Hz, 82Hz and 128Hz); the fourth peak remains in the same frequency.

The amplitude of the peaks is reduce except for the peak with the lowest frequency. The first frequency shows a considerable increment when the sleeper is not supported by the ballast.

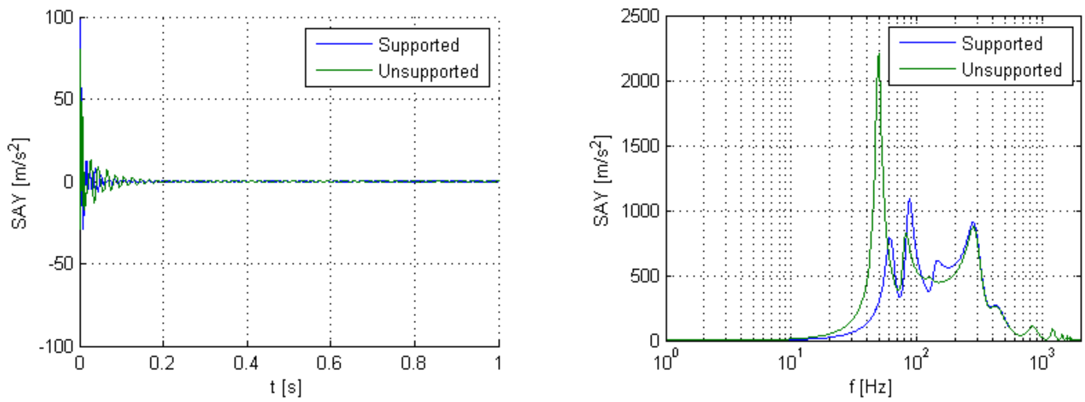

(a) Time domain (b) Frequency domain

Figure 5-7: Sleeper acceleration

Chapter 6

Transient analysis

In this chapter, a vehicle running over the model is simulated. Different track conditions are considered and the effects of these conditions are studied. The analysis is performed using the model described in Chapter 4.

6-1 Cases for analysis

Four cases are studied in the transient analysis. Each case is a combination of the presence of two variables:

- Weld in rail
- Void under sleeper

Table 6-1 shows the four cases according to the combination of *weld* and *void* in the track. A description of each case is given in further subsections.

Case	Weld	Void
1	No	No
2	Yes	No
3	Yes	Yes
4	No	Yes

Table 6-1: Track condition

6-1-1 Case 1: Perfect track

In the first case, the track does not have irregularities in the rolling surface of the rail (no weld) and the condition of the substructure is normal (Figure D-1). The results obtained from this analysis are used as control data.

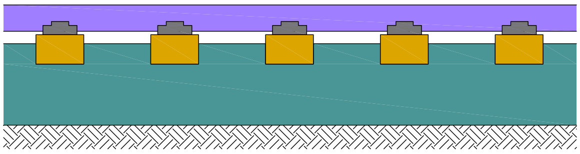

Figure 6-1: Perfect track

6-1-2 Case 2: Renewed rail

In the second case to analyse, a weld exists in the rail (Figure 6-2). The weld is located at midspan between sleepers 2 and 3; the rest of the track elements are in good condition. This case emulates the condition of the track when a CWR has been recently installed in the track.

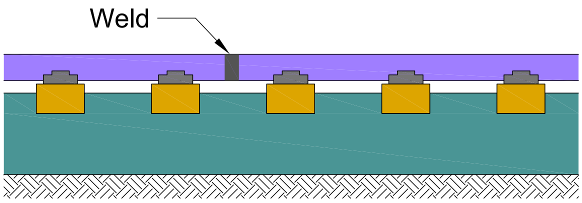

Figure 6-2: Renewed rail

6-1-3 Case 3: Degraded ballast

The granular material in the vicinity of the weld has degraded and a void is present under sleeper 3 (Figure 6-3). This condition is observed in the field when the granular material has deteriorated and major maintenance is required.

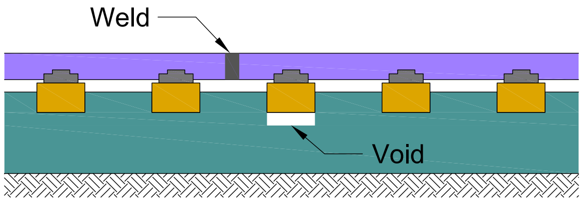

Figure 6-3: Degraded ballast

6-1-4 Case 4: Re-renewed rail

The rail is renewed and the weld is retired from the structure (Figure 6-4). However, the substructure is no longer in good condition. Deterioration of the granular material under the sleepers has occurred.

This situation can be considered as an unrealistic condition. Degradation of the ballast will not happen unless an amplification of the vertical forces occur. The amplification of forces can only happen when a discontinuity in the rolling surface exists (Section 3-3). If no weld is present in the rail, the ballast will not degrade.

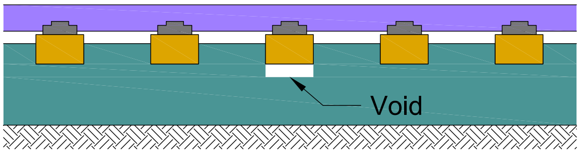

Figure 6-4: Re-renewed rail

6-2 Load on track

The vehicle used in the simulation is a single car locomotive with two bogies and two axles per bogie (Figure 6-5). The model considers only half of the track by symmetry, therefore, half of the vehicle is taken into account.

In order to simplify the computational work, the vehicle is reduced to four point loads (Figure 6-6). Each load represents the vertical force transmitted by the wheels to the rail. The wheel forces are applied to the structure using load steps, similar approach as the one followed in Section 5-2 during the harmonic analysis.

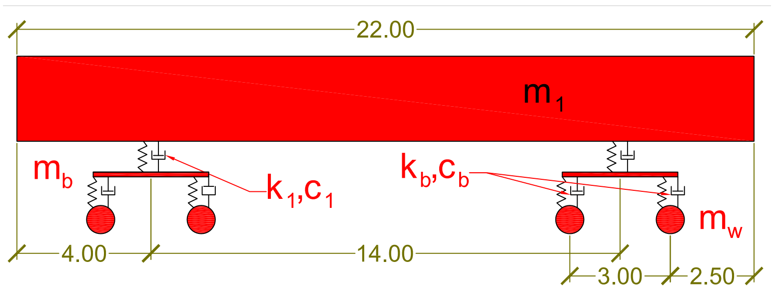

Figure 6-5: Vehicle for transient analysis

For each load step, a position and magnitude of the wheel force is determined. The histories of wheel-rail forces are obtained using DARTS software. The explanation of how the histories are calculated is given in Appendix D for further revision.

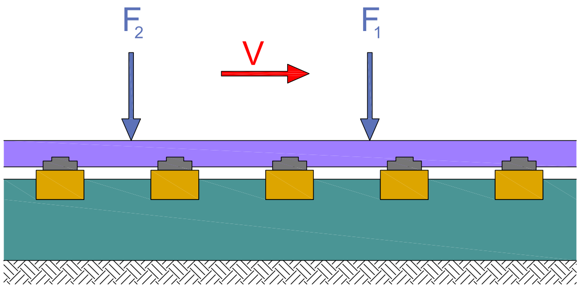

Figure 6-6: Moving point loads

6-3 Modelling of track condition

6-3-1 Weld in rail

The weld is simulated in the analysis by modifying the magnitude of the wheel-rail force applied to the structure. In Appendix D, the process to obtain the histories of forces is explained.

In Figure 6-7, the time-dependent wheel-rail force is plotted for the situation when no weld is present (cases 1 and 4) and when a weld is present in the rail (cases 2 and 3).

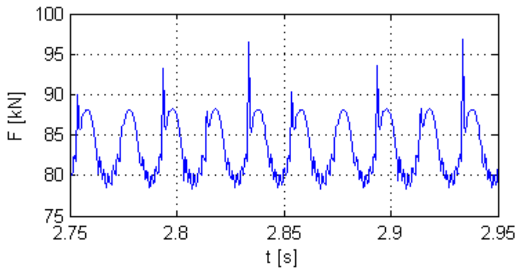

(a) No weld in rail

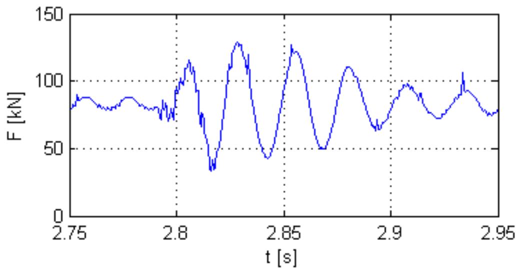

(b) Weld in rail

Figure 6-7: Wheel-rail force according to presence of a weld

6-3-2 Unsupported sleeper

The void under the sleeper for cases 3 and 4 is modelled by inserting a gap between the ballast (COMBIN40) and the sleeper (MASS21) elements (Section 4-2-3). The size of the void is fixed to $0.001m$; variation of the magnitude of the void is not considered in this analysis.

Chapter 7

Transient analysis results

The results from the computational simulations described in Chapter 6 are described in this chapter. The results correspond to the four cases described in Section 6-1. Case 1 is used as control data to compare the results from the other three cases.

7-1 Case 2

In Figure 7-1 the results corresponding to case 2 are presented. The plots show rail displacement, sleeper displacement and sleeper acceleration in time and frequency domain.

For both rail and sleeper displacement (Figure 7-1(b) and Figure 7-1(d)), it is observed that the presence of a weld in the rail produces amplification in the FRF. Such amplification is located between 30Hz to 60Hz. In this range, the characteristic vibration mode of the structure is the full-track vibration.

The sleeper acceleration FRF is plotted in Figure 7-1(f). Similar to the displacement, the acceleration of the sleeper presents an amplification in the frequency range between 30Hz and 60Hz.

From this results, it is observed that the presence of a weld in the rail affects the full-track vibration of the structure. The sleeper has larger accelerations which translates into larger forces transmitted to the ballast.

7-2 Case 3

Results for the analysis of case 3 are plotted in Figure 7-2. In this case, a weld and a void under the sleeper are present in the structure.

In Figure 7-2(b), the FRF of rail displacement shows an amplification in the range from 30Hz to 60Hz. This response corresponds to the presence of the weld as observed in case 2. The effect of the void under the sleeper can be recognised in the figure as well. Amplification is noted for low frequency range between 1Hz and 20Hz. The displacement of the sleeper has a similar behaviour as the rail displacement.

The sleeper acceleration shows amplification in three frequency ranges: 30Hz to 60Hz, 120Hz to 180Hz and a peak around 80Hz. The lowest range corresponds to the effect of the weld; the other range and the peak are consequence of having a void under the sleeper.

7-3 Case 4

Results from this case are shown in Figure 7-3; the plots exhibit the effect of having a void only. Amplification in the rail and sleeper displacement are observed in the frequency range 1Hz to 20Hz. On the other hand, sleeper acceleration amplification can be found in higher frequency ranges: 75Hz to 85Hz and 120Hz to 180Hz.

The existence of a void between the sleeper and the ballast produces forces with frequencies in the mid and high ranges. Moreover, a peak is generated ($f \approx 80Hz$) with a large amplitude.

7-4 Summary of transient analysis results

Case	Rail displacement	Sleeper displacement	Sleeper acceleration
Weld	30Hz-60Hz	30Hz-60Hz	30Hz-60Hz
Void	1Hz-20Hz	1Hz-20Hz	75Hz-85Hz 120Hz-180Hz

Table 7-1: Threshold for FRF amplification according to study case and track element

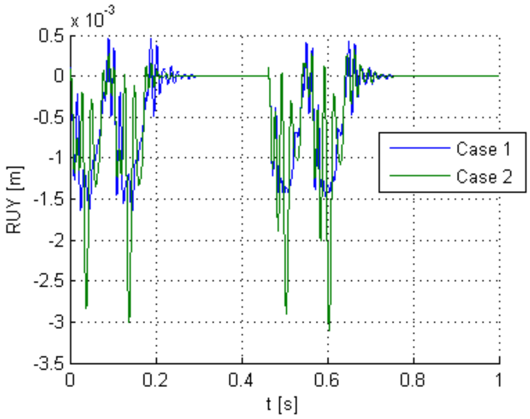

(a) Rail displacement, time domain

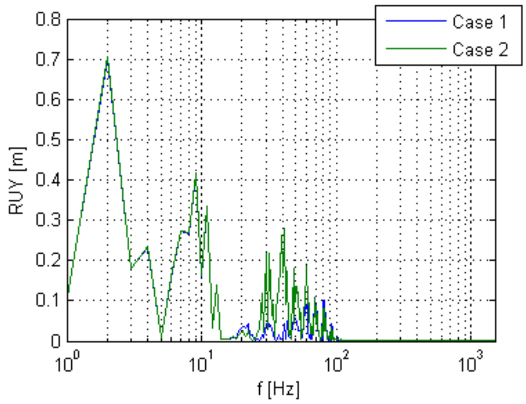

(b) Rail displacement, frequency domain

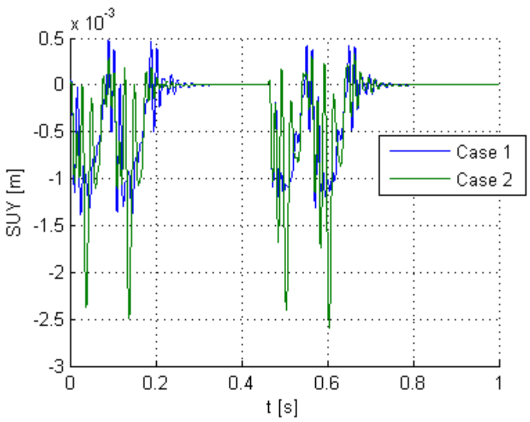

(c) Sleeper displacement, time domain

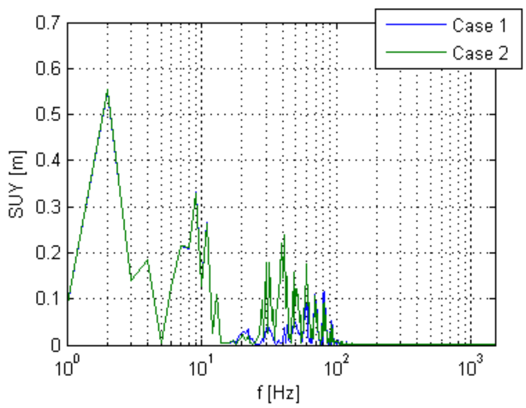

(d) Sleeper displacement, frequency domain

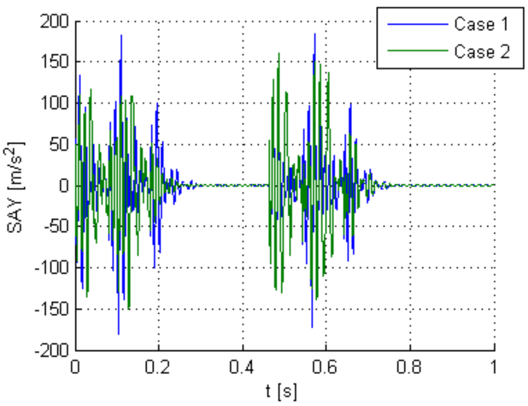

(e) Sleeper acceleration, time domain

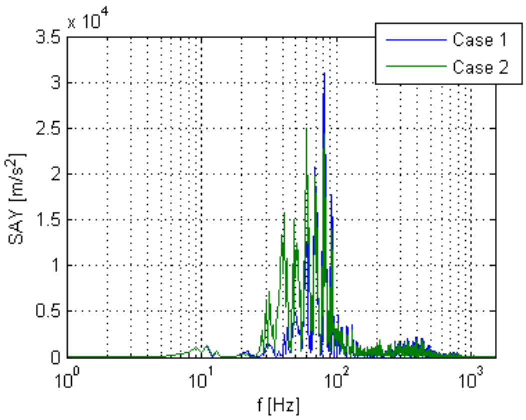

(f) Sleeper acceleration, frequency domain

Figure 7-1: Transient analysis results, case 2

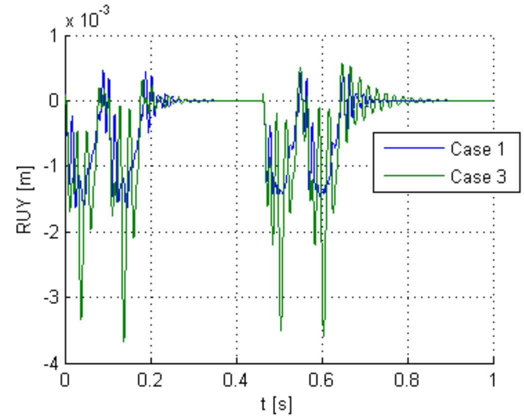

(a) Rail displacement, time domain

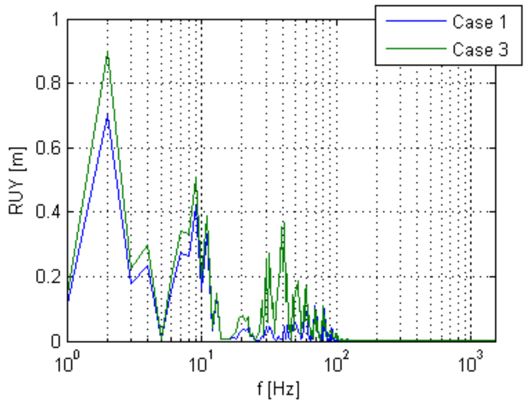

(b) Rail displacement, frequency domain

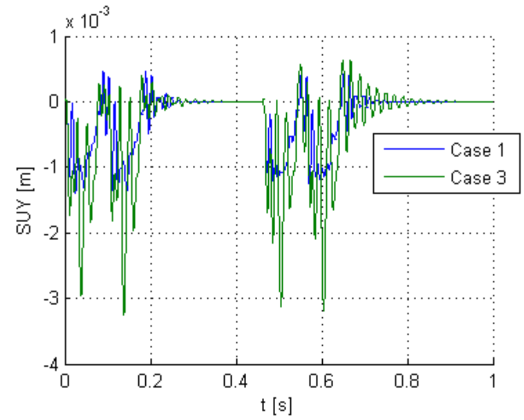

(c) Sleeper displacement, time domain

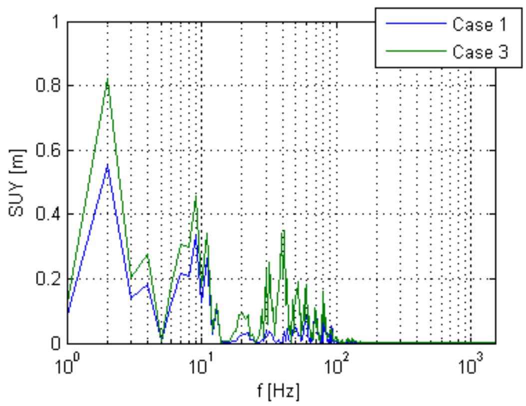

(d) Sleeper displacement, frequency domain

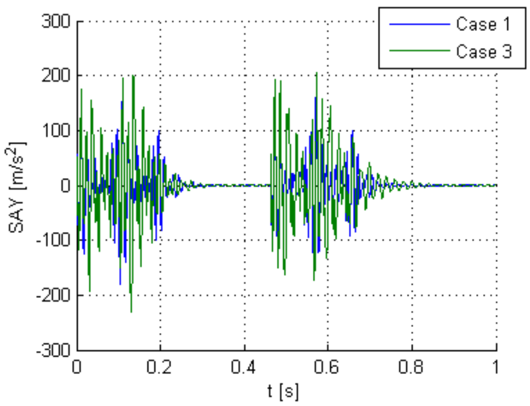

(e) Sleeper acceleration, time domain

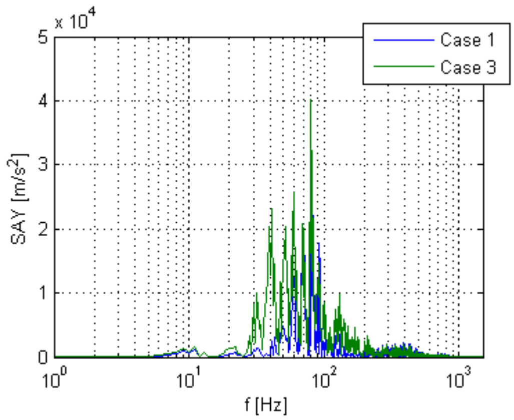

(f) Sleeper acceleration, frequency domain

Figure 7-2: Transient analysis results, case 3

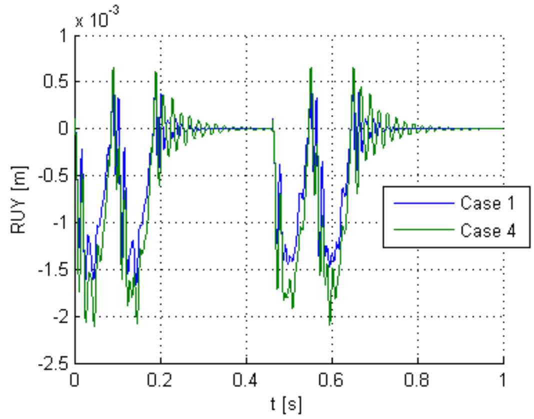

(a) Rail displacement, time domain

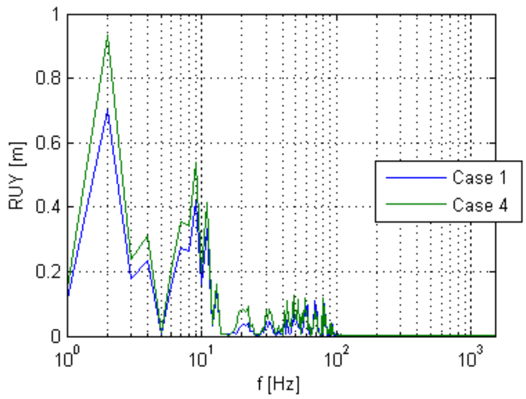

(b) Rail displacement, frequency domain

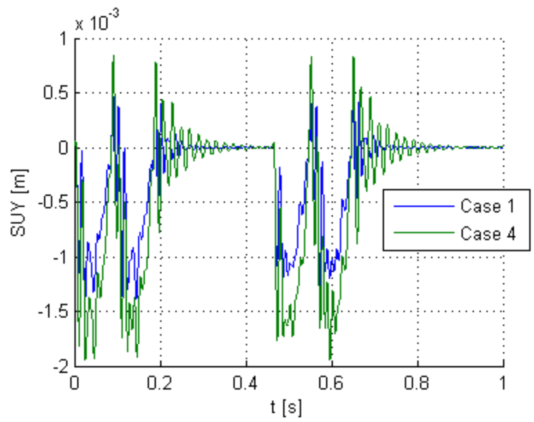

(c) Sleeper displacement, time domain

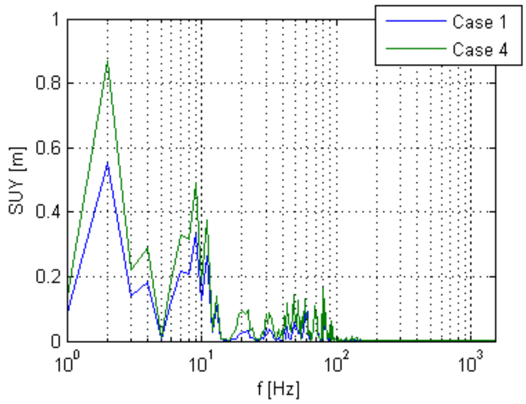

(d) Sleeper displacement, frequency domain

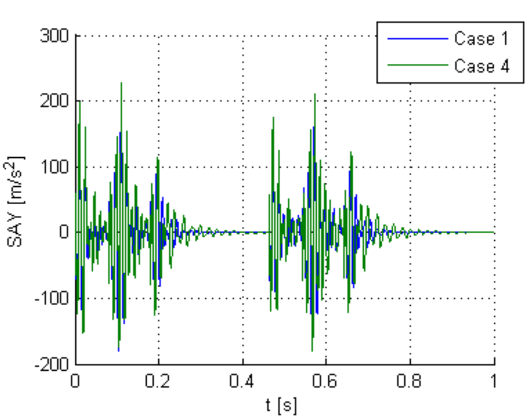

(e) Sleeper acceleration, time domain

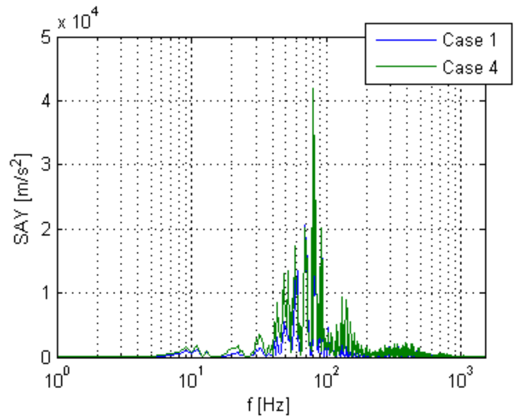

(f) Sleeper acceleration, frequency domain

Figure 7-3: Transient analysis results, case 4

Chapter 8

Field test

The results obtained from the transient analysis in Chapter 7 are compared against data measured in field. The tests performed in the field consist of measuring the vertical displacement of the rail with a specialised electronic instrument.

The measurements are taken at different stages of the rail service life, i.e., the condition of the track (substructure and superstructure) varies through the set of measurements. These conditions are almost similar to the study cases revised in Section 6-1.

8-1 Instrumentation

The Elektronische SystemAnalyse Herzstijckbereich - Mobil (ESAH-M) device is a measurement tool for analysis of wheel-rail contact in the common crossing area [15]. The instrument consists of a number of elements; a description of each of them is listed below. Figure 8-1 shows the system and it's components installed over a common-cross.

- Two inductive sensors to determine the number of axles and the vehicle velocity.
- Magnetic triaxial accelerometer to measure accelerations of the rail in three dimensions.
- Sleeper displacement sensor.
- Main battery powered unit to process the signals and save/transmit the recollected field data.

Installation of the device can be done in less than one minute [20] allowing the field work to be performed during service hours while reducing the invasion to the track to a minimum (Figure 8-2).

(a) Inductive sensors

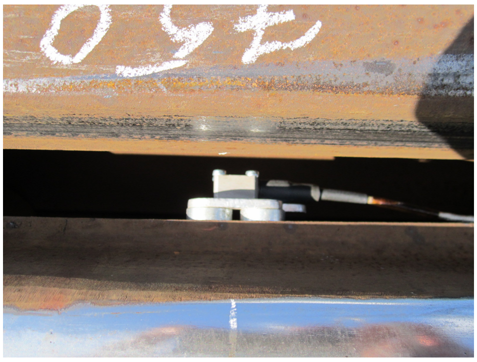

(b) Accelerometer

(c) Main unit

(d) Sleeper displacement sensor

Figure 8-1: ESAH-M device components

(a)

(b)

Figure 8-2: Installation of ESAH-M device

8-2 Location

The chosen location for the field tests is a straight track between train station **Lage Zwaluwe** and bridge **Moerdijk** (*Moerdijkbrug*), in the Rotterdam-Breda railway line (*Staatslijn I*).

The railway line is a heavily used track that connects the provinces of Zuid-Holland and Noord-Brabant. The traffic in the railway consists of passenger and freight trains. The train frequency can reach up to eight trains per hour.

(a) Map showing test location

(b) General view of Moerdijkbrug site

Figure 8-3: Moerdijk site for testing

8-3 Measurements

A large number of measurements have been done in the field. The measurements were taken in different sections of the track trying to emulate the study cases described in Section 6-1. However, not all the track conditions were present in the field when the measurements were completed. Following visual identification of the track, available field data can be organised as shown in Table 8-1.

(a) Instruments on straight track (b) Weld in rail

Figure 8-4: Variation of track condition during field tests

Test	File	Train	V [km/h]	V [m/s]
C101	W0001–2013-08-13–15-36-25	Intercity	141.40	39.28
C102	W0001–2013-08-13–15-40-48	Intercity	137.00	38.06
C103	W0001–2013-08-13–15-48-47	Intercity	135.10	37.53
C104	W0001–2013-08-13–15-52-09	Locomotive	99.90	27.75
C301	W0001–2013-08-13–14-16-27	Freight	98.20	27.28
C302	W0001–2013-08-13–14-18-34	Intercity	130.80	36.33
C303	W0001–2013-08-13–14-24-15	Freight	98.70	27.42
C304	W0001–2013-08-13–14-33-02	Intercity	139.30	38.69
C305	W0001–2013-08-13–14-41-19	Freight	111.10	30.86
C306	W0001–2013-08-13–14-48-16	Sprinter	140.10	38.92
C307	W0001–2013-08-13–15-04-07	Sprinter	128.10	35.58
C308	W0001–2013-08-13–15-06-50	Sprinter	145.60	40.44
C309	W0001–2013-08-13–15-10-20	Intercity	129.50	35.97
C310	W0001–2013-08-13–15-19-33	Other	90.90	25.25
C401	W0001–2013-08-13–11-34-04	Intercity	140.40	39
C402	W0001–2013-08-13–11-41-14	Intercity	134.60	37.39
C403	W0001–2013-08-13–11-46-33	Freight	72.70	20.19
C404	W0001–2013-08-13–11-49-44	Sprinter	102.80	28.56
C405	W0001–2013-08-13–12-04-14	Intercity	143.10	39.75
C406	W0001–2013-08-13–12-08-35	Other	141.30	39.25
C407	W0001–2013-08-13–12-11-10	Other	130.20	36.17
C408	W0001–2013-08-13–12-16-51	Freight	83.70	23.25
C409	W0001–2013-08-13–12-19-04	Intercity	49.80	13.83
C410	W0001–2013-08-13–12-22-23	Freight	89.50	24.86
C411	W0001–2013-08-13–12-33-38	Intercity	144.50	40.14
C412	W0001–2013-08-13–12-42-06	Intercity	122.30	33.97
C413	W0001–2013-08-13–12-49-15	Sprinter	95.20	26.44
C414	W0001–2013-08-13–12-53-02	Freight	87.50	24.31
C415	W0001–2013-08-13–13-02-55	Intercity	142.30	39.53
C416	W0001–2013-08-13–13-06-44	Sprinter	142.50	39.58
C417	W0001–2013-08-13–13-11-23	Intercity	111.80	31.06
C418	W0001–2013-08-13–13-32-52	Other	147.80	41.06
C419	W0001–2013-08-13–13-40-36	Intercity	137.50	38.19
C420	W0001–2013-08-13–13-49-38	Sprinter	115.80	32.17
C421	W0001–2013-08-13–13-51-10	Locomotive	117.90	32.75
C422	W0001–2013-08-13–14-04-12	Intercity	144.70	40.19
C423	W0001–2013-08-13–14-07-52	Other	133.40	37.06
C424	W0001–2013-08-13–14-09-56	Other	135.10	37.53

Table 8-1: Field measurements by vehicle and velocity

Chapter 9

Field test results

The results from the field tests completed with ESAH-M device are presented. The post-processing of the raw data obtained from the instrument is thoroughly explained in Appendix F.

The results included in this chapter are subject to a number of considerations. Firstly, the axle load, number of axles and velocity of the vehicle for each test are variable. The comparison of results between tests is done for tests with similar conditions.

Secondly, the units of the results are given in Volts [V]. This is a feature of the ESAH-M software that could not be changed before running the tests. At the moment of developing this thesis, the scaling to convert such units into Length units was not available. Therefore, the analysis done in this chapter does not focus in magnitude of the results, only in the shape of the histories and the FRF.

9-1 Good condition vs degraded ballast, Intercity 1

Two tests are compared in the time and frequency domain. The details of the tests are given in Table 9-1

Case C101 corresponds to a track in good condition; the velocity of the vehicle is $v \approx 40m/s$. Case C411 corresponds to a similar vehicle running over a track with degraded ballast under the sleeper.

Test	File	Train	V [km/h]	V [m/s]
C101	W0001–2013-08-13–15-36-25	Intercity	141.40	39.28
C411	W0001–2013-08-13–12-33-38	Intercity	144.50	40.14

Table 9-1: Data for tests C101 and C411

In Figure 9-2, the sleeper displacement of both cases is plotted in the frequency domain. It is that the response of the sleeper is larger in the case of having an unsupported element. The amplification of the displacement is observed in the low frequency range. Similar behaviour was obtained in Section 7-3 for the study case with the unsupported sleeper.

The acceleration of the sleeper is shown in Figure 9-4, the data is presented in the frequency domain as well. In the figure, no considerable difference is appreciated between the two tests. Only a peak at $f \approx 60Hz$ can be recognised. This point might belong to the 75Hz-85Hz region defined in the transient analysis results for study case 4 (Section 7-3).

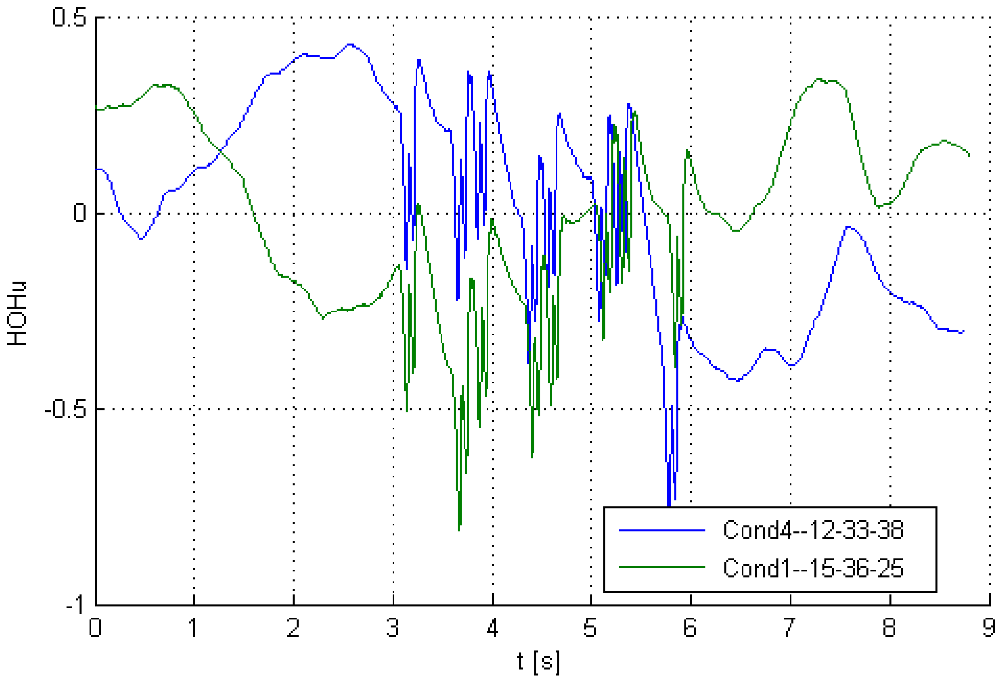

Figure 9-1: Test C101 vs Test C411, sleeper displacement, time domain

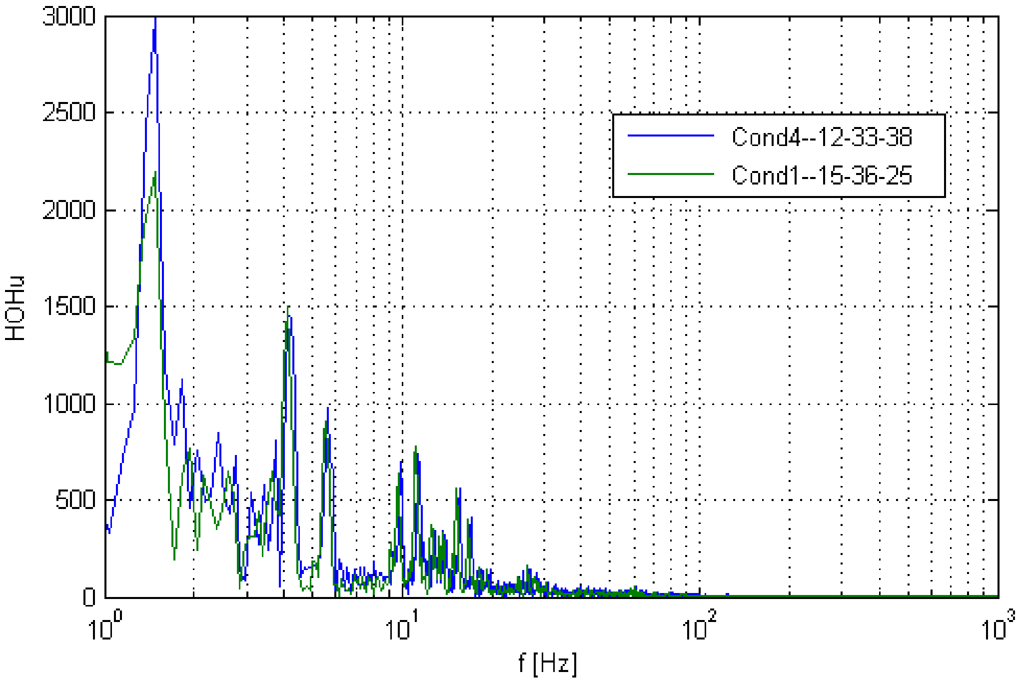

Figure 9-2: Test C101 vs Test C411, sleeper displacement, frequency domain

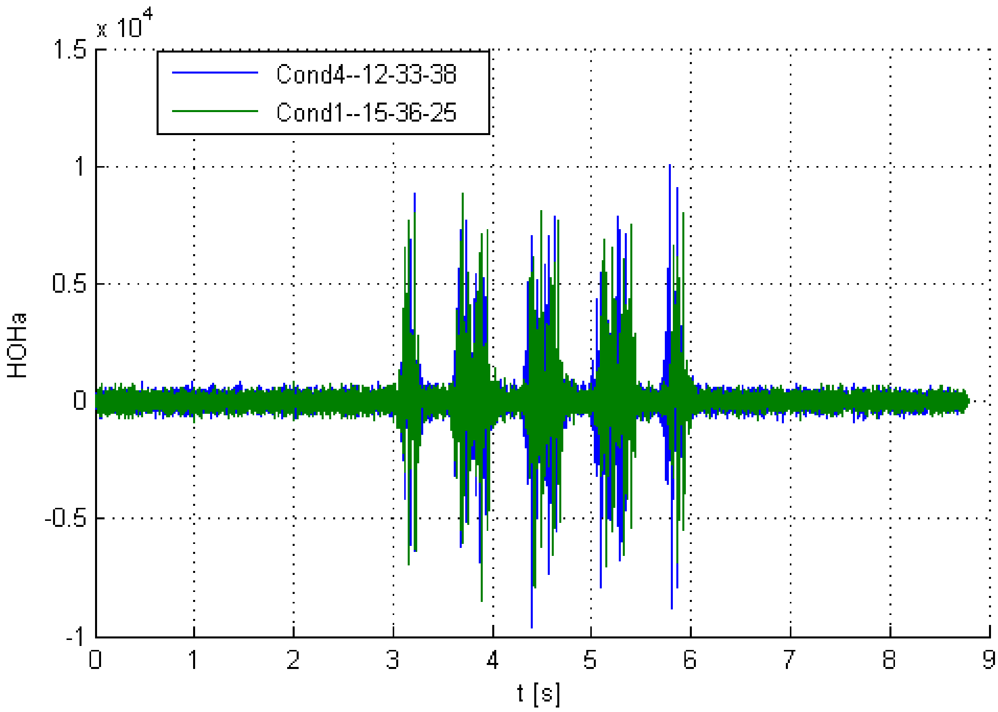

Figure 9-3: Test C101 vs Test C411, sleeper acceleration, time domain

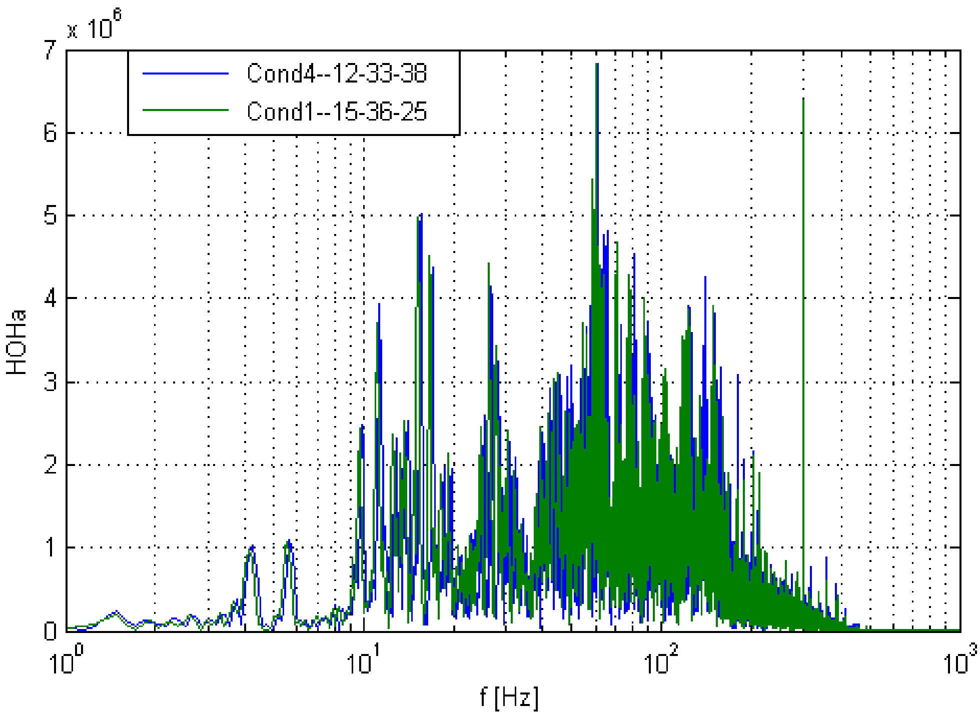

Figure 9-4: Test C101 vs Test C411, sleeper acceleration, frequency domain

9-2 Good condition vs degraded ballast, Intercity 2

C102 and C402 are similar tests as the ones discussed in the last section. However, the number of axles for these tests is larger. The description of the cases is given in Table 9-2.

Test	File	Train	V [km/h]	V [m/s]
C102	W0001–2013-08-13–15-40-48	Intercity	137.00	38.06
C402	W0001–2013-08-13–11-41-14	Intercity	134.60	37.39

Table 9-2: Data for tests C102 and C402

Figure 9-6 shows the FRF for sleeper displacement of the two cases. Resembling the condition of an unsupported sleeper, the lower frequencies amplitude shows an increment for test C402. Above this range, the response of the sleeper is practically the same.

In Figure 9-8, a significant increase of the sleeper acceleration response is clearly noted in the frequency range between 80Hz and 150Hz. This behaviour is clearly a consequence of having degraded granular material under the sleeper (Figure 7-3(f), Section 7-3).

These observations indicate that the number of consecutive axles over the track plays an important role in the sleeper response for mid frequency ranges.

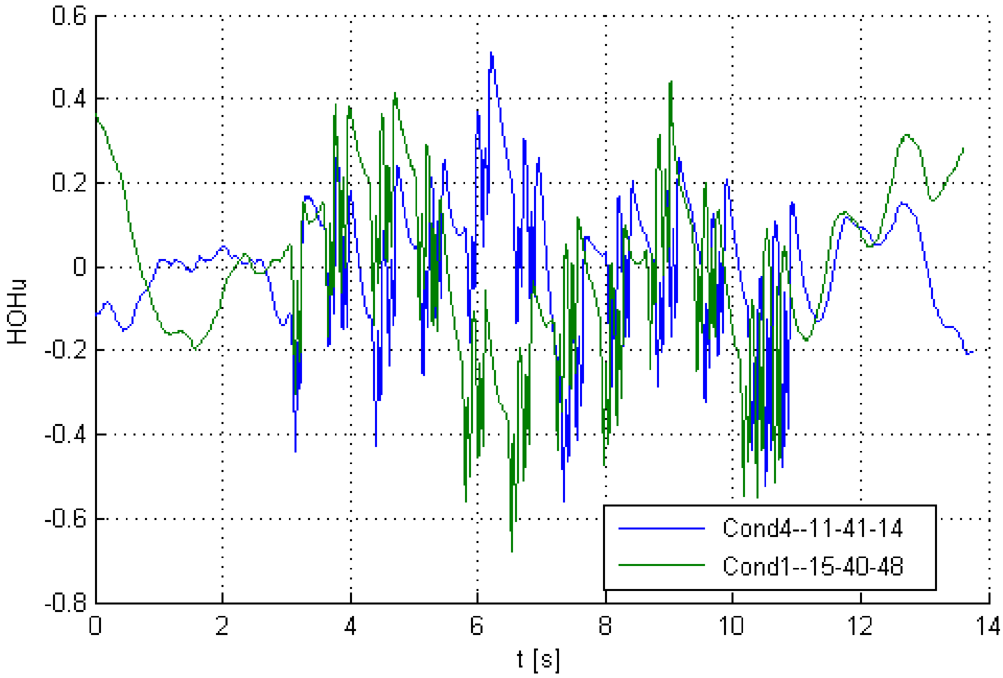

Figure 9-5: Test C102 vs Test C402, sleeper displacement, time domain

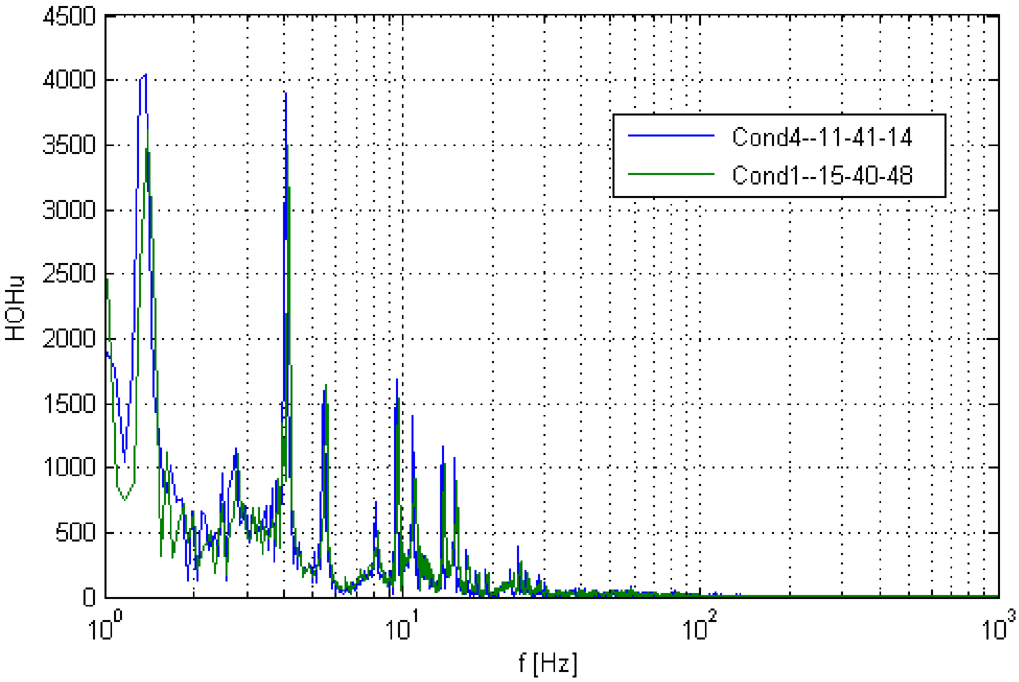

Figure 9-6: Test C102 vs Test C402, sleeper displacement, frequency domain

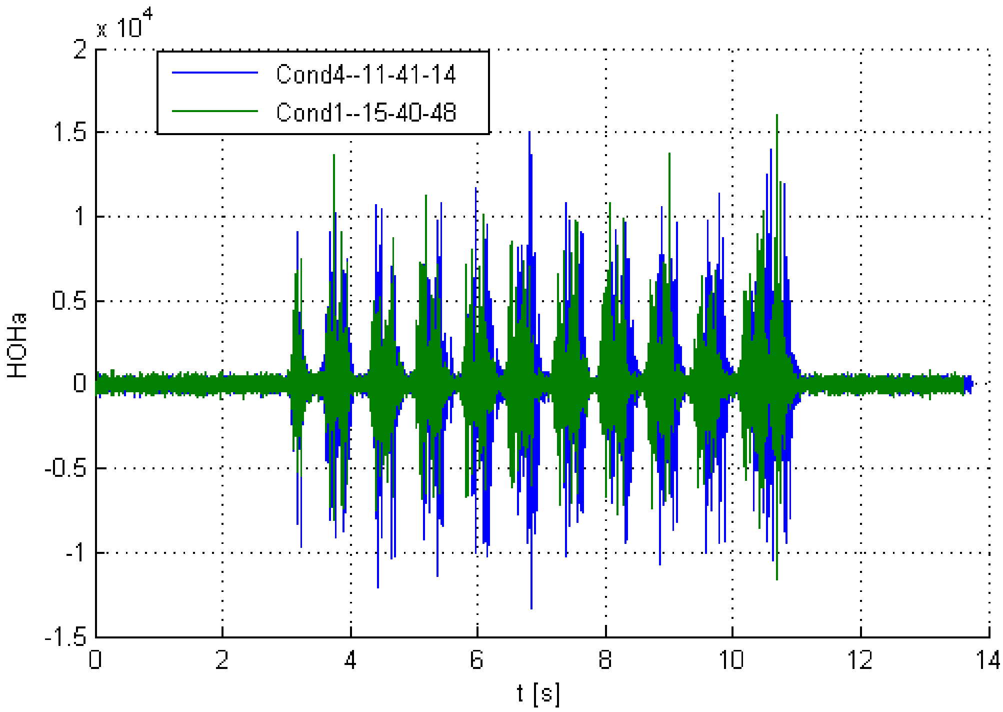

Figure 9-7: Test C102 vs Test C402, sleeper acceleration, time domain

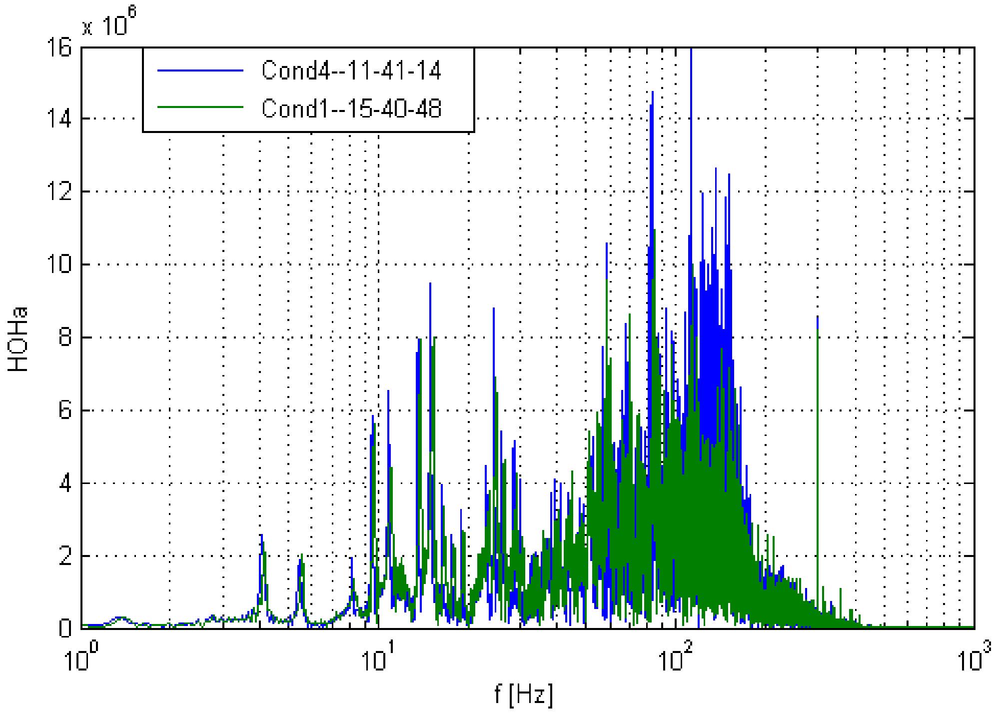

Figure 9-8: Test C102 vs Test C402, sleeper acceleration, frequency domain

9-3 Good condition vs degraded ballast, Intercity 3

Similar comparison as in the two previous sections. Amplification of sleeper displacement and acceleration are observed with alike characteristics.

Test	File	Train	V [km/h]	V [m/s]
C103	W0001–2013-08-13–15-48-47	Intercity	135.10	37.53
C415	W0001–2013-08-13–13-02-55	Intercity	142.30	39.53

Table 9-3: Data for tests C101 and C415

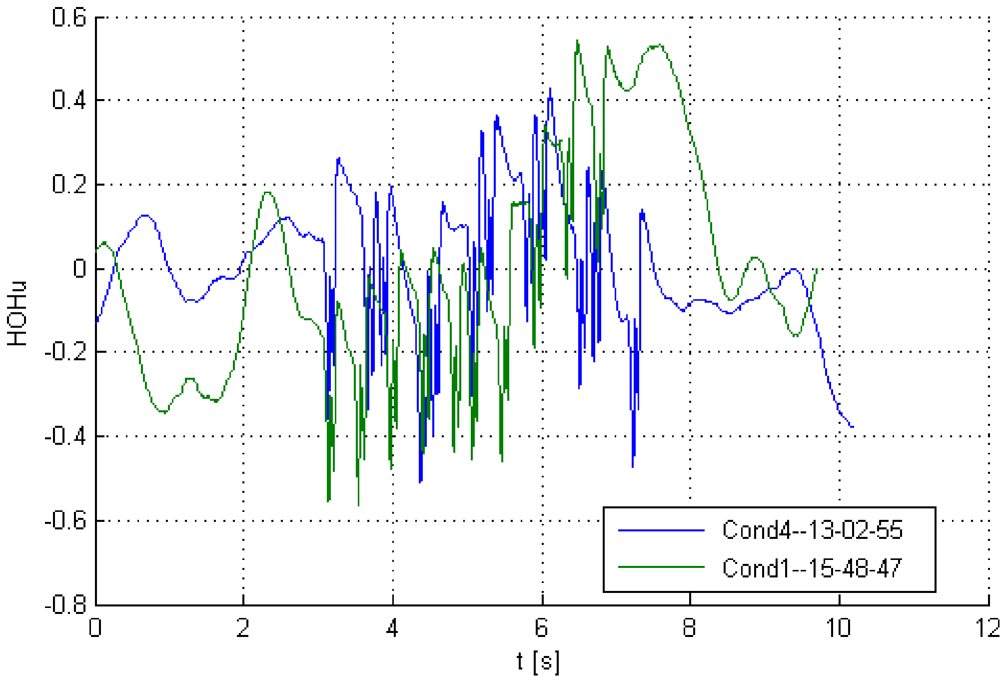

Figure 9-9: Test C103 vs Test C415, sleeper displacement, time domain

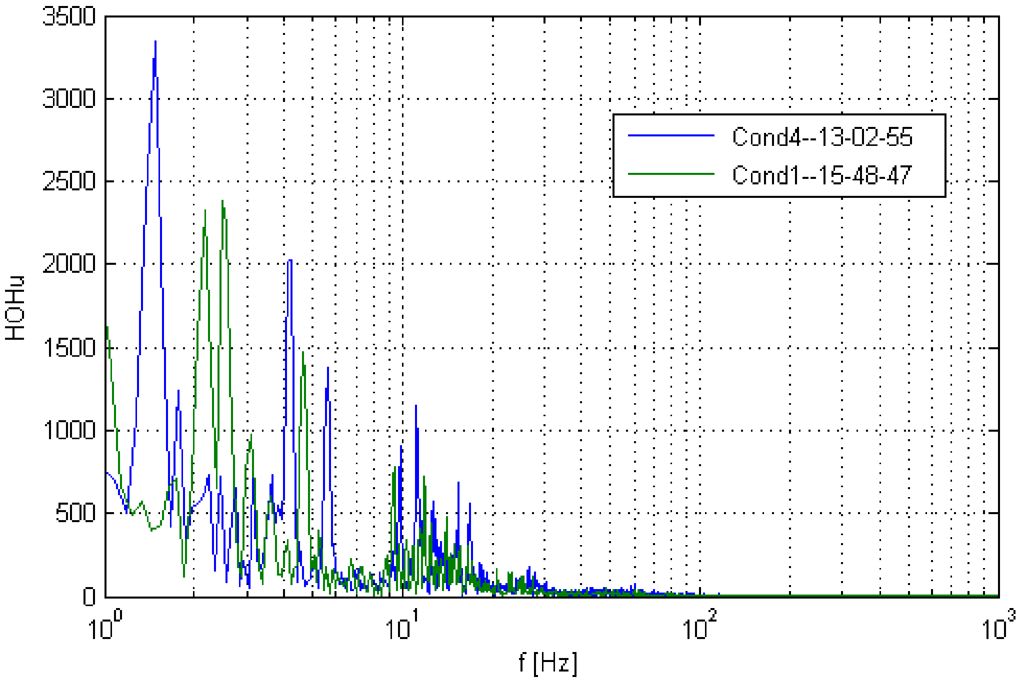

Figure 9-10: Test C103 vs Test C415, sleeper displacement, frequency domain

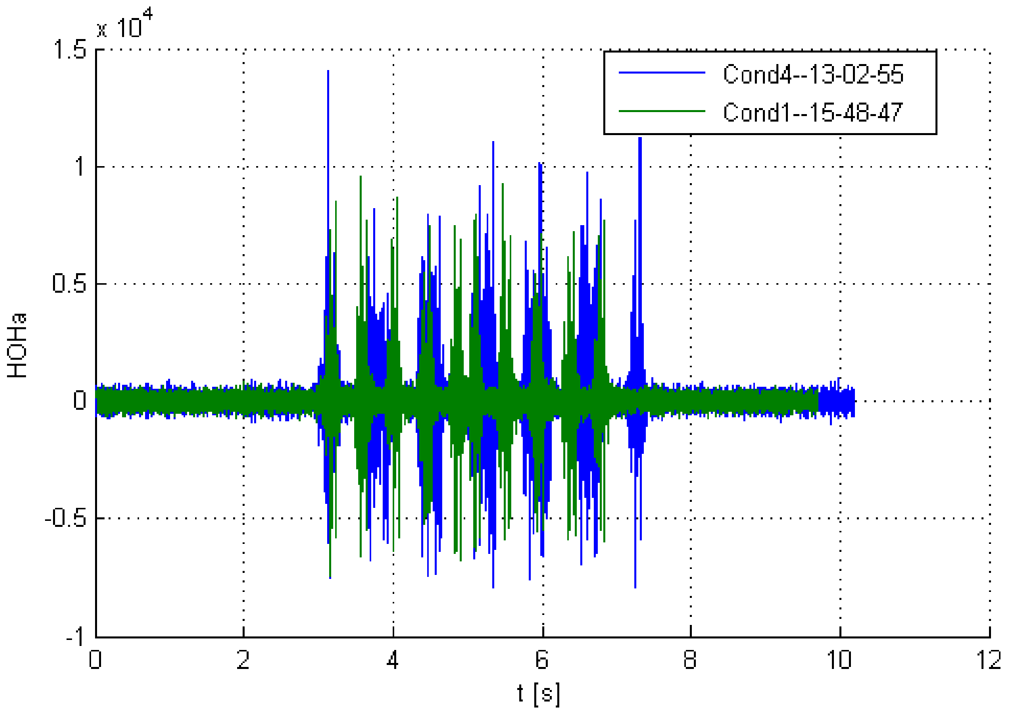

Figure 9-11: Test C103 vs Test C415, sleeper acceleration, time domain

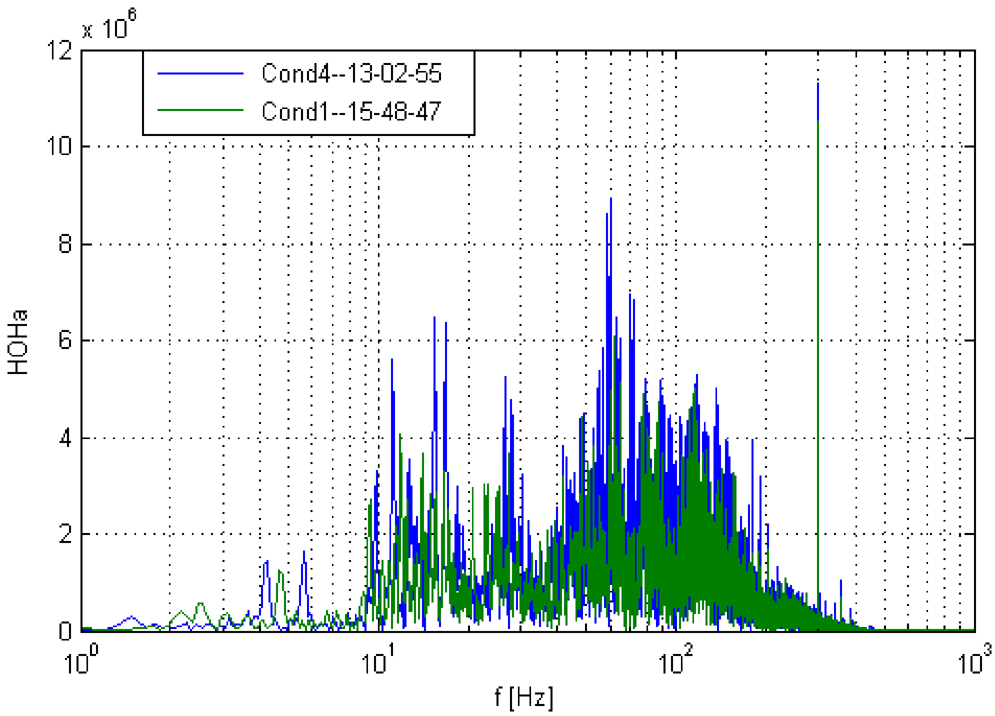

Figure 9-12: Test C103 vs Test C415, sleeper acceleration, frequency domain

9-4 Degraded ballast and weld in rail, Freight 1

Test C410 consisted in the passing of a freight train over a track with degraded ballast. Test C303 was also recorded from the running of a freight train, however, the track condition included both a weld in the rail and an unsupported sleeper.

Test	File	Train	V [km/h]	V [m/s]
C410	W0001–2013-08-13–12-22-23	Freight	89.50	24.86
C303	W0001–2013-08-13–14-24-15	Freight	98.70	27.42

Table 9-4: Data for tests C101 and C303

Analogous to previous sections, the existence of a void under the sleeper is clearly observed in the low frequency range for sleeper displacement (Figure 9-14) and in the mid frequency range for sleeper acceleration (Figure 9-16).

Added to this, the presence of a weld in the rail is now noted in the response from test C303. In Figure 9-14, the displacement of the sleeper shows larger amplitudes between 10Hz and 20Hz. Sleeper acceleration response shows several peaks in the low and mid frequency ranges (Figure 9-16). These alterations can be attributed to the presence of the weld.

In addition, it can be seen that the axle load is a determining factor for the sleeper behaviour and the response of the structure.

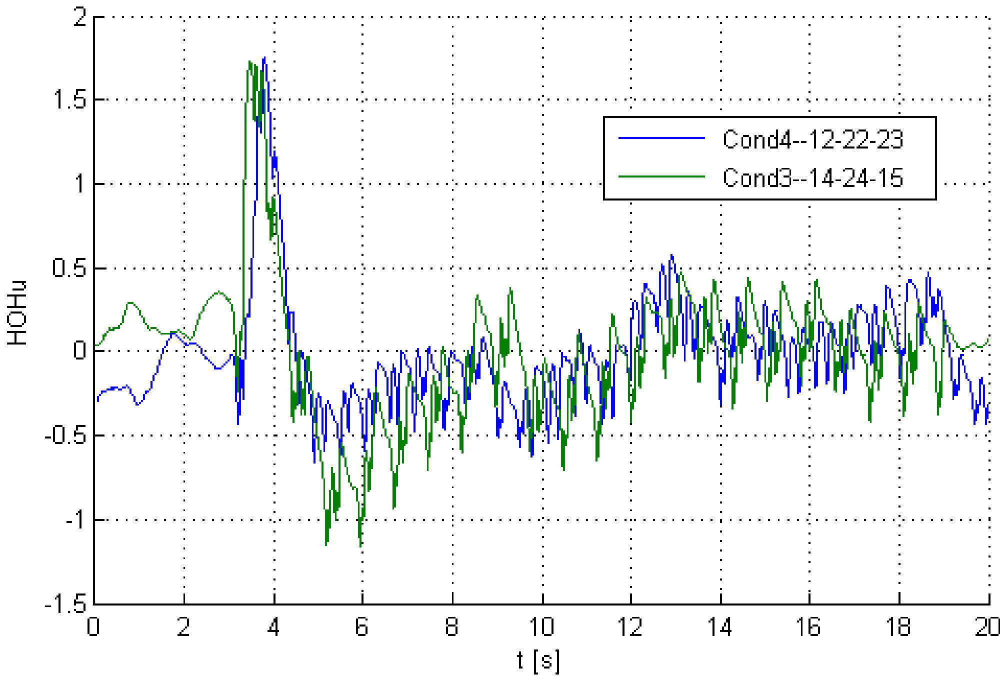

Figure 9-13: Test C410 vs Test C303, sleeper displacement, time domain

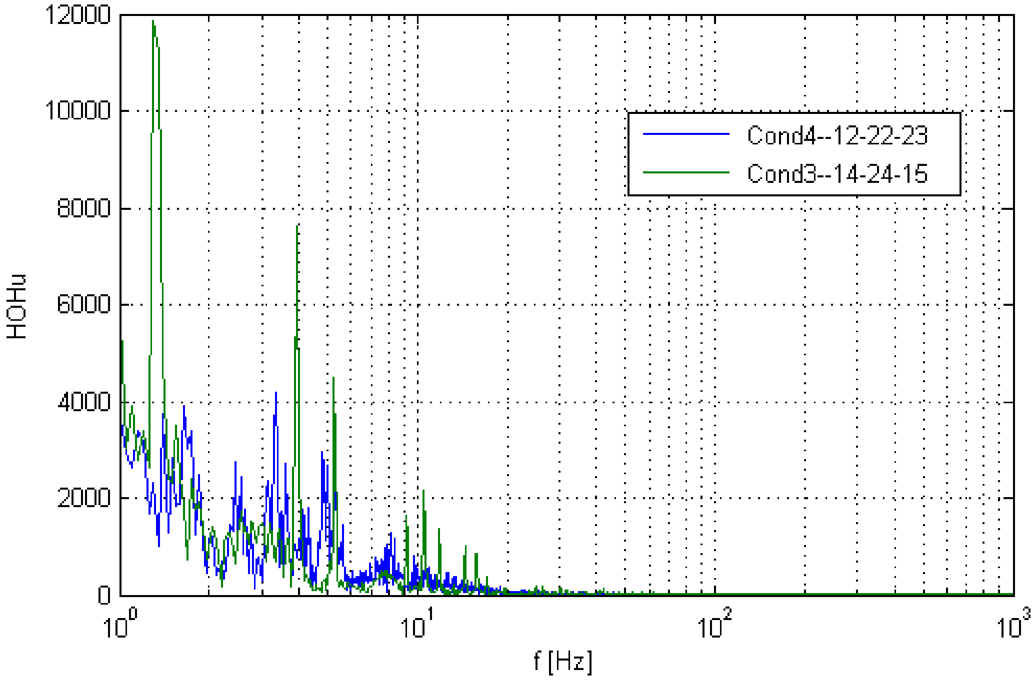

Figure 9-14: Test C410 vs Test C303, sleeper displacement, frequency domain

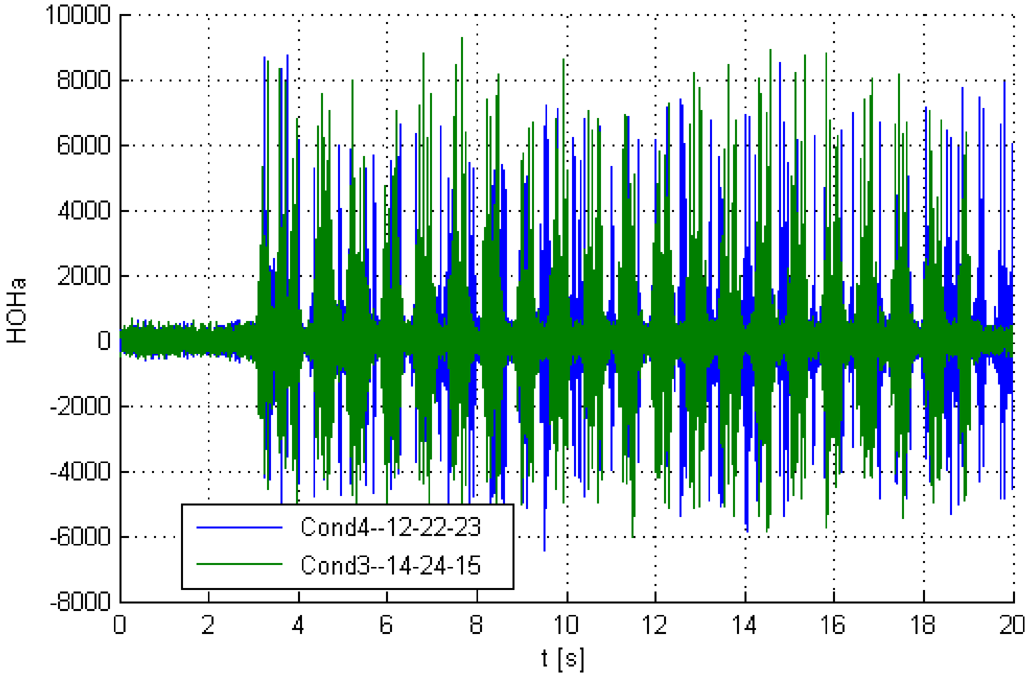

Figure 9-15: Test C410 vs Test C303, sleeper acceleration, time domain

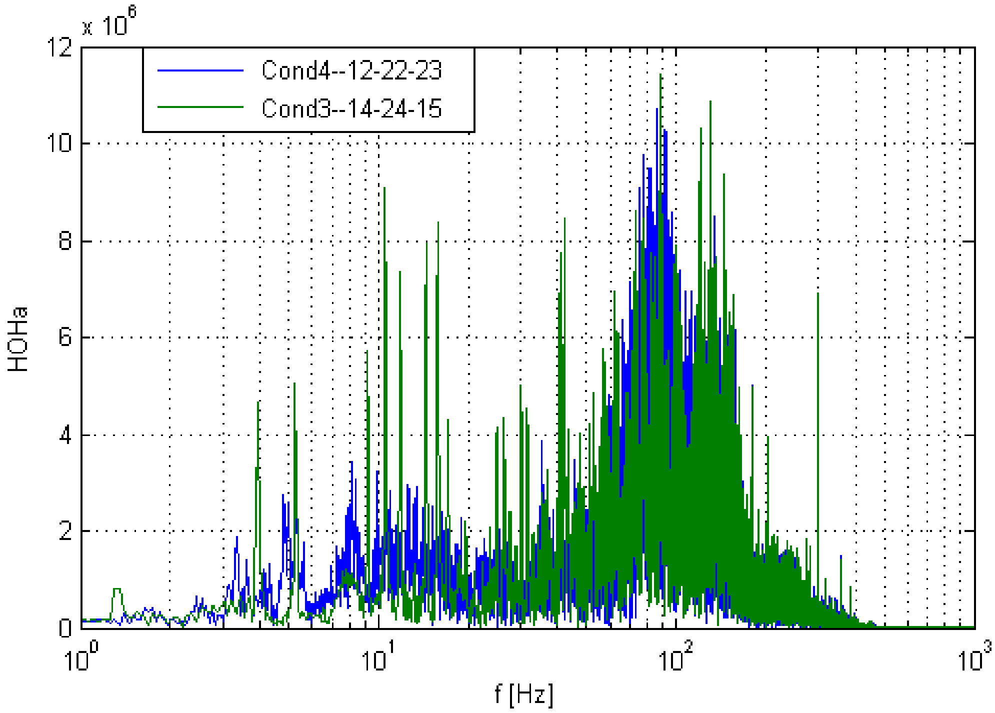

Figure 9-16: Test C410 vs Test C303, sleeper acceleration, frequency domain

Chapter 10

Sensitivity analysis

10-1 Magnitude of the gap

Firstly, the effect of varying the magnitude of the gap is studied. The gap is present under the sleeper located at $x = 1.20m$; the velocity of the vehicle in the simulations is $v = 30m/s$. The results of the analysis are presented in Figure 10-1 to Figure 10-6.

The rail displacement is amplified when the size of the gap increases (Figure 10-1). There is a direct relation between gap size and displacement of the rail. This statement is valid for the displacement of the sleeper as well (Figure 10-3).

In addition, the increment of gap size amplifies the displacement response in the mid frequency region (Figure 10-4). The frequency ($f \approx 50Hz$) corresponds to the full-track vibration frequency.

In Figure 10-6, the FRF of the sleeper acceleration is shown. Between $f = 100Hz$ and $f = 200Hz$, amplification of the response is observed for gap sizes $0.001m$ and $0.002m$. These amplifications are produced by the impact of the sleeper with the ballast when the gap closes. In the case of $gap = 0.003m$, these impact frequencies are not observed.

When $gap = 0.003m$, the maximum vertical displacement obtained is $w_{max} = 2.96 \times 10^{-3}m$. For larger gap sizes, the maximum vertical displacement remains the same. These results suggest that after the $0.003m$ mark, the sleeper is hanging and the gap between ballast bed and sleeper does not close. The rail is behaving as a beam of span $l = 1.20m$ supported by adjacent sleepers. This condition generates high horizontal stresses in the rail and increases the vertical stresses that neighbouring sleepers must resist.

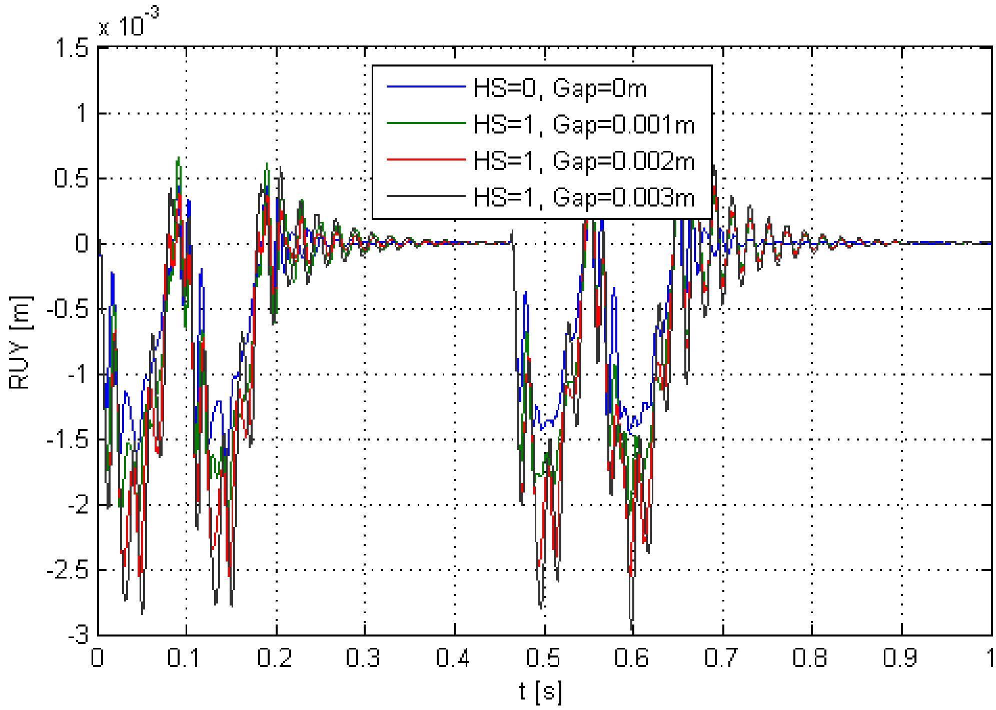

Figure 10-1: Rail displacement in time domain, different gap size for 1 unsupported sleeper

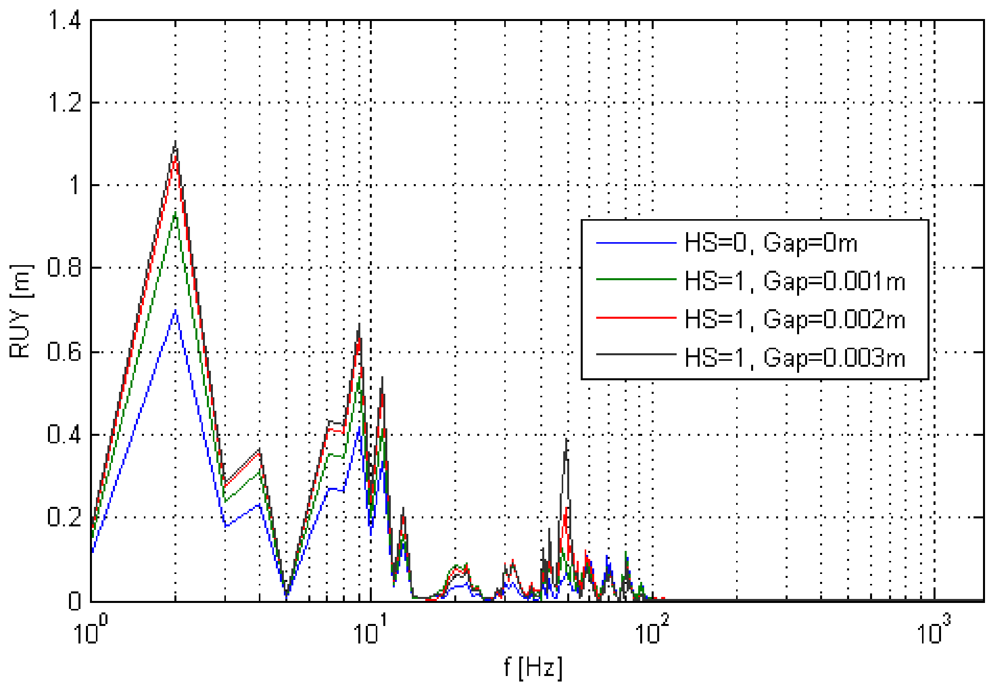

Figure 10-2: Rail displacement in frequency domain, different gap size for 1 unsupported sleeper

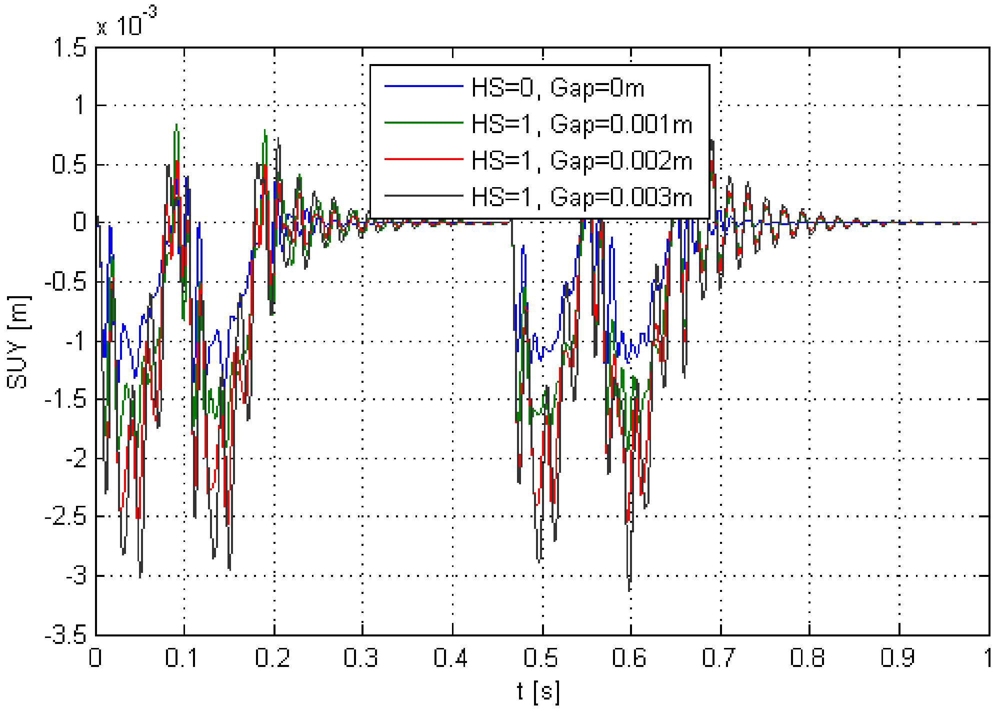

Figure 10-3: Sleeper displacement in time domain, different gap size for 1 unsupported sleeper

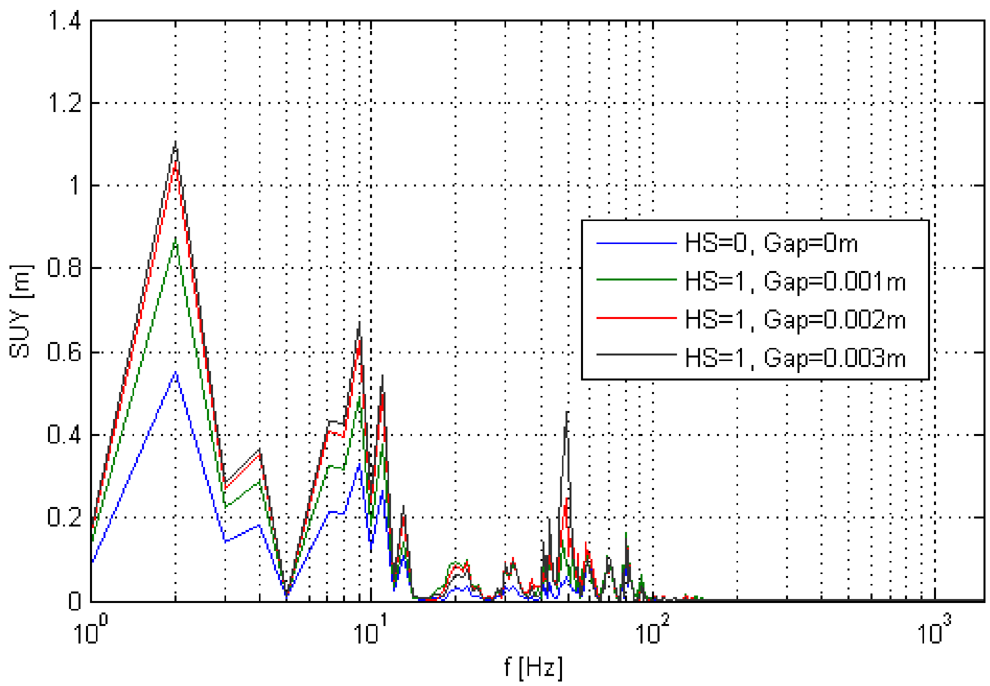

Figure 10-4: Sleeper displacement in frequency domain, different gap size for 1 unsupported sleeper

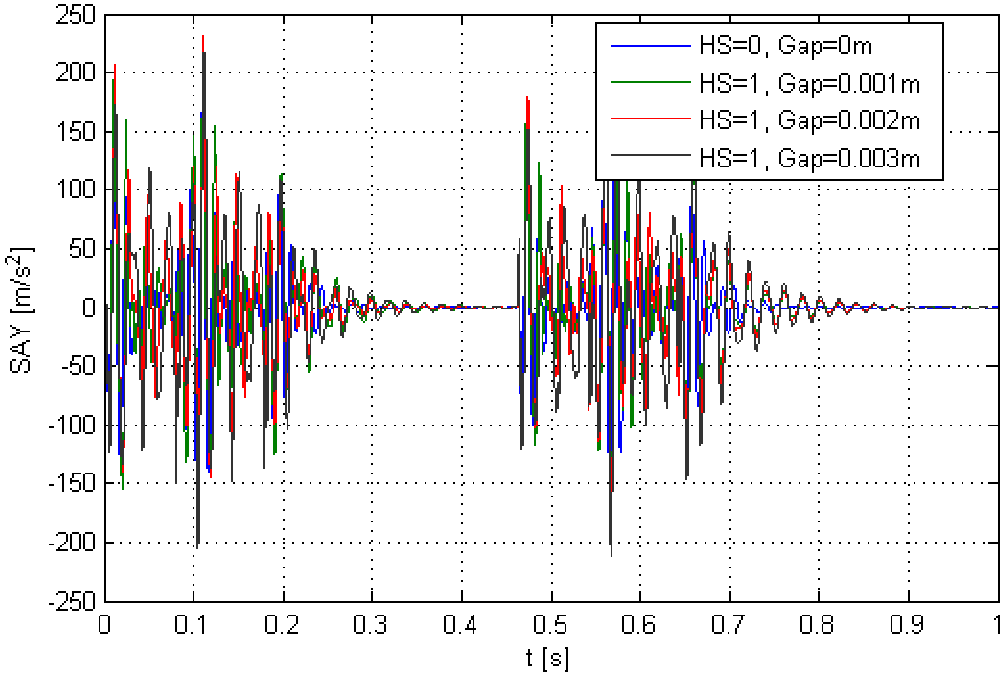

Figure 10-5: Sleeper acceleration in time domain, different gap size for 1 unsupported sleeper

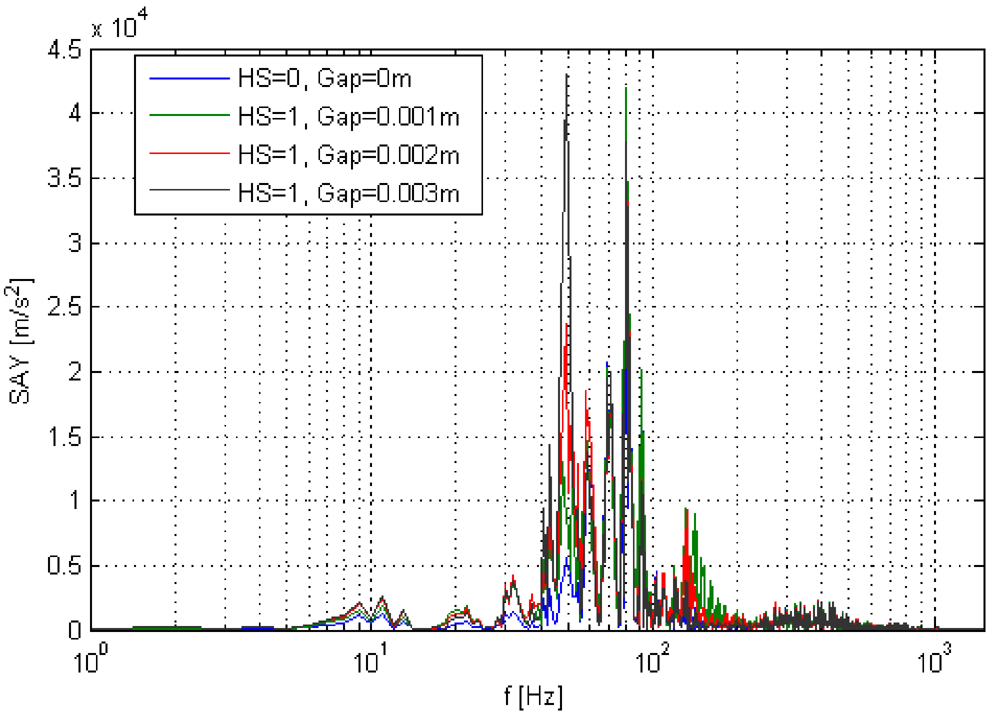

Figure 10-6: Sleeper acceleration in frequency domain, different gap size for 1 unsupported sleeper

10-2 Number of unsupported sleepers

In this section, the number of unsupported sleepers is increased from 1 to 3. A gap is present between sleeper and ballast bed at $x = 0.60m$, $x = 1.20m$ and $x = 1.80m$.

First, a fixed size of gap is used to observe the effect of increasing the number of unsupported sleepers. The size of the gap for this analysis is $0.005m$. Results are presented in Figure 10-7 to Figure 10-12.

The increment of unsupported sleepers produces larger deformations of the structure (Figure 10-7). In Figure 10-8, the FRF of rail displacement shows that larger amplifications are generated when the track has three unsupported sleepers.

Moreover, the response of the rail shifts to the left into lower frequencies. The full-track vibration frequency is no longer found in the mid frequency region but in the low frequency region. The increment of unsupported sleepers amplifies the displacement of the rail and the track response is excited by lower frequencies.

The sleeper acceleration has a similar response when the number of unsupported sleepers is increased. In Figure 10-12, a shift is observed from $f \approx 50Hz$ to $f \approx 30Hz$. Additionally, the impact frequencies between $100Hz$ and $200Hz$ are present again.

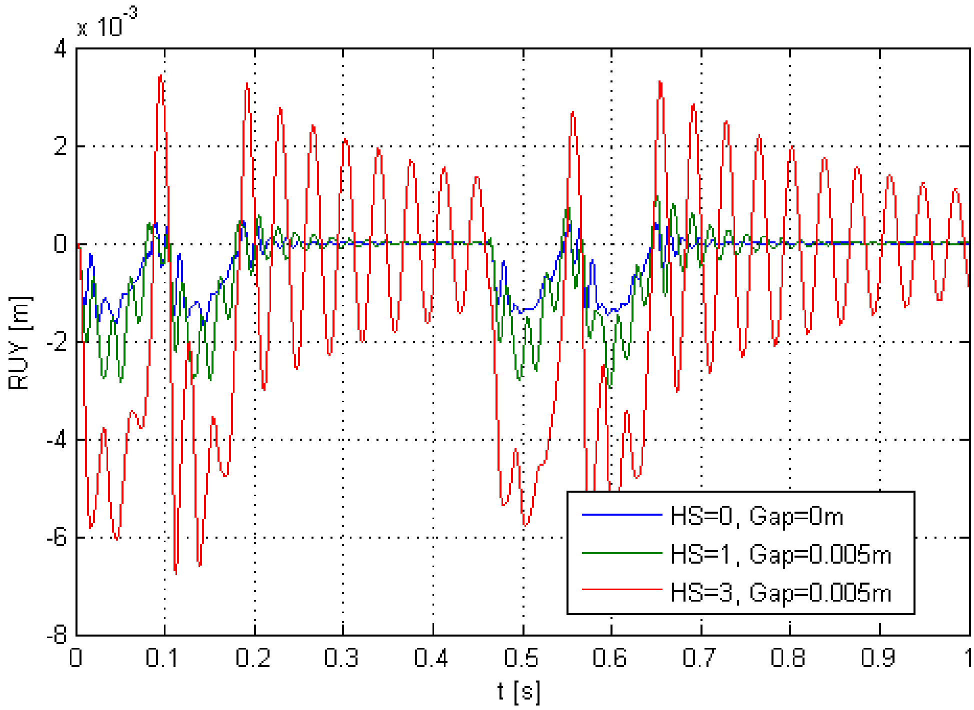

Figure 10-7: Rail displacement in time domain, different gap size for 3 unsupported sleepers

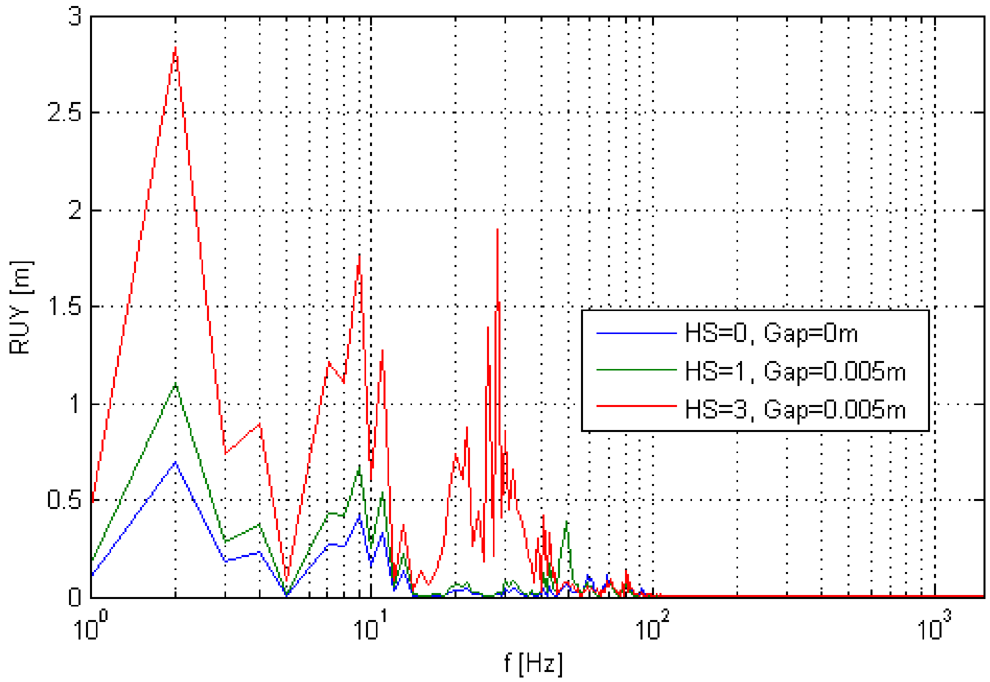

Figure 10-8: Rail displacement in frequency domain, different gap size for 3 unsupported sleepers

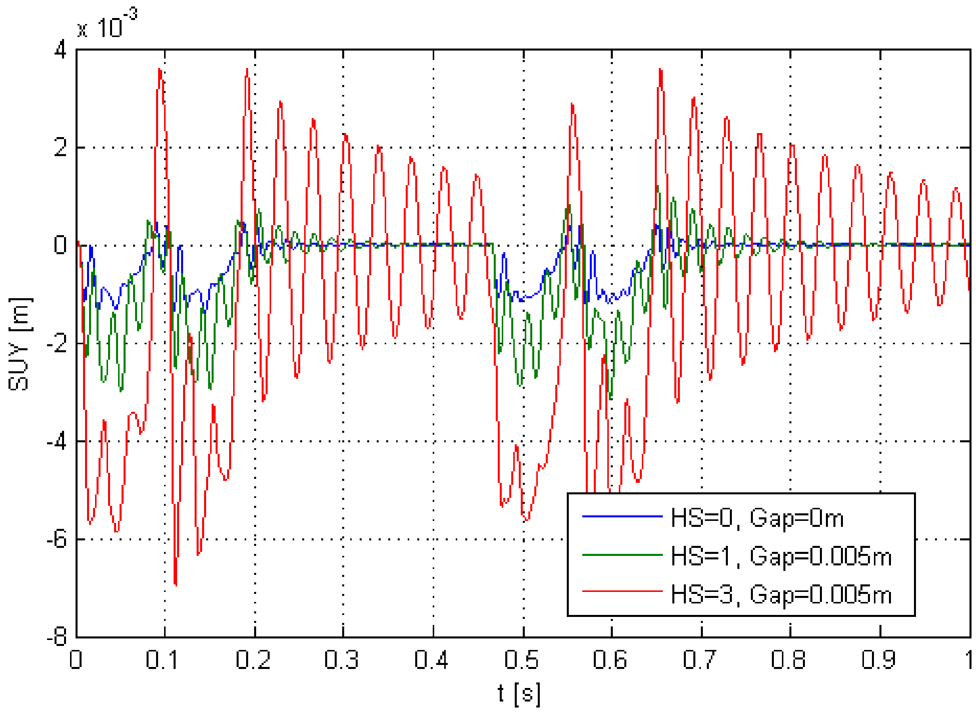

Figure 10-9: Sleeper displacement in time domain, different gap size for 3 unsupported sleepers

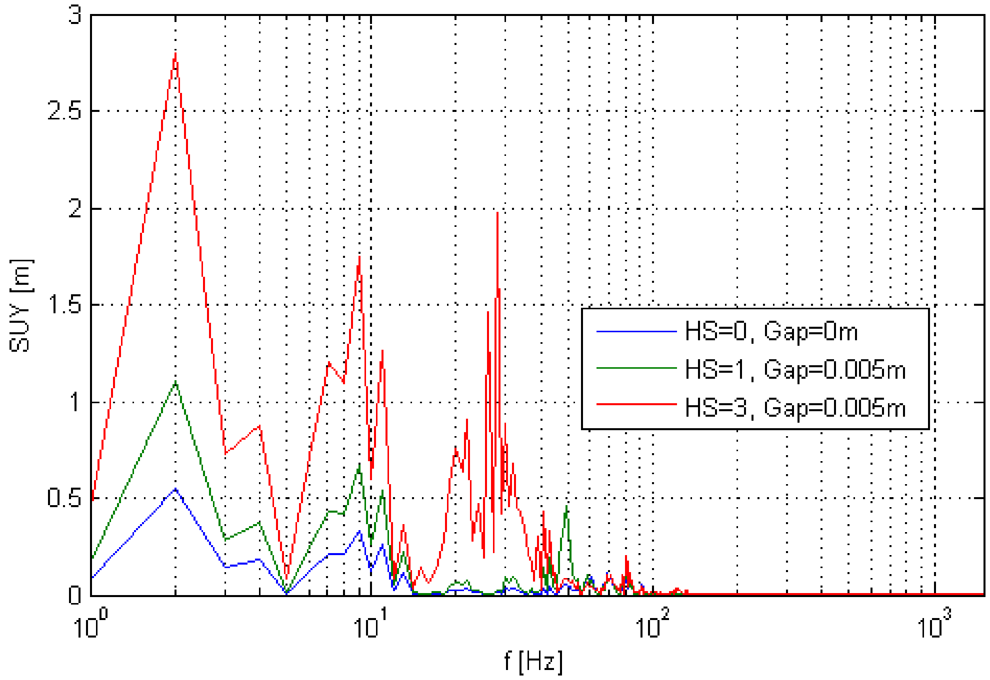

Figure 10-10: Sleeper displacement in frequency domain, different gap size for 3 unsupported sleepers

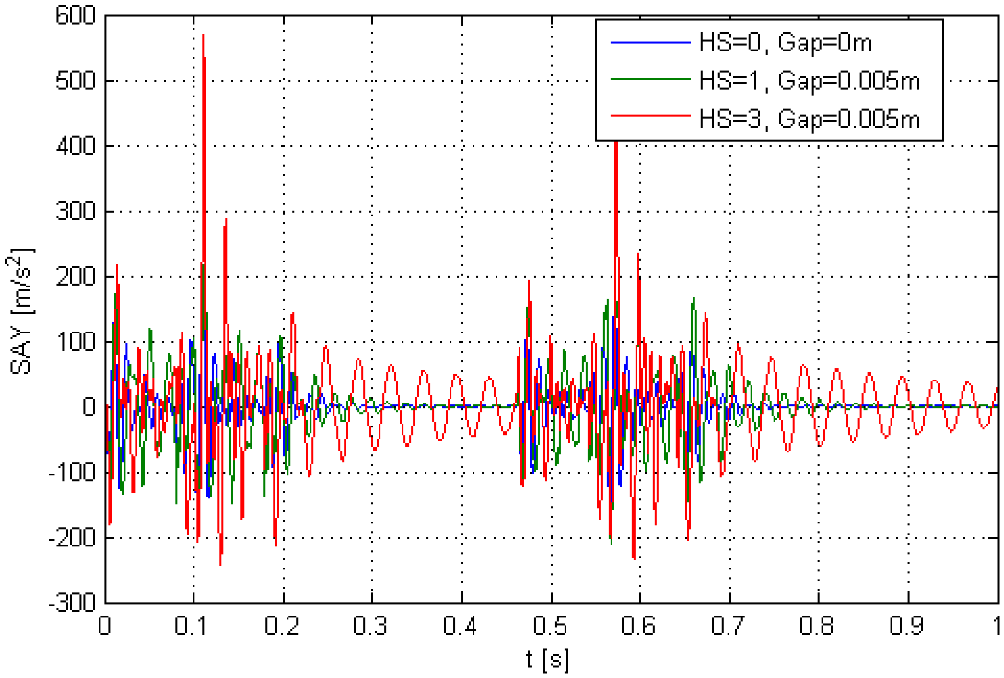

Figure 10-11: Sleeper acceleration in time domain, different gap size for 3 unsupported sleepers

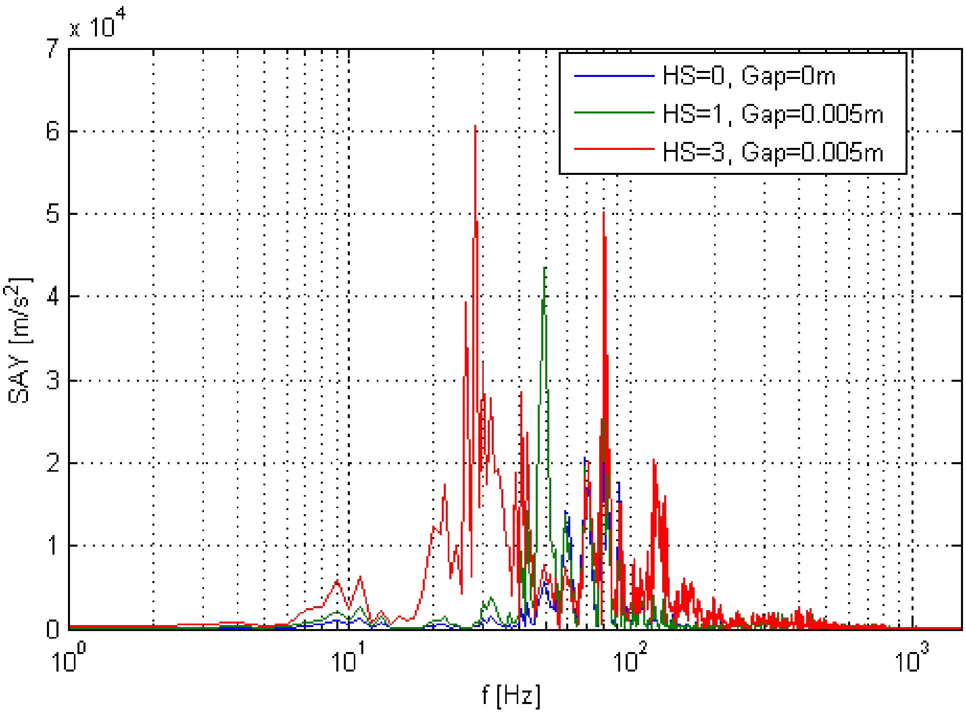

Figure 10-12: Sleeper acceleration in frequency domain, different gap size for 3 unsupported sleepers

10-3 Limitation of the model

In Figure 10-13, comparison of maximum vertical displacement of the rail for different number of unsupported sleepers and gap sizes is presented. As stated in Section 10-1, in case of having one unsupported sleeper, the displacement of the rail reaches a maximum value of $2.96mm$ for gap sizes larger than $3mm$.

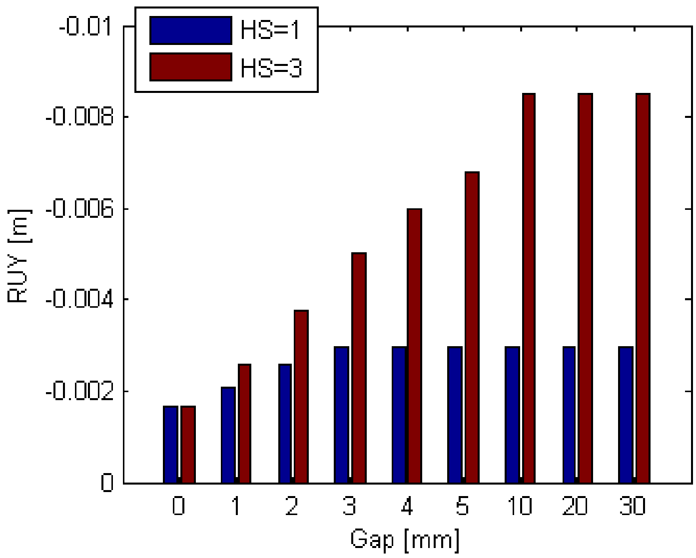

Figure 10-13: Maximum rail displacement for different gap sizes and unsupported sleepers

When the number of unsupported sleepers is increased to three, the maximum vertical displacement obtained is $8.49mm$. This displacement is found for gap sizes larger than $0.010m$. In this condition, the rail is acting as a beam of span $l = 2.40m$, only supported by the end sleepers at both sides of the model.

The limitations of the model does not allow to explore larger number of unsupported sleepers. However, it is important to point out that a vertical displacement of almost $10mm$ was reached using only three unsupported sleepers.

10-4 Velocity of the vehicle

In the following analyses, different vehicle velocities are studied. The velocities used in the simulations are shown in Table 10-1. The analysis is performed for gap size $0.010m$. Only frequency domain results from the analyses are presented.

m/s	km/h
01	3.60
10	36
20	72
30	108

Table 10-1: Vehicle velocities for sensitivity analysis

Figure 10-14 shows the rail displacement FRF for four different velocities. The largest response of the rail moves to lower frequencies when the velocity of the train is reduced. The amplitude of the response is not affected by the velocity of the train, only the position in the frequency spectrum.

On the other hand, the sleeper acceleration response shows an amplification when large vehicle velocities are used (Figure 10-16). The position of the peak response does not change, only the amplitude.

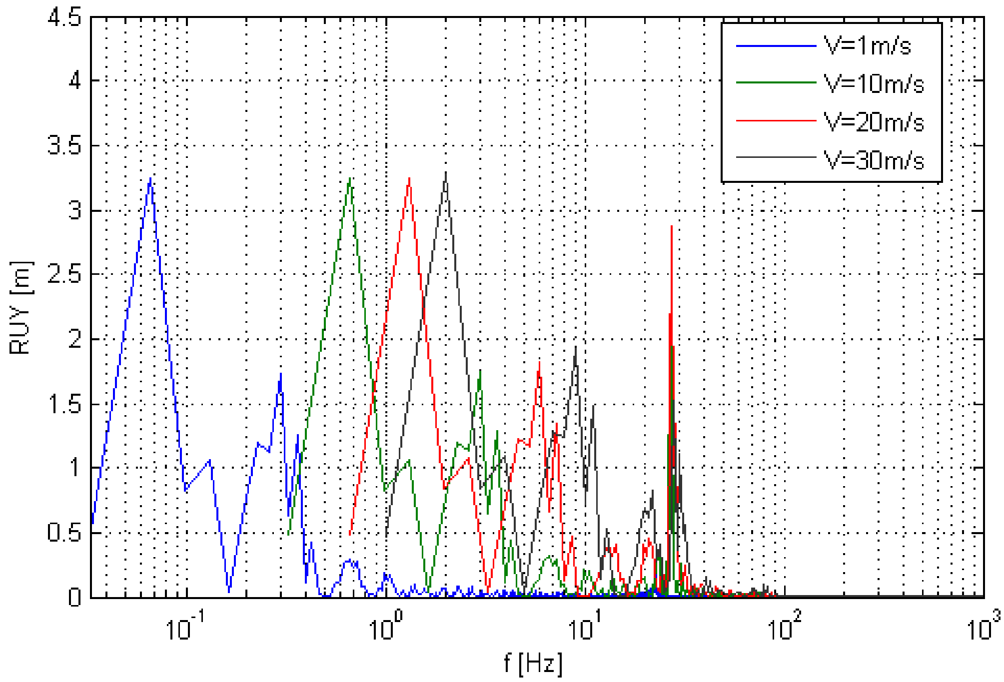

Figure 10-14: Rail displacement in frequency domain, different velocities for gap=0.010m

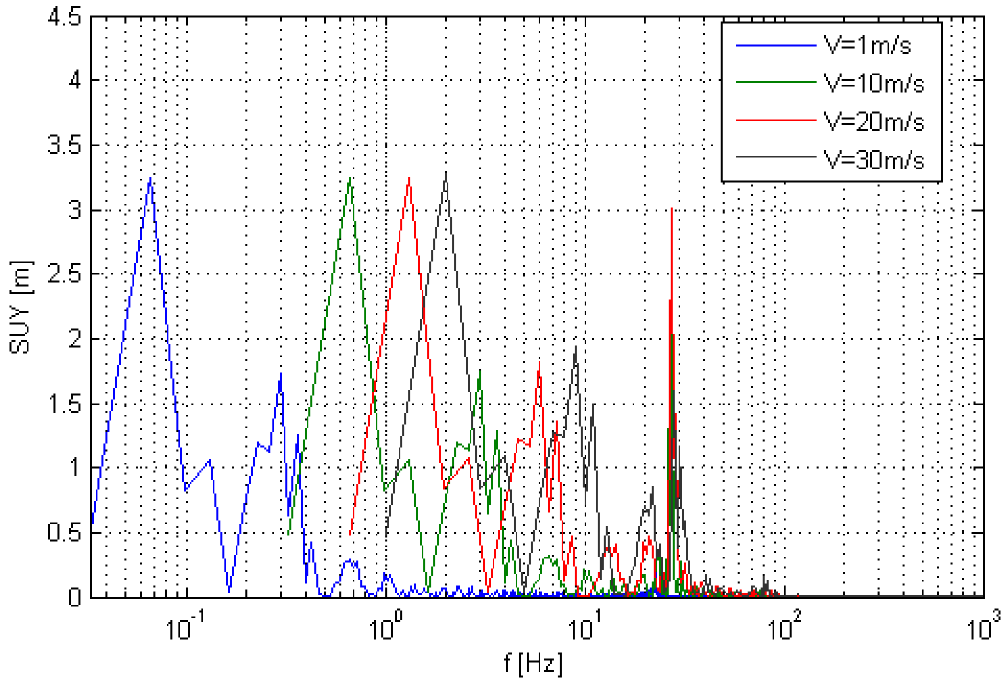

Figure 10-15: Sleeper displacement in frequency domain, different velocities for gap=0.010m

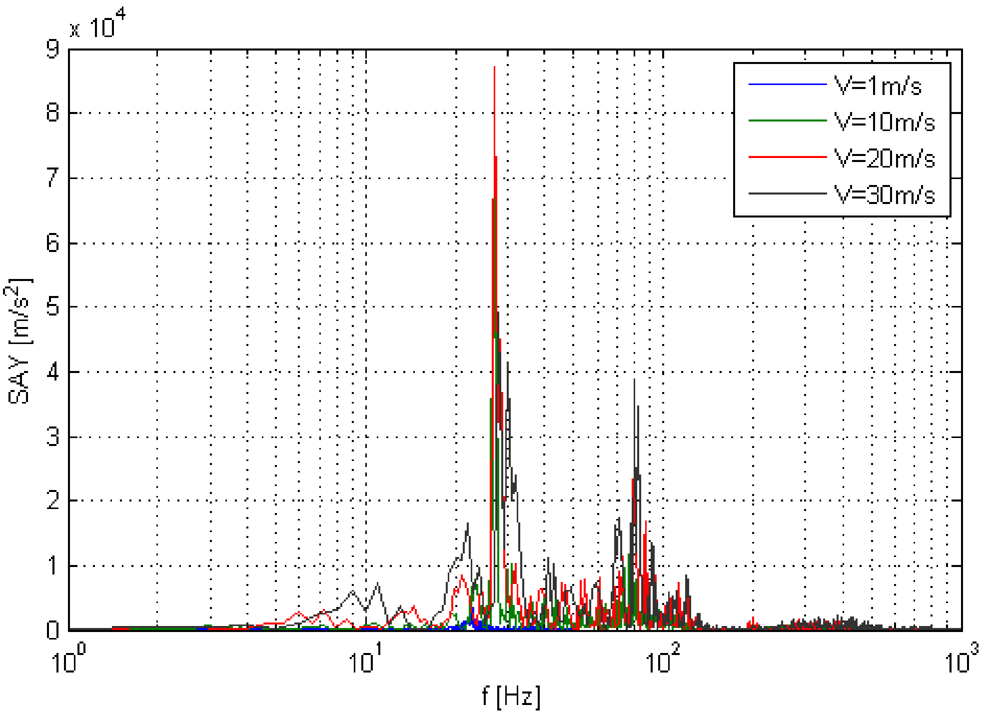

Figure 10-16: Sleeper acceleration in frequency domain, different velocities for gap=0.010m

10-5 Summary of results

10-5-1 General results

From the sensitivity analysis, the following information is obtained:

- The model is limited to simulate a track with maximum three unsupported sleepers.
- Following the model limitation, gap sizes larger than $0.010m$ generate the same vertical displacement.
- Large gap sizes generates large vertical displacement of the rail.
- Increment of the gap size shifts the track vibration frequencies to low frequency region.
- Impact between sleeper and ballast produces frequencies in the mid frequency range ($100Hz$ to $200Hz$).
- Decrement of the vehicle velocity amplifies lower frequencies in the displacement FRF.

10-5-2 Maximum rail displacement

Figure 10-17 shows the maximum vertical displacement of the rail for different velocities and gap sizes using three unsupported sleepers. The maximum displacement ($w_{max} = 9.15 \times 10^{-3}m$) was obtained for $v = 10m/s = 36km/h$ and a gap size of $0.010m$.

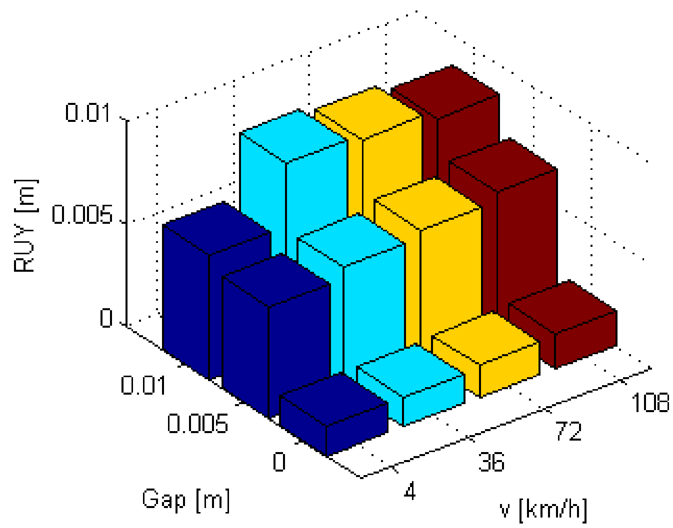

Figure 10-17: Maximum rail displacement for different gap sizes and vehicle velocities, three unsupported sleepers

10-6 Relation between displacement, velocity and frequency

From the sensitivity analysis, it is known the effect of a gap in the dynamic response of the track. This effect is related to the forces acting in the track through the frequency of the loads. The maximum frequency that a train can exert to the track is defined by the minimum distance between two axles. In the case of the locomotive used in the simulations (Figure 6-5), the frequency of the load f_{load} can be calculated as:

$$f_{load} = \frac{1}{t} = \frac{v}{l} \tag{10-1}$$

Where v is the velocity of the vehicle and l is the distance between axles. Substitution of different values for v and l in Eq. (10-1) generates the surface presented in Figure 10-18. The figure shows the relation between velocity, axle distance and frequency of the load.

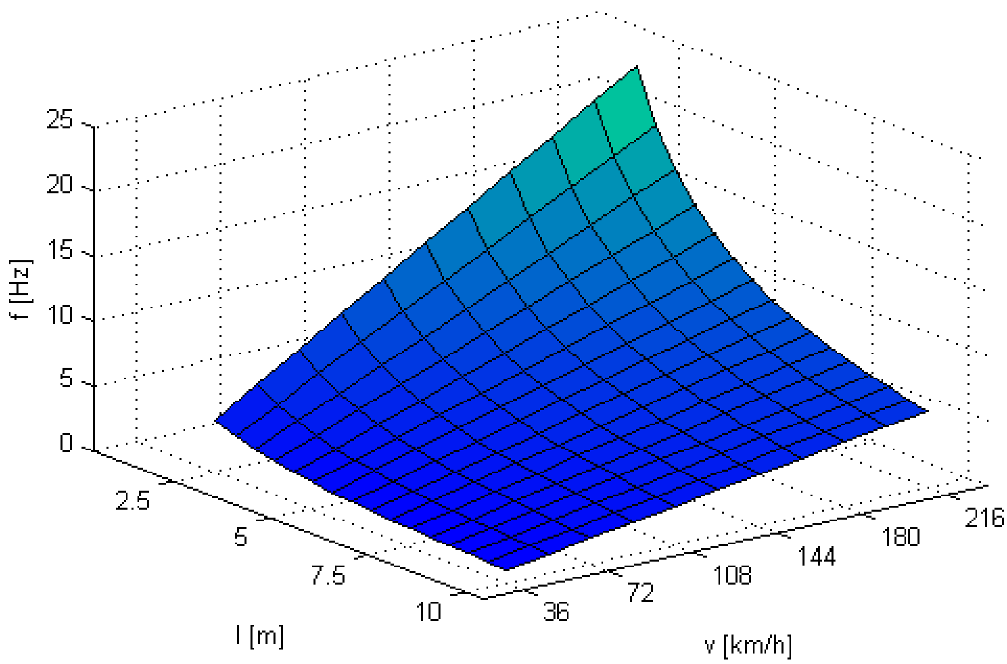

Figure 10-18: Load frequency for different distance between loads (l) and vehicle velocity (v)

In theory, the frequency that can be generated by a train is $f \leq 25Hz$. The vibration frequencies of the track without gaps are located above this value. However, from previous analysis, it was shown that the vibration frequency of the track is shifted to lower frequency values when large displacements of the rail are present.

In Figure 10-19, different load frequencies are plotted as a function of the vehicle velocity. In the same figure, the value for full-track vibration frequency with and without gap are plotted as dotted lines.

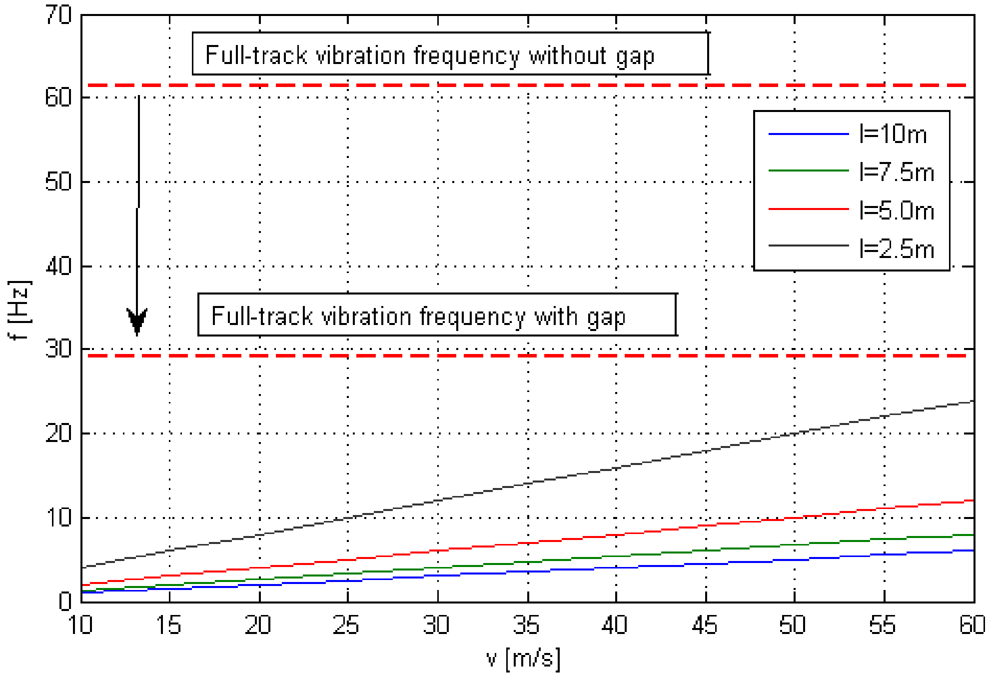

Figure 10-19: Track vibration frequency modification due to presence of a gap compared to frequency of the load for different vehicle velocities

Due to the limitation in the model, it is not possible to explore larger vertical displacement values that can generate lower vibration frequencies of the track. However, the results obtained in this analysis properly show the relation between vehicle velocity, track vibration frequency and vertical displacement of the track.

10-7 Use of Under-Sleeper Pad

An analysis is performed using USP elements between sleepers and ballast bed. The track is in good condition and the velocity of the vehicle is $v = 30m/s$. Results of the analysis are graphically displayed in Figure 10-20 to Figure 10-25.

The amplitude of rail displacement and sleeper acceleration are increased by the presence of the USP in the model. Figure 10-21 shows clearly how the flexibility added by the USP amplifies the response of the rail displacement. Same effect is observed in the displacement of the sleeper (Figure 10-23).

In Figure 10-25, the acceleration of the sleeper shows larger response when USP are included in the model. The added flexibility reduces the response of the acceleration in the range between 100Hz and 150Hz. However, the amplitude of the response in this frequency range is negligible.

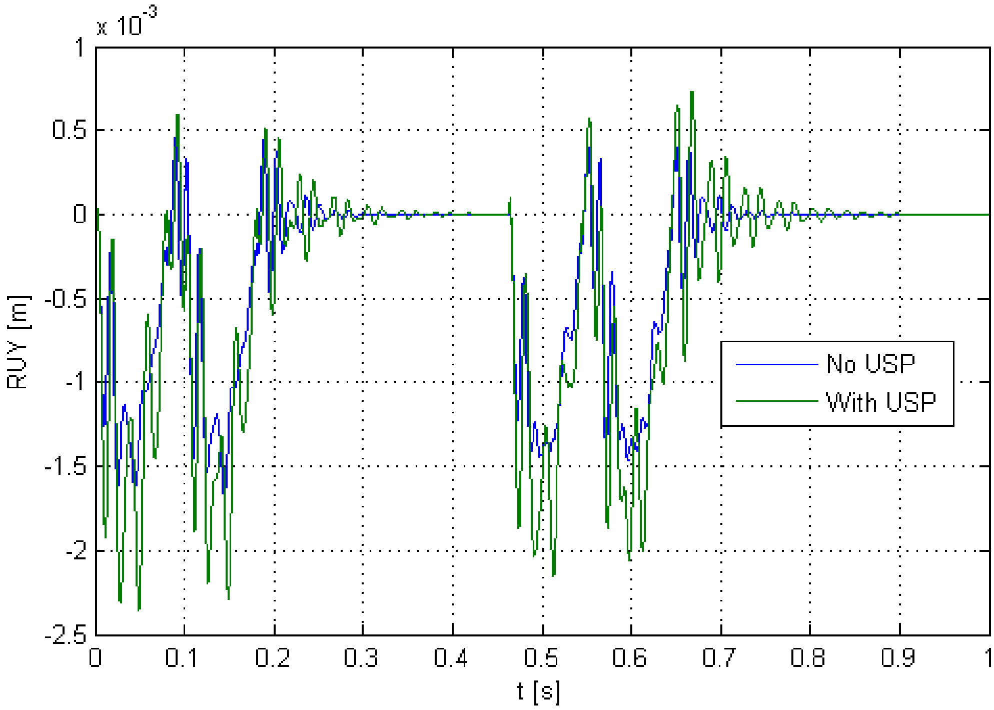

Figure 10-20: Rail displacement in time domain with and without **USP!**

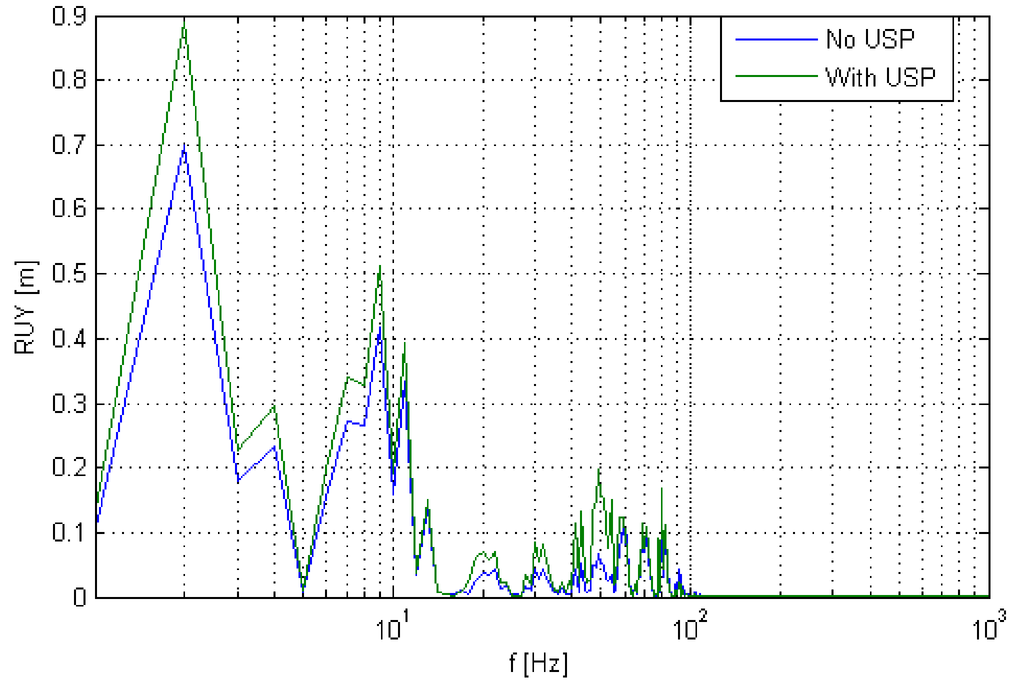

Figure 10-21: Rail displacement in frequency domain with and without **USP!**

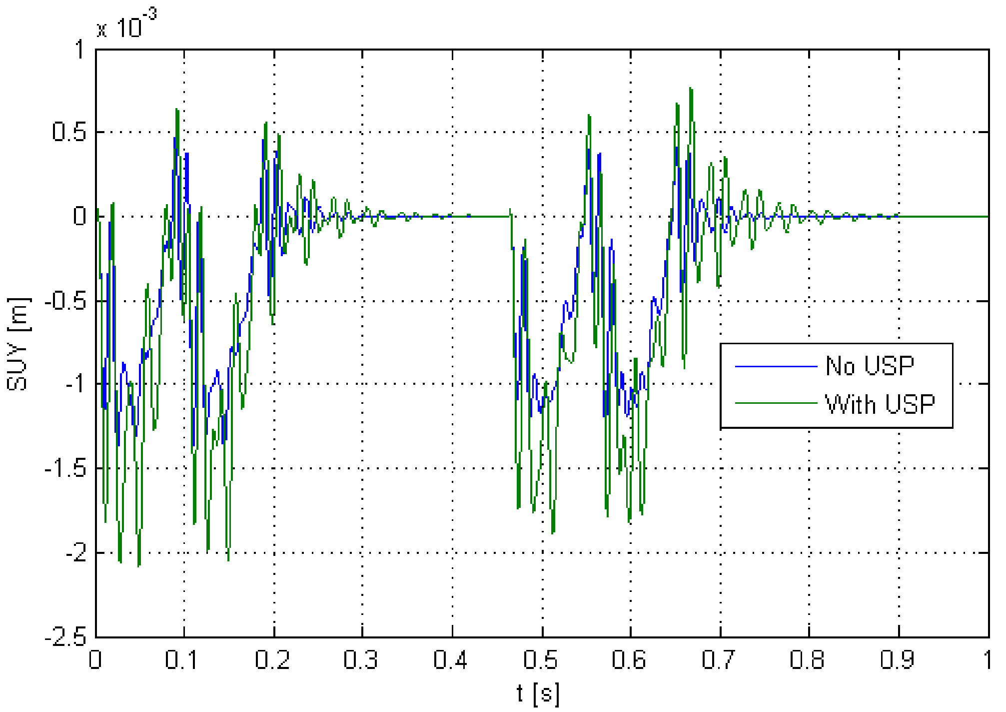

Figure 10-22: Sleeper displacement in time domain with and without **USP!**

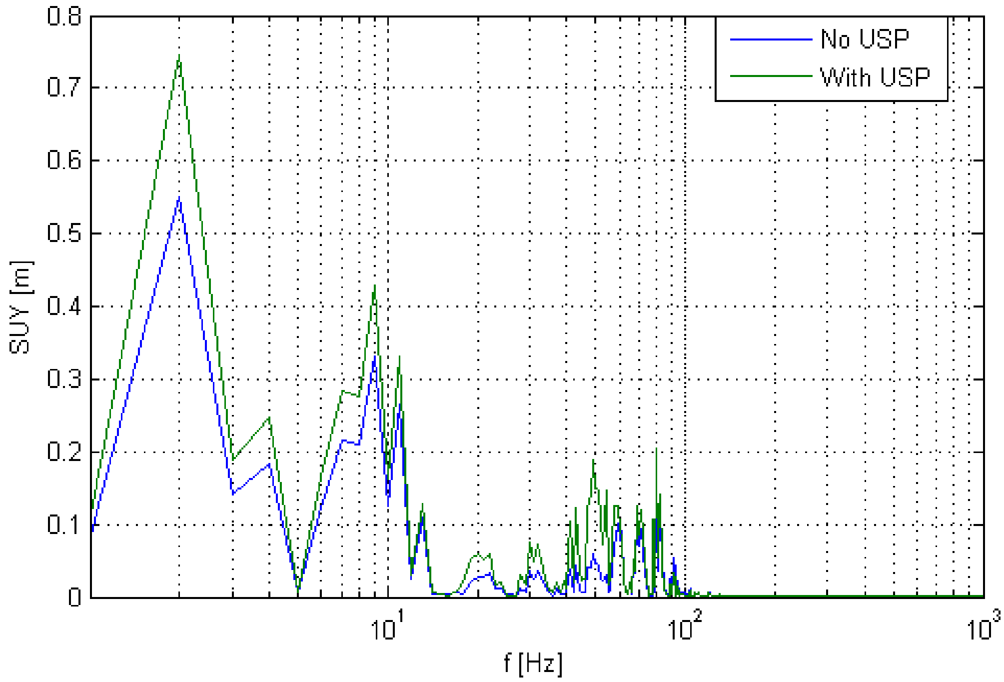

Figure 10-23: Sleeper displacement in frequency domain with and without **USP!**

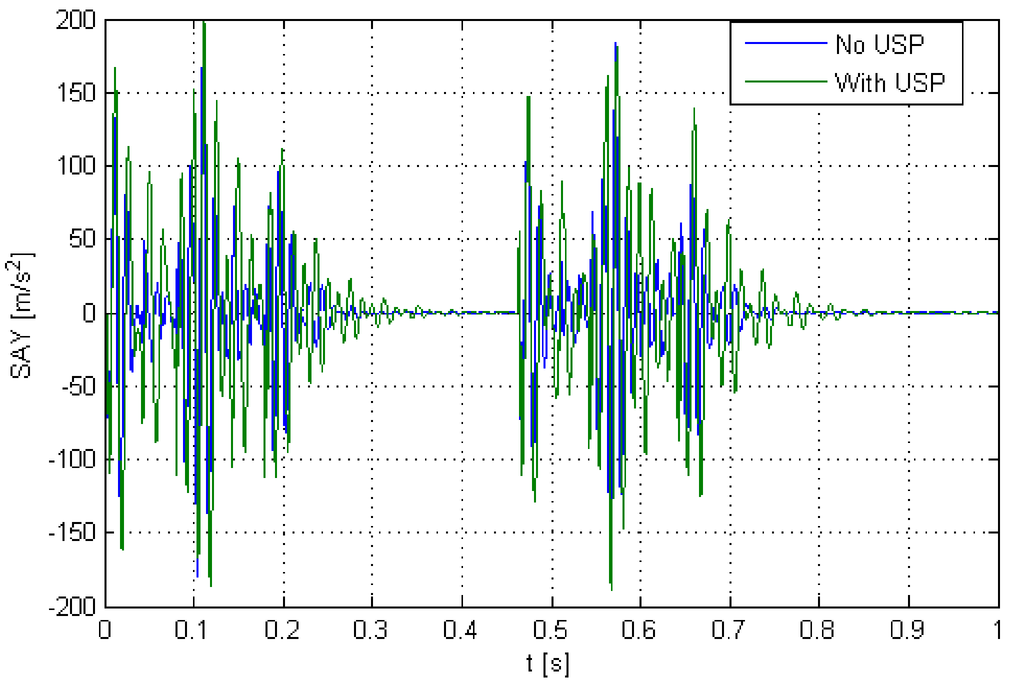

Figure 10-24: Sleeper acceleration in time domain with and without **USP!**

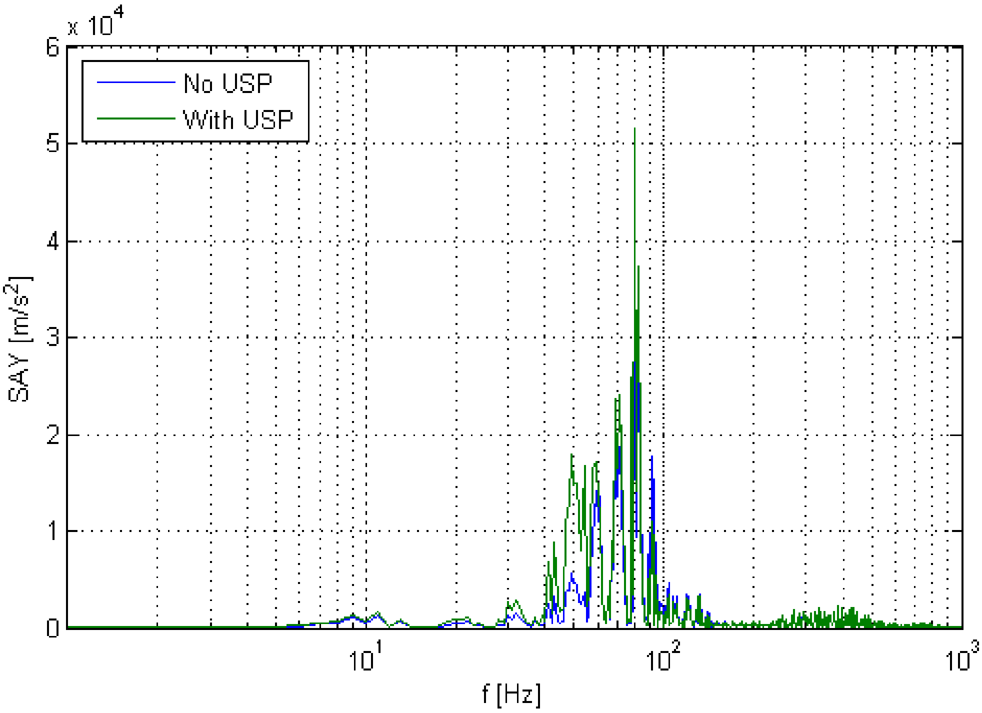

Figure 10-25: Sleeper acceleration in frequency domain with and without **USP!**

Chapter 11

Conclusions

11-1 Condition of the track

The ESAH-M instrument was tested in the field to measure the vertical dynamic behaviour of the railway track. The system was selected for the following reasons:

- Reduced weight of the system and simple transportation.
- Capability of measuring accelerations and displacements of rail and sleeper.
- Installation of the system requires a short period of time. The presence of working personal in the track is reduced.
- Results are saved in a practical output format that can be post-processed with commercially available numerical computing software.
- System has a sampling rate of 10kHz, suitable for analyses in the high frequency region.

Good correlation was found between simulation results and field measurements. It is possible to measure the vertical displacement of the rail by using the ESAH-M system.

Considerations must be taken when using ESAH-M in the field:

- The system is designed to measure local response of the track. Every measurement is limited to one vehicle running over one point of the railway.
- Installation of the system requires that a working team must enter the track. This fieldwork can occur during or out of track service hours.

Overall, ESAH-M had a promising performance in the field.

11-2 Evaluation of the norm

A computational model of a short section of railway track was built. The model was revised using modal analysis and data recollected in the field. After validation of the model, a sensitivity analysis was performed.

Three variables were considered in the analysis to explore the dynamic response of the track:

- Gap size between unsupported sleeper and ballast bed (void)
- Number of unsupported sleepers in the track
- Velocity of the vehicle

During the analysis, the largest vertical displacement of the rail obtained with the model was $w_{max} = 9.15 \times 10^{-3}m$. The research sought to explore displacements larger than $w = 0.010m$; the capabilities of the model are limited to this value. The conclusions presented are drawn according to this limitation.

The analysis showed that the vertical displacement of the rail is directly proportional to the size of the gap under the sleeper. The FRF of the track elements is shifted into the low frequency region when larger gaps are present.

The number of unsupported sleepers has a significant effect in the response of the track. Larger vertical displacements are obtained when the number of unsupported sleepers is increased. The vibration frequencies of the track are reduced when more than one sleeper is not supported properly.

Using the distance between axles of different trains and their velocity, it was calculated that the frequency of the loads applied to a railway track belong to the low frequency region. It is desired that the frequency of the load does not match the vibration frequencies of the structure.

The third variable, velocity of the vehicle, showed that larger velocities amplify the displacements and accelerations of the rail and sleeper. For vertical displacements close to $w = 0.010m$, a threshold was found at $v = 10m/s$ ($v = 36km/h$). The limitations of the model prevented the research to deepen into this threshold.

The use of USP in the construction of the track was analysed as well. From the analysis it was confirmed that the USP provides flexibility to the structure. This modification in the stiffness generates larger displacements and accelerations of the rail and sleeper. No positive effects of using USP in the track were identified.

The length of the model limited the scope of the research. Despite the information obtained from the sensitivity analysis, no answer to the second research question can be given; only recommendations.

11-3 Track condition indicator

The displacement of the rail is an elementary and easy understandable parameter. In this research, the relation between displacement and quality of the track has been proved. The magnitude of the rail displacement is measurable in the field and the measurement provides direct information on the quality of the track: larger displacement, lower quality.

For simplicity of a norm, a basic displacement unit (m) is preferred over more complex units (m/s^2 or kN/m). It is reasonable for a standard to limit displacements rather than other parameters.

The vertical displacement of the rail is a good indicator to regulate the quality of the track. It is concluded that the displacement of the rail is the most suitable parameter to be standardised by ProRail norms.

Chapter 12

Recommendations

- Before using the ESAH-M system in the field, the instrument must be correctly configured. The measuring units for displacement and acceleration should be declared before any field work.
- The relation displacement - velocity - frequency was not completed due to the limitation of the model. It is recommended to expand the model and include more track elements in the simulations. Then, larger displacements can be obtained and the norm can be assessed.
- Do a sensitivity analysis to include the ballast hardening phenomenon when the granular material is pulverised.
- Explore the use of USP with different stiffness and damping properties.
- If forces acting on the track are of interest, measuring accelerations directly from the structure is a more reliable source than displacements. It is possible to convert displacements into forces, however, information is lost in the transformation process (differentiation).

Appendix A

ANSYS elements

The elements used to define the computational model in Chapter 4 are decribed in this appendix. Where necessary, examples are given to revise the element behaviour.

A-1 BEAM188

The element is based in the Timoshenko beam theory; it is suitable for two-dimensional slender elements. The beam profile can be defined using a IGES file. Longitudinal dimension of the element is given in [*Length*].

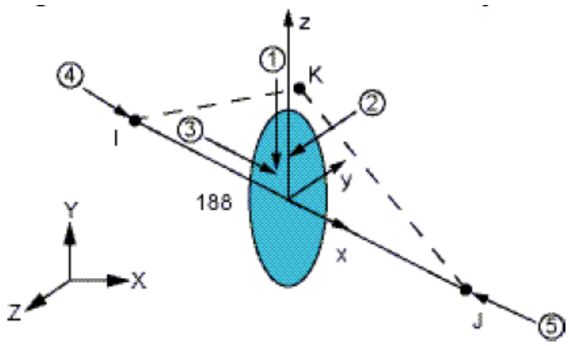

Figure A-1: Element BEAM188 definition

A-1-1 Element verification for BEAM188

A simple static example is performed in ANSYS in order to revise the correct behaviour of element BEAM188. The exercise consists in calculating the vertical displacement (δ) of a cantilever beam of length L, Young's Modulus E and moment of inertia I, loaded with a point

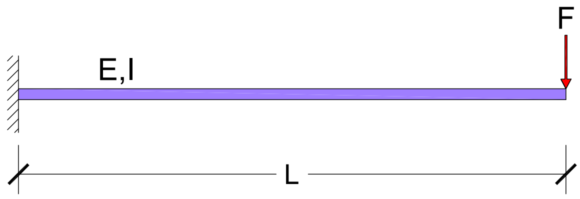

Figure A-2: Cantilever beam

Parameter	Value	Unit
E	2.10×10^{8}	kN/m^2
I	3.04×10^{-5}	m^4
L	5.00	m
F	1.00	kN

Table A-1: Parameters for cantilever beam example

force F at $x = L$ (Figure A-2). The parameters considered for the example are presented in Table A-1.

The vertical displacement is calculated using the well-known deflection equation for cantilever beam (Eq. (A-1)):

$$\delta = \frac{FL^3}{3EI} \tag{A-1}$$

$$\delta = \frac{1.00(5.00)^3}{3(2.10\times10^8)(3.04\times10^{-5})} \tag{A-2}$$

$$\delta = 0.006505m \tag{A-3}$$

The example is modelled in ANSYS using the element BEAM188 and defining the properties previously used (Figure A-3). The maximum vertical displacement calculated by the software is $\delta = 0.006545m$ (Figure A-4). The result from the simulation is equal to the analytical result obtained from Eq. (A-1). Therefore, the element BEAM188 has the expected response.

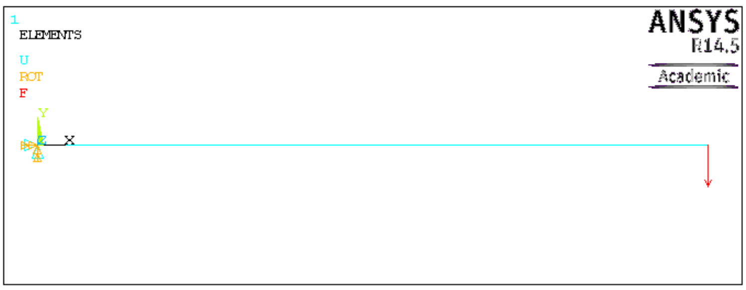

Figure A-3: ANSYS model for cantilever beam

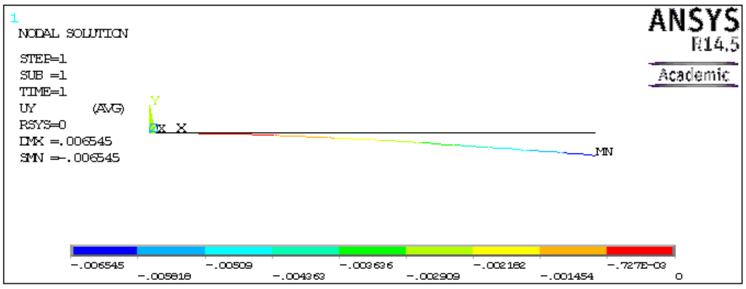

Figure A-4: Static displacement for cantilever beam

A-2 MASS21 and COMBIN14

MASS21 is a lumped element defined by a single node (Figure A-5(a)). The mass unit is given in $[Force * Time^2/Length]$ and can be defined with rotational properties if necessary.

COMBIN14 is a linear spring-damper system defined by two nodes (Figure A-5(b)). Longitudinal stiffness and damping of the element is given by direct parameters during the element definition. The system does not resist bending. Dimensions for stiffness and damping are $[Force/Length]$ and $[Force * Time/Length]$, respectively.

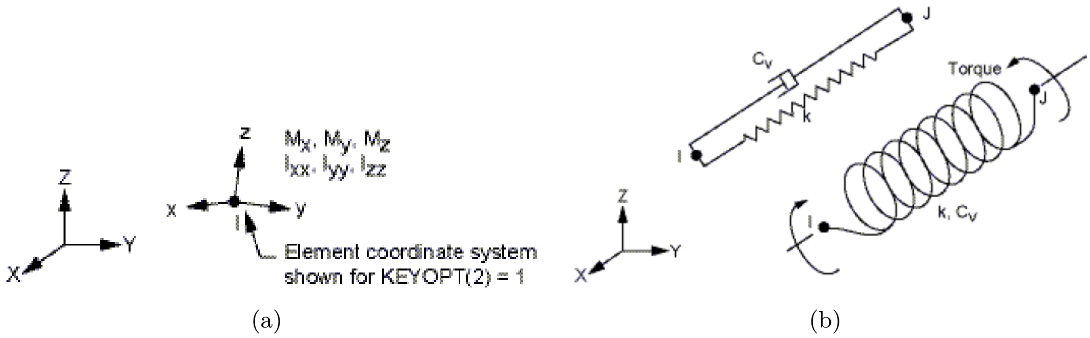

Figure A-5: Definition of MASS21 and COMBIN14

A-2-1 Element verification for MASS21 and COMBIN14

A dynamic analysis is used to verify the mechanical behaviour of MASS21 and COMBIN14 elements. The system used for the analysis is the mass-spring-damper system shown in Figure A-6. The system is excited by a set of initial conditions u_0 and v_0. The parameters to consider in the exercise are resumed in Table A-2.

Firstly, the initial value problem is solved analytically using ordinary differential equations. The equation of motion of the system is defined using the displacement method (Eq. (A-4)).

$$m\ddot{x} + c\dot{x} + kx = 0 \tag{A-4}$$

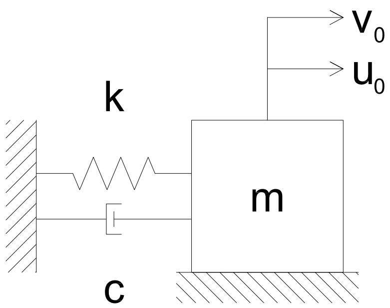

Figure A-6: Mass-spring-damper system

Parameter	Value	Unit
m	1.00	kg
c	1.00	Ns/m
k	100	N/m
u_0	0.01	m
v_0	0.00	m/s

Table A-2: Parameters for mass-spring-damper example

The solution of the equation of motion introduces the natural frequency and the viscous damping of the system.

$$w_n = \sqrt{\frac{k}{m}} \tag{A-5}$$

$$n = \frac{c}{2\,m} \tag{A-6}$$

$$w_1 = \sqrt{w_n^2 - n^2} \tag{A-7}$$

The amplitude and phase angle of the free vibration are given by Eq. (A-8) and Eq. (A-9).

$$A_0 = \sqrt{u_0^2 + \left(\frac{v_0}{w_1} + \frac{n\,u_0}{w_1}\right)^2} \tag{A-8}$$

$$\varphi_0 = \arctan\left(\frac{v_0 + n\,u_0}{u_0\,w_1}\right) \tag{A-9}$$

The time-dependent solution for the displacement of the mass is given by Eq. (A-10).

$$X(t) = A_0\,\exp(-nt)\,\cos(w_1\,t - \varphi_0) \tag{A-10}$$

The solution is dependent of the initial conditions of the mass displacement and velocity. The parameters and the initial conditions presented in Table A-2 are substituted to complete the analytical solution of the problem.

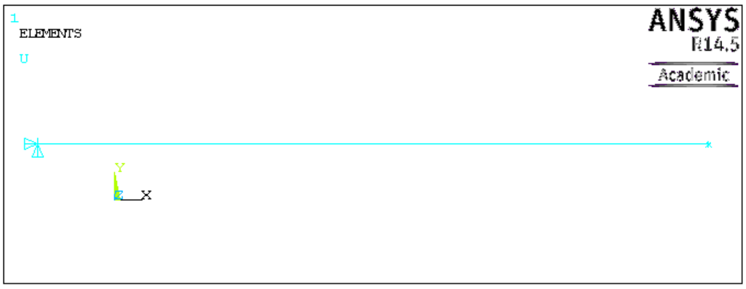

Figure A-7: Mass-spring-damper model in ANSYS

Now, the same initial condition problem is solved using ANSYS. The three elements (mass, spring and damper) are defined using elements MASS21 and COMBIN14. Figure A-7 shows a screenshot of the software GUI with the modelled system.

A transient analysis is run and the time-dependent solution is extracted and processed. In Figure A-8, a graphical comparison of the results obtained from Eq. (A-10) and ANSYS analysis is presented. The response obtained from both methods are virtually equal. Therefore, elements MASS21 and COMBIN14 have the mechanical behaviour sought for the research.

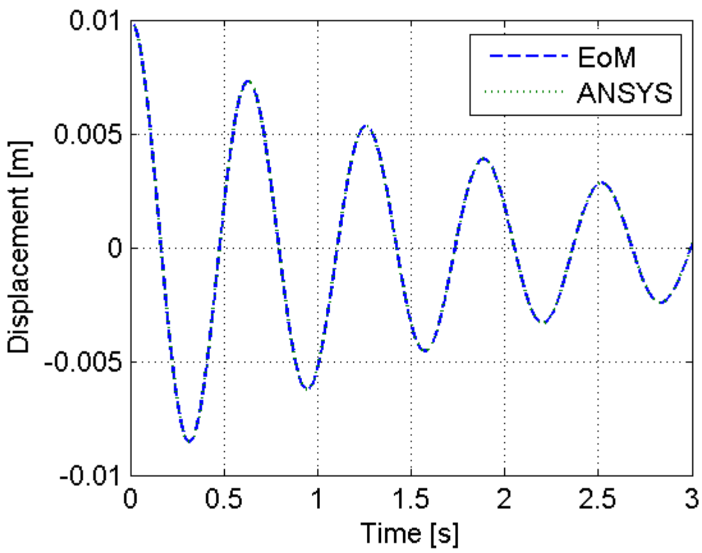

Figure A-8: Histories of displacement for both methods

A-3 COMBIN40

The element description is similar to COMBIN14. It consists of a spring and a dashpoint working between two nodes. However, a *gap* property can be included in the definition of the system to obtain a non-linear behaviour. Dimensions for stiffness and damping remain as in the previous case; the dimension for *gap* is $[Length]$.

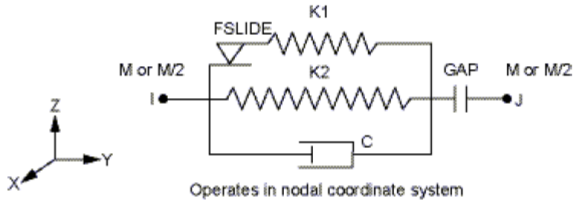

Figure A-9: COMBIN40 definition

A-3-1 Element verification for COMBIN40

To verify the non-linearity of the system, a transient analysis is performed on the model shown in Figure A-10. The model consists of a beam supported by three spring-damper elements. The central support presents a gap at the connection with the beam.

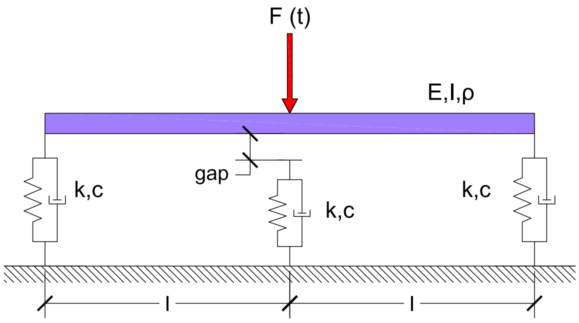

Figure A-10: Beam supported by three elements

The beam is modelled using a BEAM188 element; the supports at the ends are COMBIN14 elements and the central support is defined as a COMBIN40 element. The numerical information used in the model is shown in Table A-3.

Parameter	Value	Unit
l	0.60	m
E	2.10×10^{8}	kN/m^2
I	2.89×10^{-5}	m^4
ρ	7850	kg/m^3
k	1.00	kN/m
c	100	kN/m
gap	0.001	m

Table A-3: Parameters for COMBIN40 verification

A point harmonic load excites the system at the top of the beam. The force is described by Eq. (A-11).

$$F(t) = -100 \sin(\pi t) \tag{A-11}$$

The transient analysis is run using ANSYS. Figure A-11(a) shows the histories of displacement at the center of the beam. The force response of the middle support is shown in Figure A-11(b).

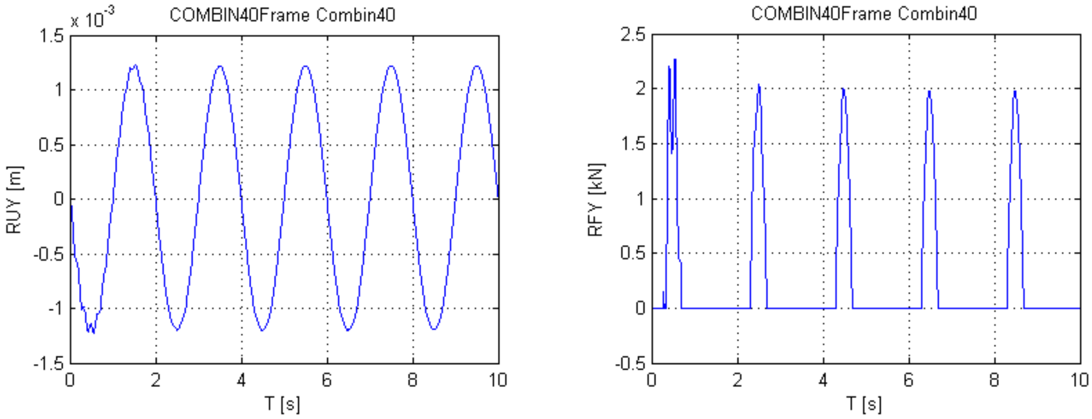

(a) Node displacement (b) Non-linear force response

Figure A-11: Mechanical response for COMBIN40

As expected, the behaviour of element COMBIN40 is nonlinear. When the beam has a displacement larger than the size of the gap ($\delta = 0.001m$), the spring-damper system has a reaction. Otherwise, the element shows no force reaction.

Appendix B

ANSYS Parametric Design Language

ANSYS Parametric Design Language (APDL) is a scripting language used to automate tasks in ANSYS. The language uses parameters to define elements of a model and to perform analysis. The number of commands integrated to the design language is large. The reader is referred to the Help & Documentation section of the computational package for more information.

In this appendix, only the APDL command files used during the modal and harmonic analysis in Chapter 5 are included. The APDL command files of the transient analysis (Chapter 6) are basically identical to the harmonic analysis commands. The difference reside in the definition of the load steps (Appendix C and Appendix E).

B-1 Model creation

The first command file defines the general information of the project, generates the model geometry, defines the structural elements and their properties, meshes the elements and defines boundary conditions and constrains of the model.

```
!==============
!= PREPROCESS =
!==============
*ASK,jbnm,Jobname,'I500modal'
/FILNAME,jbnm,1
/PREP7

!= RAIL =
!========
ET,1,BEAM188
MP,DENS,1,7.85 !density
MP,EX,1,210000000 !E
MP,PRXY,1,0.3 !poisson
```

```
SECTYPE,1,BEAM,MESH,UIC60 !section
SECOFFSET,CENT,,,
SECREAD,'D:\ANSYS\Sections\UIC60','SECT',,MESH

!= SLEEPER =
!===========
ET,2,MASS21
KEYOPT,2,1,0
KEYOPT,2,2,0
KEYOPT,2,3,4
R,1,0.150, !mass

!= PAD =
!=======
ET,3,COMBIN14
KEYOPT,3,1,0
KEYOPT,3,2,0
KEYOPT,3,3,0
R,2,100000,15, , , , , !kp, cp
RMORE, ,

!= BALLAST =
!===========
R,3,27000,12.3, , , , , !kb, cb
RMORE, ,

!= HS1 =
!=======
ET,4,COMBIN40
KEYOPT,4,1,0
KEYOPT,4,3,2
KEYOPT,4,4,0
KEYOPT,4,6,0
R,4,27000,12.3, ,0.001, , , !kb, cb, gap

!================
!= IMPORT MODEL =
!================
/AUX15
IOPTN,IGES,SMOOTH
IOPTN,MERGE,YES
IOPTN,SOLID,YES
IOPTN,SMALL,YES
IOPTM,GTOLER,FILE
IGESIN,'I500','iges','D:\AutoCAD\'
LPLOT

!=====================
!= GENERATE ELEMENTS =
!=====================

!= RAIL =
!========
```

```
LSEL,S,LOC,Y,0.305
/PREP7
TYPE,1
MAT,1
REAL,1
ESYS,0
SECNUM,1
TSHAP,LINE
LESIZE,ALL,0.01, , , ,1, , ,1, !dx
LMESH,ALL
ALLSEL,ALL

!= PAD =
!=======
LSEL,S,LOC,Y,0.301,.304
/PREP7
TYPE,3
MAT,1
REAL,2
ESYS,0
SECNUM,1
TSHAP,LINE
LESIZE,ALL, , ,1, ,1, , ,1,
LMESH,ALL
ALLSEL,ALL
NUMMRG,NODE, , , ,LOW

!= BALLAST =
!===========
LSEL,S,LOC,Y,0,0.3
/PREP7
TYPE,3
MAT,1
REAL,3
ESYS,0
SECNUM,1
TSHAP,LINE
LESIZE,ALL, , ,1, ,1, , ,1,
LMESH,ALL
ALLSEL,ALL
NUMMRG,NODE, , , ,LOW

!= SLEEPER =
!===========
KSEL,S,LOC,Y,0.3
/PREP7
TYPE,2
MAT,1
REAL,1
ESYS,0
SECNUM,1
TSHAP,PILO
KMESH,ALL
```

```
ALLSEL,ALL

!= CONSTRAINTS =
!==============
NSEL,S,LOC,Y,0
D,ALL, , , , , ,ALL, , , , ,
ALLSEL,ALL

NSEL,S,LOC,Y,0.1,0.5
D,ALL, , , , , ,UX,UZ, , , ,
ALLSEL,ALL

!= VIEW =
!========
/VIEW,1,,,1
/ANG,1
/REP,FAST
EPLOT

!========
!= SAVE =
!========
*GET,jbnm,ACTIVE,0,JOBNAM, , ,
SAVE,STRCAT(jbnm,'Mod.db')
FINISH
```

B-2 Analysis and solution

B-2-1 Modal analysis solution

The modal analysis is limited to 1500Hz or the first 1000 vibration modes of the structure. Further description is given in Section 5-1.

```
!============
!= SOLUTION =
!============
/SOLU
ANTYPE,2
MODOPT,LANB,1000
EQSLV,SPAR
MXPAND,1000, , ,0
LUMPM,0
PSTRES,0
MODOPT,LANB,1000,0,1500, ,OFF

/STATUS,SOLU
SOLVE

SAVE,STRCAT(jbnm,'Solfrf.db')
FINISH
```

B-2-2 Harmonic analysis solution

The solution of the harmonic analysis is performed using load step files as described in Section 5-2.

```
!============
!= SOLUTION =
!============
/NERR,200,99999999,,0,5
/SOLU
LSSOLVE,1,3,1,

SAVE,STRCAT(jbnm,'Solfrf.db')
FINISH
```

B-3 Analysis results

The post-process tool included in Analysis System (ANSYS) is used to generate a CSV file. This file contains the time-dependent solution for the rail and the sleeper elements of the model. For each element, the next three variables are extracted:

- Acceleration of the element
- Displacement of the element
- Forces exerted on the element

```
!================
!= READ RESULTS =
!================
/POST26
FILE,jbnm,'rst','.'
/UI,COLL,1
NUMVAR,200
SOLU,191,NCMIT
STORE,MERGE
FILLDATA,191,,,,1,1
REALVAR,191,191

!= Rail UY =
!===========
NSOL,2,122,U,Y,RUY,
STORE,MERGE

!= Rail AY =
!===========
NSOL,3,122,A,Y,RAY,
STORE,MERGE

!= Rail FY =
!===========
FORCE,TOTAL
ESOL,4,243,122,F,Y,RFY,
STORE,MERGE

!= Sleeper UY=
!=============
FORCE,TOTAL
NSOL,5,245,U,Y,SUY,
STORE,MERG

!= Sleeper AY=
!=============
FORCE,TOTAL
NSOL,6,245,A,Y,SAY,
STORE,MERG
```

```
!= Sleeper FY=
!=============
FORCE,TOTAL
ESOL,7,253,245,F,Y,SFY,
STORE,MERGE

!= Ballast FY=
!=============
FORCE,TOTAL
ESOL,8,248,245,F,Y,BFY,
STORE,MERGE

!= TABLE =
!=========
*CREATE,scratch,gui
*DEL,_P26_EXPORT
*DIM,_P26_EXPORT,TABLE,8000,8
VGET,_P26_EXPORT(1,0),1
VGET,_P26_EXPORT(1,1),2
VGET,_P26_EXPORT(1,2),3
VGET,_P26_EXPORT(1,3),4
VGET,_P26_EXPORT(1,4),5
VGET,_P26_EXPORT(1,5),6
VGET,_P26_EXPORT(1,6),7
VGET,_P26_EXPORT(1,7),8

!= CSV FILE =
!============
/OUTPUT,'SE253','csv','.'
*VWRITE,'TIME','RUY','RAY','RFY','SUY','SAY','SFY','BFY'
%C, %C, %C, %C, %C, %C, %C, %C
*VWRITE,_P26_EXPORT(1,0),_P26_EXPORT(1,1),_P26_EXPORT(1,2),_P26_EXPORT(1,3),...
_P26_EXPORT(1,4),_P26_EXPORT(1,5),_P26_EXPORT(1,6),_P26_EXPORT(1,7)
%G, %G, %G, %G, %G, %G, %G, %G
/OUTPUT,TERM
*END
/INPUT,scratch,gui

FINISH
/EXIT,ALL
```

Appendix C

Load steps for harmonic analysis

In Chapter 5, the harmonic analysis is performed using a series of load steps Figure C-1. In this appendix, the script files for those load steps are reported.

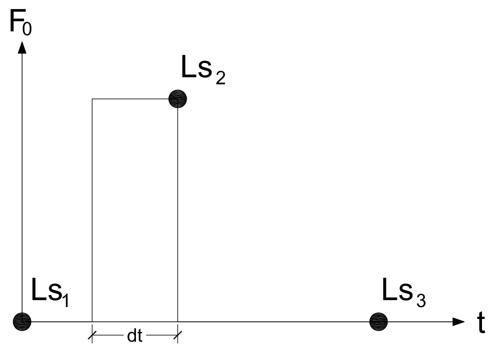

Figure C-1: Load step for harmonic analysis

C-1 Load step 1

```
/COM,ANSYS RELEASE 14.5    UP20120918       18:44:00    02/08/2014
/NOPR
/TITLE,
_LSNUM=      1
ANTYPE, 4
TRNOPT,FULL,,DAMP
TREF,  0.00000000
IRLF,  0
BFUNIF,TEMP,_TINY
ACEL,  0.00000000    ,  0.00000000    ,  0.00000000
OMEGA,  0.00000000    ,  0.00000000    ,  0.00000000
DOMEGA,  0.00000000    ,  0.00000000    ,  0.00000000
```

```
CGLOC,  0.00000000     ,  0.00000000     ,  0.00000000
CGOMEGA,  0.00000000     ,  0.00000000     ,  0.00000000
DCGOMG,  0.00000000     ,  0.00000000     ,  0.00000000

DELTIM, 5.000000000E-04,  0.00000000     ,  0.00000000     ,
KUSE,      0
TIME, 5.000000000E-04
ALPHAD,  0.00000000
BETAD,  0.00000000
DMPRAT,  0.00000000
TIMINT,ON  ,STRU
TINTP,R8.1, 5.000000000E-03,,,
TINTP,R8.1, -1.00000000     , 0.500000000     , -1.00000000     ,,,,
TINTP,R8.1, 5.000000000E-03,  0.00000000

CRPLIM, 0.100000000     ,   0
CRPLIM,  0.00000000     ,   1
NCNV,     1,  0.00000000     ,     0,  0.00000000     ,  0.00000000

NEQIT,     0
ERESX,DEFA
OUTRES, ALL, ALL,
D,    250,UX  ,  0.00000000     ,  0.00000000
D,    250,UY  ,  0.00000000     ,  0.00000000
D,    250,UZ  ,  0.00000000     ,  0.00000000
D,    250,ROTX,  0.00000000     ,  0.00000000
D,    250,ROTY,  0.00000000     ,  0.00000000
D,    250,ROTZ,  0.00000000     ,  0.00000000
D,    251,UX  ,  0.00000000     ,  0.00000000
D,    251,UY  ,  0.00000000     ,  0.00000000
D,    251,UZ  ,  0.00000000     ,  0.00000000
D,    251,ROTX,  0.00000000     ,  0.00000000
D,    251,ROTY,  0.00000000     ,  0.00000000
D,    251,ROTZ,  0.00000000     ,  0.00000000
D,    252,UX  ,  0.00000000     ,  0.00000000
D,    252,UY  ,  0.00000000     ,  0.00000000
D,    252,UZ  ,  0.00000000     ,  0.00000000
D,    252,ROTX,  0.00000000     ,  0.00000000
D,    252,ROTY,  0.00000000     ,  0.00000000
D,    252,ROTZ,  0.00000000     ,  0.00000000
D,    253,UX  ,  0.00000000     ,  0.00000000
D,    253,UY  ,  0.00000000     ,  0.00000000
D,    253,UZ  ,  0.00000000     ,  0.00000000
D,    253,ROTX,  0.00000000     ,  0.00000000
D,    253,ROTY,  0.00000000     ,  0.00000000
D,    253,ROTZ,  0.00000000     ,  0.00000000
D,    254,UX  ,  0.00000000     ,  0.00000000
D,    254,UY  ,  0.00000000     ,  0.00000000
D,    254,UZ  ,  0.00000000     ,  0.00000000
D,    254,ROTX,  0.00000000     ,  0.00000000
D,    254,ROTY,  0.00000000     ,  0.00000000
D,    254,ROTZ,  0.00000000     ,  0.00000000
/GOPR
```

C-2 Load step 2

```
/COM,ANSYS RELEASE 14.5    UP20120918       18:46:38    02/08/2014
/NOPR
/TITLE,
_LSNUM=      2
ANTYPE, 4
TRNOPT,FULL,,DAMP
TREF,  0.00000000
IRLF,  0
BFUNIF,TEMP,_TINY
ACEL,  0.00000000    ,  0.00000000    ,  0.00000000
OMEGA,  0.00000000    ,  0.00000000    ,  0.00000000
DOMEGA,  0.00000000    ,  0.00000000    ,  0.00000000
CGLOC,  0.00000000    ,  0.00000000    ,  0.00000000
CGOMEGA,  0.00000000    ,  0.00000000    ,  0.00000000
DCGOMG,  0.00000000    ,  0.00000000    ,  0.00000000

DELTIM, 5.000000000E-04,  0.00000000    ,  0.00000000    ,
KUSE,     0
TIME, 1.000000000E-03
ALPHAD,  0.00000000
BETAD,  0.00000000
DMPRAT,  0.00000000
TIMINT,ON  ,STRU
TINTP,R8.1, 5.000000000E-03,,,
TINTP,R8.1, -1.00000000    , 0.500000000    , -1.00000000    ,,,,
TINTP,R8.1, 5.000000000E-03,  0.00000000

CRPLIM, 0.100000000    ,   0
CRPLIM,  0.00000000    ,   1
NCNV,     1,  0.00000000    ,     0,  0.00000000    ,  0.00000000

NEQIT,     0

ERESX,DEFA
OUTRES, ALL, ALL,

D,     250,UX  ,  0.00000000    ,  0.00000000
D,     250,UY  ,  0.00000000    ,  0.00000000
D,     250,UZ  ,  0.00000000    ,  0.00000000
D,     250,ROTX,  0.00000000    ,  0.00000000
D,     250,ROTY,  0.00000000    ,  0.00000000
D,     250,ROTZ,  0.00000000    ,  0.00000000
D,     251,UX  ,  0.00000000    ,  0.00000000
D,     251,UY  ,  0.00000000    ,  0.00000000
D,     251,UZ  ,  0.00000000    ,  0.00000000
D,     251,ROTX,  0.00000000    ,  0.00000000
D,     251,ROTY,  0.00000000    ,  0.00000000
D,     251,ROTZ,  0.00000000    ,  0.00000000
D,     252,UX  ,  0.00000000    ,  0.00000000
D,     252,UY  ,  0.00000000    ,  0.00000000
```

```
D,     252,UZ  ,  0.00000000    ,  0.00000000
D,     252,ROTX,  0.00000000    ,  0.00000000
D,     252,ROTY,  0.00000000    ,  0.00000000
D,     252,ROTZ,  0.00000000    ,  0.00000000
D,     253,UX  ,  0.00000000    ,  0.00000000
D,     253,UY  ,  0.00000000    ,  0.00000000
D,     253,UZ  ,  0.00000000    ,  0.00000000
D,     253,ROTX,  0.00000000    ,  0.00000000
D,     253,ROTY,  0.00000000    ,  0.00000000
D,     253,ROTZ,  0.00000000    ,  0.00000000
D,     254,UX  ,  0.00000000    ,  0.00000000
D,     254,UY  ,  0.00000000    ,  0.00000000
D,     254,UZ  ,  0.00000000    ,  0.00000000
D,     254,ROTX,  0.00000000    ,  0.00000000
D,     254,ROTY,  0.00000000    ,  0.00000000
D,     254,ROTZ,  0.00000000    ,  0.00000000
F,      92,FY  , -60.0000000    ,  0.00000000
/GOPR
```

C-3 Load step 3

```
/COM,ANSYS RELEASE 14.5    UP20120918       18:48:04    02/08/2014
/NOPR
/TITLE,
_LSNUM=      3
ANTYPE, 4
TRNOPT,FULL,,DAMP
TREF,  0.00000000
IRLF,  0
BFUNIF,TEMP,_TINY
ACEL,  0.00000000    ,  0.00000000    ,  0.00000000
OMEGA,  0.00000000    ,  0.00000000    ,  0.00000000
DOMEGA,  0.00000000    ,  0.00000000    ,  0.00000000
CGLOC,  0.00000000    ,  0.00000000    ,  0.00000000
CGOMEGA,  0.00000000    ,  0.00000000    ,  0.00000000
DCGOMG,  0.00000000    ,  0.00000000    ,  0.00000000

DELTIM, 5.000000000E-04,  0.00000000    ,  0.00000000    ,
KUSE,     0
TIME,  5.00000000
ALPHAD,  0.00000000
BETAD,  0.00000000
DMPRAT,  0.00000000
TIMINT,ON  ,STRU
TINTP,R8.1, 5.000000000E-03,,,
TINTP,R8.1, -1.00000000    , 0.500000000    , -1.00000000    ,,,,
TINTP,R8.1, 5.000000000E-03,  0.00000000

CRPLIM, 0.100000000    ,   0
CRPLIM,  0.00000000    ,   1
NCNV,     1,  0.00000000    ,     0,  0.00000000    ,  0.00000000

NEQIT,     0

ERESX,DEFA
OUTRES, ALL, ALL,

D,     250,UX  ,  0.00000000    ,  0.00000000
D,     250,UY  ,  0.00000000    ,  0.00000000
D,     250,UZ  ,  0.00000000    ,  0.00000000
D,     250,ROTX,  0.00000000    ,  0.00000000
D,     250,ROTY,  0.00000000    ,  0.00000000
D,     250,ROTZ,  0.00000000    ,  0.00000000
D,     251,UX  ,  0.00000000    ,  0.00000000
D,     251,UY  ,  0.00000000    ,  0.00000000
D,     251,UZ  ,  0.00000000    ,  0.00000000
D,     251,ROTX,  0.00000000    ,  0.00000000
D,     251,ROTY,  0.00000000    ,  0.00000000
D,     251,ROTZ,  0.00000000    ,  0.00000000
D,     252,UX  ,  0.00000000    ,  0.00000000
D,     252,UY  ,  0.00000000    ,  0.00000000
```

```
D,     252,UZ  ,  0.00000000    ,  0.00000000
D,     252,ROTX,  0.00000000    ,  0.00000000
D,     252,ROTY,  0.00000000    ,  0.00000000
D,     252,ROTZ,  0.00000000    ,  0.00000000
D,     253,UX  ,  0.00000000    ,  0.00000000
D,     253,UY  ,  0.00000000    ,  0.00000000
D,     253,UZ  ,  0.00000000    ,  0.00000000
D,     253,ROTX,  0.00000000    ,  0.00000000
D,     253,ROTY,  0.00000000    ,  0.00000000
D,     253,ROTZ,  0.00000000    ,  0.00000000
D,     254,UX  ,  0.00000000    ,  0.00000000
D,     254,UY  ,  0.00000000    ,  0.00000000
D,     254,UZ  ,  0.00000000    ,  0.00000000
D,     254,ROTX,  0.00000000    ,  0.00000000
D,     254,ROTY,  0.00000000    ,  0.00000000
D,     254,ROTZ,  0.00000000    ,  0.00000000
/GOPR
```

Appendix D

DARTS

Dynamic Analysis of Rail Track Systems (DARTS) is a software designed for the structural analysis of a rail track on elastic foundation [7]. The software is capable of analysing different railway track structures, e.g. ballasted track and slab track. DARTS can perform dynamic analysis on large models, however, the computational tool is limited to 2-D structures and the transient analysis must remain lineal.

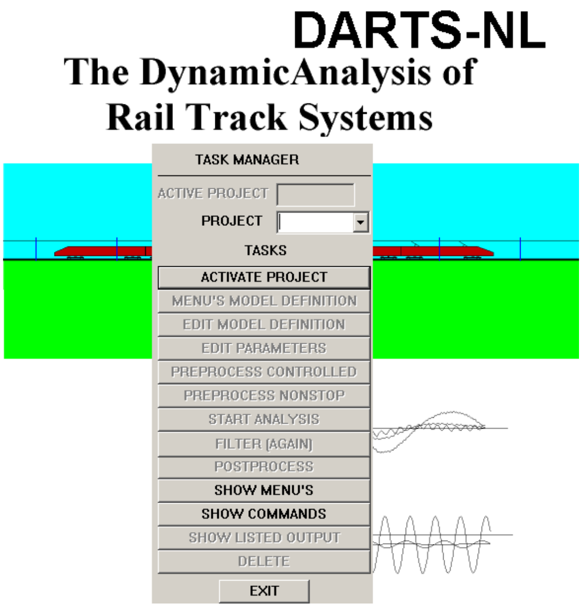

Figure D-1: DARTS GUI

D-1 Wheel-rail force

DARTS is used in the research to calculate the time-dependent forces that a moving vehicle generates while running over a railway structure. The histories of wheel-rail forces are later applied to the ANSYS model in Chapter 6 during the transient analysis.

Two simulations are completed according to the study cases described in Section 6-1. In the first simulation, a vehicle runs over a rail with perfect rolling surface. In the second simulation, a weld is present in the rail and thus the rolling surface no longer remains perfect. In this appendix, overview of both simulations is included.

D-2 Moving vehicle

The vehicle used in the simulation is a single car locomotive with two bogies and two axles per bogie, i.e. four wheels per rail. In Figure D-2, the geometry of the vehicle is shown. The mechanical properties of the vehicle and its components are presented in Table D-1. The velocity of the locomotive is fixed to $v = 30m/s$, operational velocity of most tracks in The Netherlands.

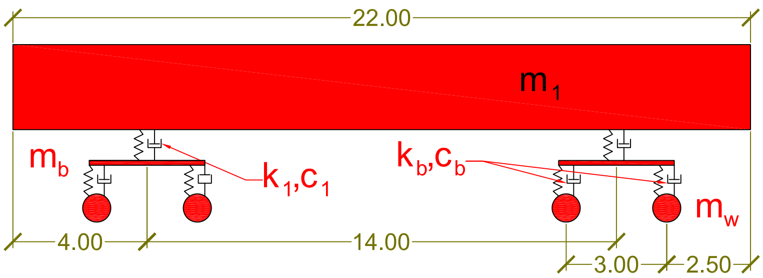

Figure D-2: Moving vehicle Locomotive

Parameter	Value	Unit
m_1	54.15	kN
m_b	2.80	kN
m_w	1.03	kN
k_1	600.00	kN/m
c_1	4.00	kNs/m
k_b	1150.00	kN/m
c_b	2.50	kNs/m

Table D-1: Mechanical properties for locomotive

D-3 Perfect rolling surface

The vehicle runs over a straight rail profile, no discontinuities are found over the length of the rail. The resulting wheel-rail time-dependent force exerted by the first wheel is plotted in Figure D-3. Even though the rolling surface has no irregularities, the presence of discrete supports (sleepers) produce fluctuations.

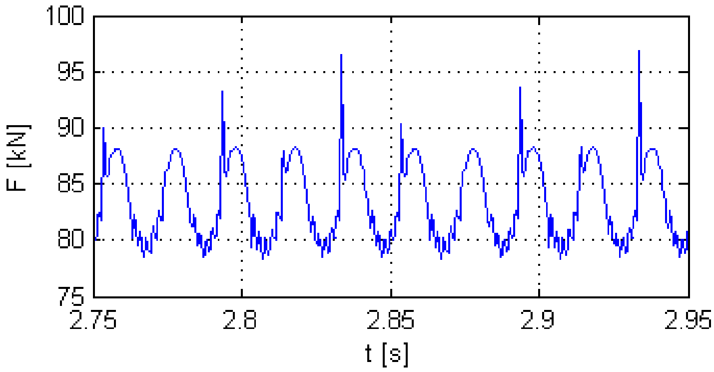

Figure D-3: Wheel-rail force on perfect rolling surface

The histories of forces are recorded and used for the transient analysis in Chapter 6. A force signal is obtained for each wheel of the vehicle and are processed separately.

D-4 Weld in rail surface

The second simulation run in DARTS is performed over a rail that has a weld. The rail profile is not perfectly straight; the surface of the rail presents irregularities.

The profile shown in Figure D-4 is 1.00m of a CWR after being welded and ground (Section 3-3-2). The weld is inserted in the model and the simulation is run as in the previous step.

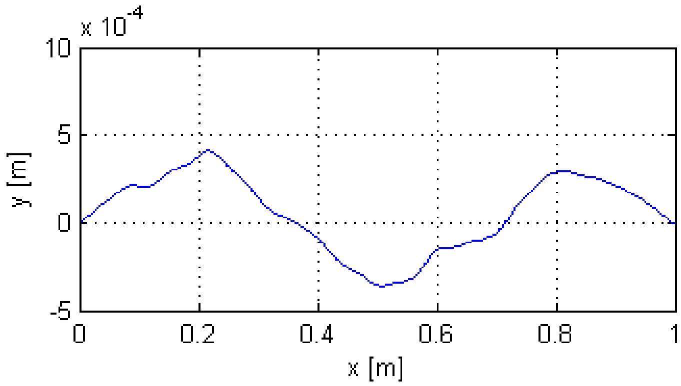

Figure D-4: Profile of weld in the rail

In Figure D-5, the time-dependent wheel-rail force of the first wheel is shown. The dynamic amplification due to the irregularities of the rail is clearly observed close to the t=2.80s mark. For each wheel, the force signal is recorded and processed to be used in the transient analysis.

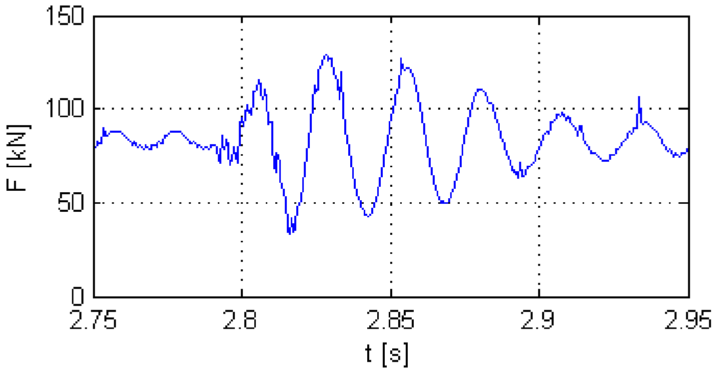

Figure D-5: Wheel-rail force on rail with weld

D-5 DARTS command file

Similar to the APDL command files, DARTS generates and solves the computational models using a simple TXT file. The command file used in the simulations of DARTS is provided in this section. The same command file is used for both simulations previously described. The only difference remains in loading the surface file that contains the weld profile: "`surface file 'weldaog' X=100 scale=1.0`".

```
RAIL 'J500'
UNIT Mete KN
BOTT LAYE BED

GENERATE CLASSIC TRACK SPACING=0.60 SLEEPER=0.30 /
BRIDGE=5 REPEAT 334
$BOUN COND on

RAIL PROP 'UIC-60'
RAIL PAD KFY=100000 CFY=15
SLEEPER MASS=0.150 WIDE=0.30
SPRING PROP K=27000 C=12.3

SURFACE FILE 'weldaog' X=100 scale=1.0
MOVI TRAI 'loco' velocity=30.0 offset=0.0
INT u=7.0 by=0.00033
ARTI DAMP rail=1. hertz=1.
FREQUENCIES LIMIT=2000.

FINISH
```

Appendix E

Load steps for transient analysis

In Chapter 6, a transient analysis is completed using a large number of load steps. The number of load steps required to performed the analysis exceeded the 3000 files. Thus, in this appendix only one load step file is presented.

The value of `TIME` and the four point forces `F` defined at the end of the file are the variables that change for each load step. For each value of `TIME`, the position and magnitude of `F` change.

```
/COM,ANSYS RELEASE 14.5    UP20120918       12:34:56    04/25/2009
/NOPR
/TITLE,
_LSNUM=2
ANTYPE, 4
TRNOPT,FULL,,DAMP
KBC,     0
TREF,  0.00000000
IRLF,  0
BFUNIF,TEMP,_TINY
ACEL,  0.00000000    ,  0.00000000    ,  0.00000000
OMEGA,  0.00000000    ,  0.00000000    ,  0.00000000
DOMEGA,  0.00000000    ,  0.00000000    ,  0.00000000
CGLOC,  0.00000000    ,  0.00000000    ,  0.00000000
CGOMEGA,  0.00000000    ,  0.00000000    ,  0.00000000
DCGOMG,  0.00000000    ,  0.00000000    ,  0.00000000

NSUBST,         1,         0,         0,
KUSE,     0
TIME,0.000660000
ALPHAD,  0.00000000
BETAD,  0.00000000
DMPRAT,  0.00000000
TIMINT,ON  ,STRU
TINTP,R8.1, 5.000000000E-03,,,
```

```
TINTP,R8.1, -1.00000000    , 0.500000000    , -1.00000000    ,,,,
TINTP,R8.1, 5.000000000E-03,  0.00000000

CRPLIM, 0.100000000    ,   0
CRPLIM,  0.00000000    ,   1
NCNV,     1,  0.00000000    ,     0,  0.00000000    ,  0.00000000

NEQIT,     0

ERESX,DEFA
OUTRES, ALL,LAST,
D,    250,UX  ,  0.00000000    ,  0.00000000
D,    250,UY  ,  0.00000000    ,  0.00000000
D,    250,UZ  ,  0.00000000    ,  0.00000000
D,    250,ROTX,  0.00000000    ,  0.00000000
D,    250,ROTY,  0.00000000    ,  0.00000000
D,    250,ROTZ,  0.00000000    ,  0.00000000
D,    251,UX  ,  0.00000000    ,  0.00000000
D,    251,UY  ,  0.00000000    ,  0.00000000
D,    251,UZ  ,  0.00000000    ,  0.00000000
D,    251,ROTX,  0.00000000    ,  0.00000000
D,    251,ROTY,  0.00000000    ,  0.00000000
D,    251,ROTZ,  0.00000000    ,  0.00000000
D,    252,UX  ,  0.00000000    ,  0.00000000
D,    252,UY  ,  0.00000000    ,  0.00000000
D,    252,UZ  ,  0.00000000    ,  0.00000000
D,    252,ROTX,  0.00000000    ,  0.00000000
D,    252,ROTY,  0.00000000    ,  0.00000000
D,    252,ROTZ,  0.00000000    ,  0.00000000
D,    253,UX  ,  0.00000000    ,  0.00000000
D,    253,UY  ,  0.00000000    ,  0.00000000
D,    253,UZ  ,  0.00000000    ,  0.00000000
D,    253,ROTX,  0.00000000    ,  0.00000000
D,    253,ROTY,  0.00000000    ,  0.00000000
D,    253,ROTZ,  0.00000000    ,  0.00000000
D,    254,UX  ,  0.00000000    ,  0.00000000
D,    254,UY  ,  0.00000000    ,  0.00000000
D,    254,UZ  ,  0.00000000    ,  0.00000000
D,    254,ROTX,  0.00000000    ,  0.00000000
D,    254,ROTY,  0.00000000    ,  0.00000000
D,    254,ROTZ,  0.00000000    ,  0.00000000
F,3,FY  , -73.812,  0.00000000
F,1,FY  , -0,  0.00000000
F,1,FY  , -0,  0.00000000
F,1,FY  , -0,  0.00000000
/GOPR
```

Appendix F

ESAH-M data post-processing

F-1 Binary to decimal

The data obtained from ESAH-M hardware is heavily packed in a DAT file. The file consists of an ASCII part and a Binary part that must be processed in order to access the information.

Matlab is used to perform such task due to the capability of working with binary information and converting the recorded signal into decimal representation. The numerical process to complete the conversion from binary to decimal is not included. Nevertheless, the Matlab routine written specifically for the task is presented in Appendix G.

The raw data from the device includes the triaxial acceleration signals and the vertical displacement of the sleeper.

F-2 Filtering the signal

During field tests, the recorded samples are subjected to environment conditions which are not controlled as those in laboratory tests. Small variation in the data recording is expected in the form of noise.

Noise is considered as a recognised random error that occurs during the recording of measurements in an experiment [18]. This error can be observed as small fluctuations of the signal as shown in Figure F-1.

The presence of noise in a signal alters the results generated while processing the data. It is desired to kept the analysis error to a minimum; therefore, the noise in the signal must be filtered. Two methods are considered for the task:

1. Moving Average Filter (MAF)
2. Band-Pass Filter (BPF)

The methods are described and compared using the concept of Signal to Noise Ratio (SNR).

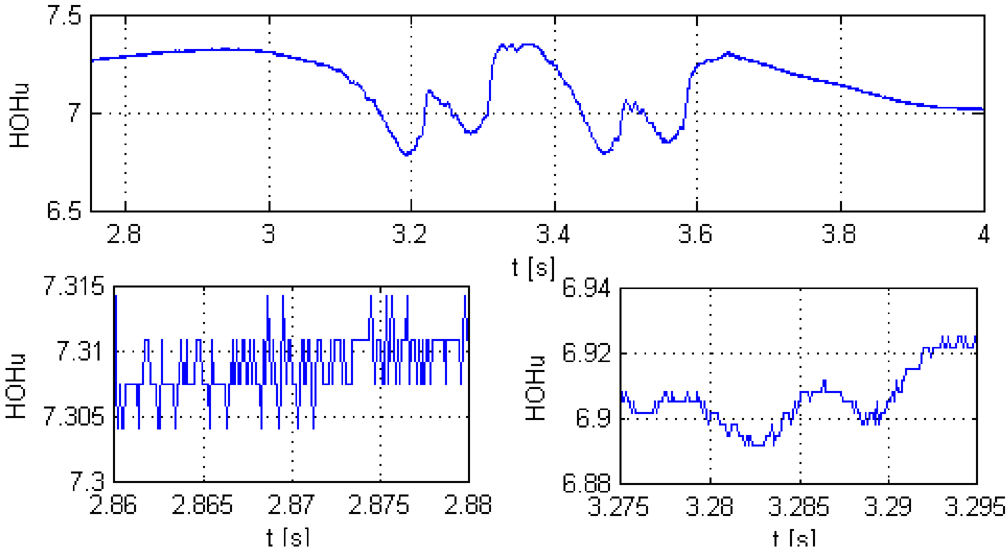

Figure F-1: Example of signal with noise

F-2-1 Signal to Noise Ratio

The Signal to Noise Ratio (SNR) is the ratio of the signal power σ_s^2 and noise power $A^2\sigma_n^2$ [2], defined in decibels (dB):

$$SNR = 10\,log\left(\frac{\sigma_s^2}{A^2\sigma_n^2}\right)[dB] \tag{F-1}$$

A signal with a ratio larger than 1.0 contains less noise and thus the quality of the recorded data is better. The library of MATLAB contains a function (**snr**) that performs the numerical operation for a selected data vector. For this research, a method with larger SNR is preferred; however, special attention must be paid to average loss of information during the filtering process.

Average loss of information ($\left|\bar{\Delta}\right|$) is the absolute mean value of the difference between original data and filtered value. A loss is calculated for each point of the vector and a mean value is obtained from this information.

$$\left|\bar{\Delta}\right| = \left|\frac{\sum_{i=1}^{n} Data_{original}(i) - Data_{filtered}(i)}{n}\right| \tag{F-2}$$

The aforementioned filtering methods are compared using the SNR and $\left|\bar{\Delta}\right|$ indicators. From the comparison, a method is selected and used to process the field measurements.

F-2-2 Method 1: Moving Average Filter

The Moving Average Filter (MAF) is a FIR filter that replaces a signal value by an average of its neighbouring values [2]. When using this method, the sharp peaks of the original signal are dimmed resulting in a smoother signal.

For this method, MATLAB contains the **smooth** function in the software's library. The function uses a MAF to rewrite a data vector into a filtered signal [16]. The number of points to consider for the mathematical operation is defined by the user.

For instance, if the number of points used in the calculation is five ($L = 5$), the algebraic operation can be written as [16]:

$$YY_k = \frac{Y_{k-2} + Y_{k-1} + Y_k + Y_{k+1} + Y_{k+2}}{L} \tag{F-3}$$

The operation is repeated for each point in the data vector. The function can be applied several times on a given vector for smoother results. However, increasing the smooth factor of the filter function reduces the presence of short wavelength signal (decrement of their amplitude).

Figure F-2 shows an example of a noisy signal being filtered using the **smooth** function fifty times. The smoothed signal does not present fluctuations, however, the loss of information is largely perceptible.

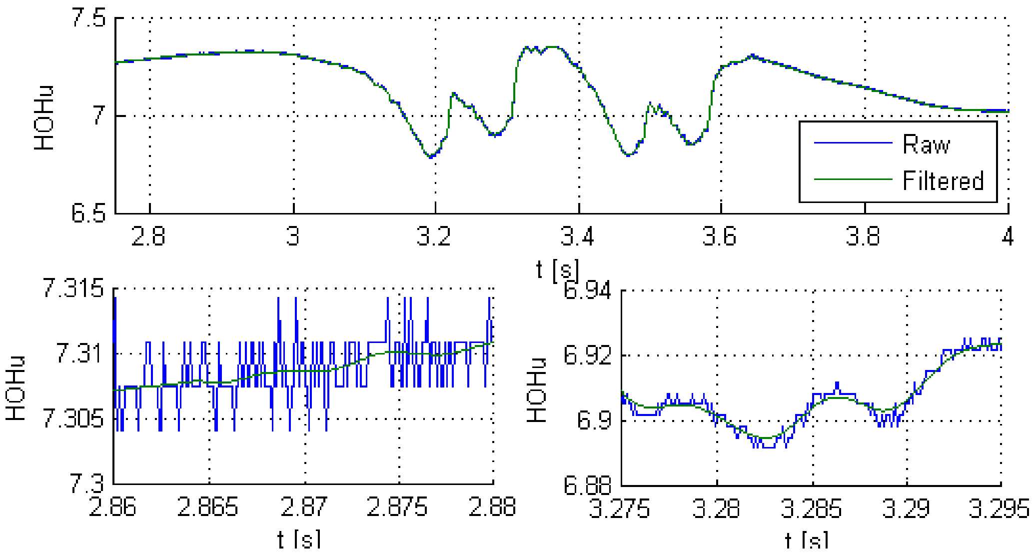

Figure F-2: Effect of smoothing the signal

F-2-3 Method 2: Band-Pass Filter

The Band-Pass Filter (BPF) is a filtering method that amplifies or attenuates selected frequency components of a signal [19]. To carry out a BPF a transformation of the data from time-domain into frequency-domain is performed using Fast Fourier Transform (FFT). The frequency range that is not desired (filtered frequencies) is set to zero. The frequency-domain data is returned to time-domain by executing an Inverse Fast Fourier Transform (IFFT).

The example given in Figure F-3 shows the raw data obtained from ESAH-M device (Figure F-3(a)), the signal is transformed to frequency domain (Figure F-3(b)), a BPF applied between frequencies f_1 and f_2 (Figure F-3(c)) and the signal transformed back to time domain (Figure F-3(d)).

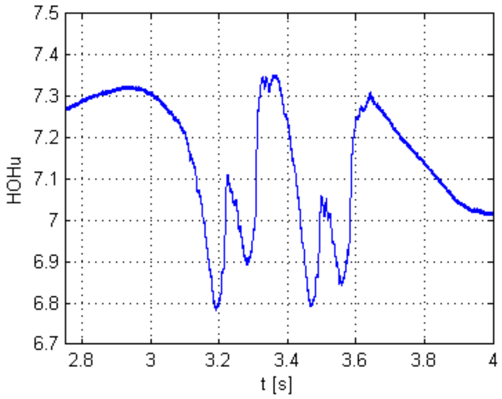

(a) Noisy signal in time domain

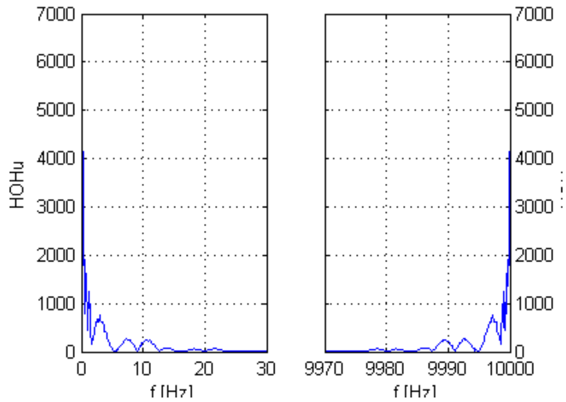

(b) Data in frequency domain

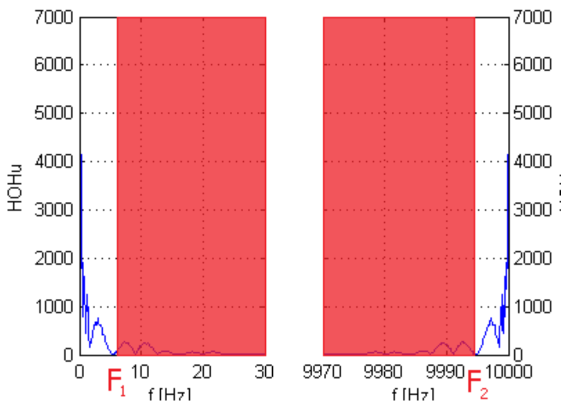

(c) Band Pass Filter

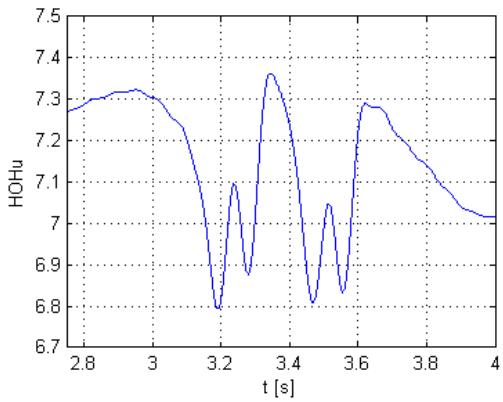

(d) Filtered signal in time domain

Figure F-3: Example of BPF application

MATLAB is the chosen computational tool to aid the numerical operation. The library of the software includes FFT and IFFT functions: **fft** and **ifft** respectively. The input for the **fft** function is the original data in time-domain. For the **ifft** function, the input is the frequency-domain data after being filtered.

The filtered signal in time-domain shows a modification in the amplitude and a delay of the response if the filter has a band-pass that includes frequencies close to the extremes (Figure F-4). As mention in [4]: *"There is a trade-off between the smoothing of the transient (attenuation of the noise) and the modification: the higher the attenuation, the more sever* *the modification."*

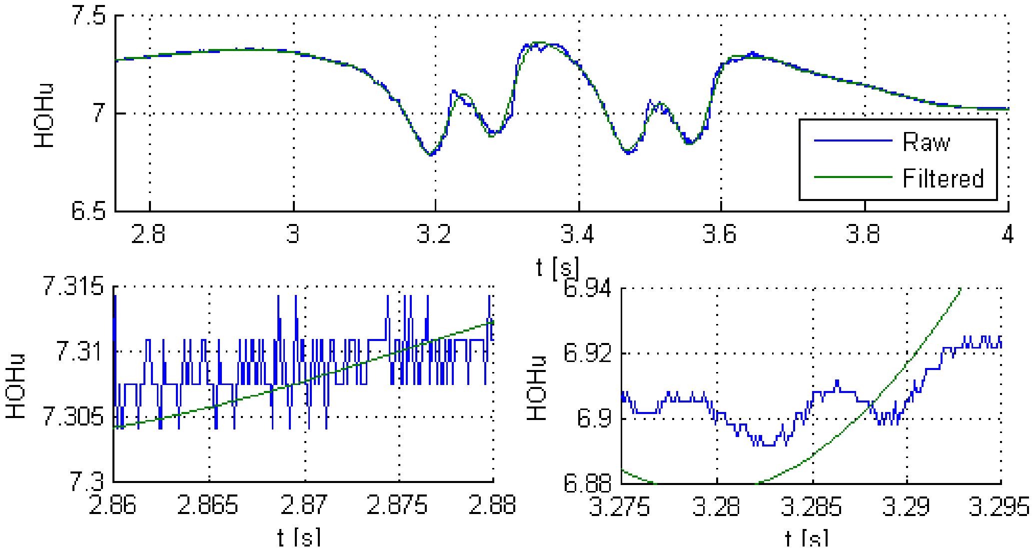

Figure F-4: Modification of signal after applying a BPF

F-2-4 Filtering method comparison

Method 1 revision

The method prompts the user to define the next two parameters:

Span
The number of points to be considered in the average calculation (Eq. (F-3)).

Repeat
The number of times to apply the **smooth** function to the signal.

Figure F-5 shows how the SNR and the $\left|\bar{\Delta}\right|$ vary for different values of *Span* and *Repeat*. Certainly, a better SNR is obtained when the *Span* and *Repeat* parameters are increased. However, the $\left|\bar{\Delta}\right|$ increases as well and with a steeper shape than the SNR. Along with this, the SNR reaches a limit value for large values of *Span* and *Repeat*.

No optimal *Span* or *Repeat* parameter is given in revised literature. On the other hand, most of the authors in the DSP study field leave to the researcher the task to choose those parameters according to the circumstances of the study.

In order to assure that the signal is properly filtered but the loss of information is not considerable, the proposed factor [Span, Repeat] is:

$$factor = [10, 20] \tag{F-4}$$

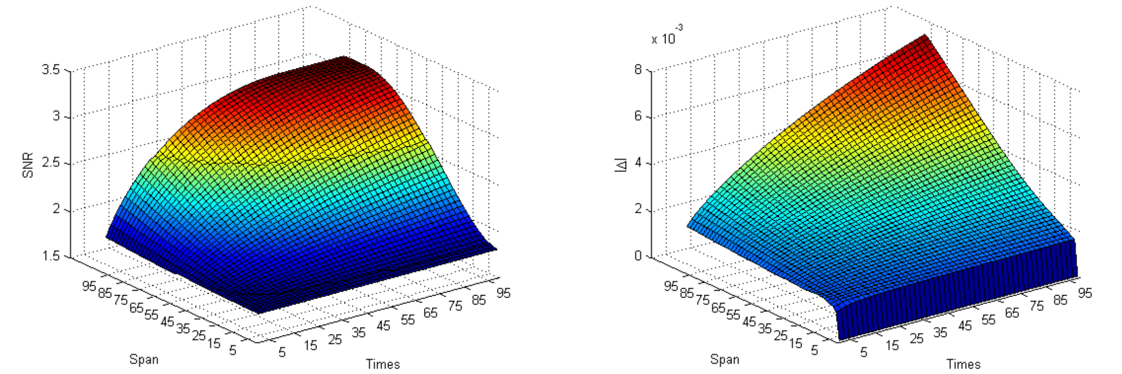

(a) Signal to Noise Ratio

(b) Average Loss of Information

Figure F-5: Effect of Span and Times variation

The average execution time for the **smooth** function, including loading and saving results, is 3.707838 seconds.

Method 2 revision

Similar approach is done for the second filtering method. Figure F-6 shows the effect of narrowing or widening the band of frequencies removed from the signal (f_1 and f_2 in Figure F-3(c)).

The SNR increases as the band widens and so does $\left|\bar{\Delta}\right|$. However, compared to the MAF method, the BPF is unable to reach large SNR values.

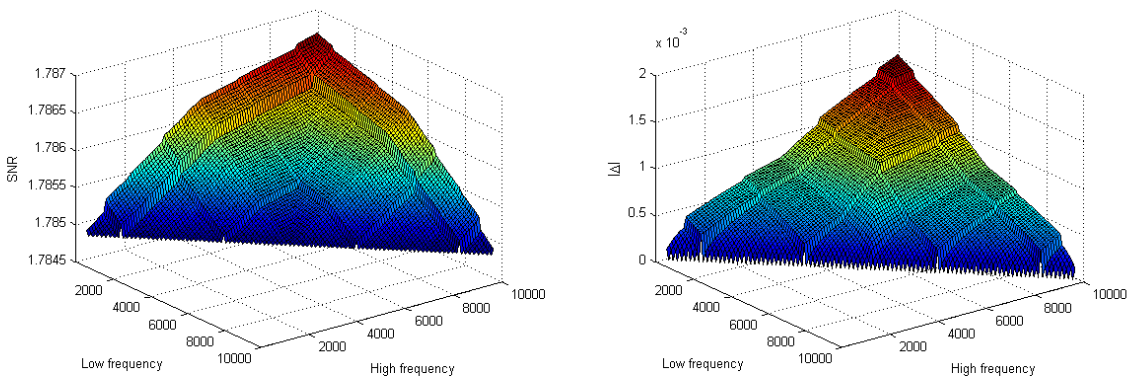

(a) Signal to Noise Ratio

(b) Average Loss of Information

Figure F-6: Effect of Low and High Frequency Band-Pass variation

The execution time for this method is in average 3.804053 seconds.

Method selection

The MAF method is preferred for better SNR performance, along with simplicity and speed in its execution. Therefore, this method is used to process all the field data generated by ESAH-M instrument.

F-3 Displacement to acceleration transformation

The data generated by the ESAH-M device is displacement of the sleeper in time-domain. The displacement vector is transformed to acceleration in order to obtain information regarding inertial forces in the system. The transformation from displacement to acceleration is performed following the calculus principle of the derivative.

F-3-1 Double derivative

From elemental calculus, it is known that the second derivative of a distance vector is the acceleration. Naturally, the most straightforward and reliable method to transform the displacement signal is by performing a double derivation of the data vector.

$$a = \frac{dv}{dt} = \frac{d^2u}{dt^2} \tag{F-5}$$

MATLAB function **diff** calculates differences between adjacent elements of a vector [16]. Using this tool, it is rather simple to convert the displacement vector into acceleration (Figure F-7).

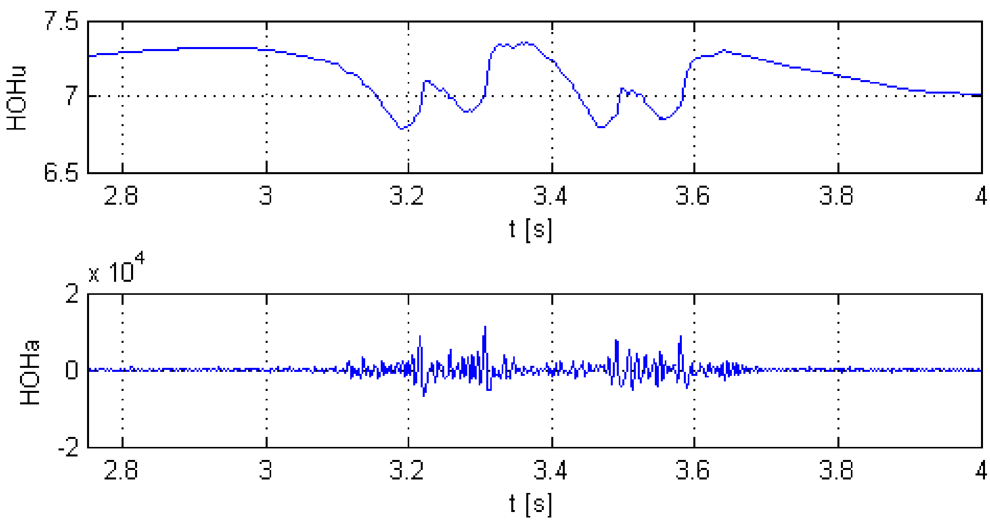

Figure F-7: Transformation of displacement to acceleration

Appendix G

Matlab functions

The Matlab functions developed during the research for different tasks are included in this appendix. The functions are organised according to the stage of the research where they were used.

Several functions were created to aid the pre-processing and post-processing of the modelling and simulations performed in ANSYS. Likewise, all data obtained from ESAH-M system was processed using Matlab.

G-1 ANSYS

G-1-1 Pre-process functions

This section contains the Matlab function *AnsysLSWeld* created for the pre-process of the ANSYS model used during the research. The function generates a set of APDL files (TXT extension) that contain the load steps applied to the computational model (Chapter 6).

AnsysLSWeld

```
function AnsysLSWeld
%AnsysLSWeld
%  Generates a set of Load Steps to be read in ANSYS. The files created
    are
%  a simple .TXT file with an extension according to the LS (Jobname.SXX)
    .
%  The Load steps uses previous information from DARTS to define the
%  wheel-rail force. Developed for J500 model.
%
%  Name: A. Ortega García
%  Date: November 2013
%  Last revision: April 2014
```

```

%% Main
format long
clear all
clc

disp 'Generate LS files to be read in ANSYS'
disp ' '
PathOut=strcat(uigetdir('','Select folder to save results'),'\'); % Results path
disp ' '
disp 'Microsmurfs working, please wait'
disp ' '
tic

%% Info and loading
temp=strfind(PathOut,'\'); % find folder separations
JobName=PathOut(temp(end-1)+1:temp(end)-1); %Project name
Weld=str2num(JobName(end-1));
%Void=str2num(JobName(end));

if Weld==0
    load('LSNoWeld');
elseif Weld==1
    load('LSWeld');
else
    load('LSStatic');
end
N=length(Time);

%% Load steps text file
LStxt=cell(N,1);
progressbar % call figure of progress and set starting time

for i=1:N
    LStxt{i,1}=cell(73,1);
    LStxt{i,1}{1,1}='/COM,ANSYS RELEASE 14.5    UP20120918       12:34:56 04/25/2009';
    LStxt{i,1}{2,1}='/NOPR';
    LStxt{i,1}{3,1}='/TITLE,';
    LStxt{i,1}{4,1}=strcat('_LSNUM=',num2str(i)); %Change Load Step number
    LStxt{i,1}{5,1}='ANTYPE, 4';
    LStxt{i,1}{6,1}='TRNOPT,FULL,,DAMP';
    LStxt{i,1}{7,1}='KBC,      0';
    LStxt{i,1}{8,1}='TREF,  0.00000000';
    LStxt{i,1}{9,1}='IRLF,  0';
    LStxt{i,1}{10,1}='BFUNIF,TEMP,_TINY';
    LStxt{i,1}{11,1}='ACEL,  0.00000000     ,  0.00000000     ,  0.00000000     ';
    LStxt{i,1}{12,1}='OMEGA,  0.00000000     ,  0.00000000     ,  0.00000000';
```

```
    LStxt{i,1}{13,1}='DOMEGA,  0.00000000     ,  0.00000000     ,  0.00000000';
    LStxt{i,1}{14,1}='CGLOC,  0.00000000     ,  0.00000000     ,  0.00000000';
    LStxt{i,1}{15,1}='CGOMEGA,  0.00000000     ,  0.00000000     ,  0.00000000';
    LStxt{i,1}{16,1}='DCGOMG,  0.00000000     ,  0.00000000     ,  0.00000000';
    LStxt{i,1}{17,1}='';
    LStxt{i,1}{18,1}='NSUBST,         1,          0,          0,';
    LStxt{i,1}{19,1}='KUSE,     0';
    LStxt{i,1}{20,1}=strcat('TIME, ',num2str(Time(i,1),'%0.9f')); %Change time at the end of load step
    LStxt{i,1}{21,1}='ALPHAD,  0.00000000';
    LStxt{i,1}{22,1}='BETAD,  0.00000000';
    LStxt{i,1}{23,1}='DMPRAT,  0.00000000';
    LStxt{i,1}{24,1}='TIMINT,ON  ,STRU';
    LStxt{i,1}{25,1}='TINTP,R8.1, 5.000000000E-03,,,';
    LStxt{i,1}{26,1}='TINTP,R8.1, -1.00000000     , 0.500000000     , -1.00000000     ,,,,';
    LStxt{i,1}{27,1}='TINTP,R8.1, 5.000000000E-03,  0.00000000';
    LStxt{i,1}{28,1}='';
    LStxt{i,1}{29,1}='';
    LStxt{i,1}{30,1}='';
    LStxt{i,1}{31,1}='CRPLIM, 0.100000000     ,   0';
    LStxt{i,1}{32,1}='CRPLIM,  0.00000000     ,   1';
    LStxt{i,1}{33,1}='NCNV,     1,  0.00000000     ,     0,  0.00000000     ,  0.00000000';
    LStxt{i,1}{34,1}='';
    LStxt{i,1}{35,1}='NEQIT,     0';
    LStxt{i,1}{36,1}='';
    LStxt{i,1}{37,1}='ERESX,DEFA';
    LStxt{i,1}{38,1}='OUTRES, ALL,LAST,';
    LStxt{i,1}{39,1}='';

    %Constrains
    LStxt{i,1}{39,1}='D,    250,UX  ,  0.00000000     ,  0.00000000     ';
    LStxt{i,1}{40,1}='D,    250,UY  ,  0.00000000     ,  0.00000000     ';
    LStxt{i,1}{41,1}='D,    250,UZ  ,  0.00000000     ,  0.00000000     ';
    LStxt{i,1}{42,1}='D,    250,ROTX,  0.00000000     ,  0.00000000     ';
    LStxt{i,1}{43,1}='D,    250,ROTY,  0.00000000     ,  0.00000000     ';
    LStxt{i,1}{44,1}='D,    250,ROTZ,  0.00000000     ,  0.00000000     ';
    LStxt{i,1}{45,1}='D,    251,UX  ,  0.00000000     ,  0.00000000     ';
    LStxt{i,1}{46,1}='D,    251,UY  ,  0.00000000     ,  0.00000000     ';
    LStxt{i,1}{47,1}='D,    251,UZ  ,  0.00000000     ,  0.00000000     ';
    LStxt{i,1}{48,1}='D,    251,ROTX,  0.00000000     ,  0.00000000     ';
    LStxt{i,1}{49,1}='D,    251,ROTY,  0.00000000     ,  0.00000000     ';
    LStxt{i,1}{50,1}='D,    251,ROTZ,  0.00000000     ,  0.00000000     ';
    LStxt{i,1}{51,1}='D,    252,UX  ,  0.00000000     ,  0.00000000     ';
    LStxt{i,1}{52,1}='D,    252,UY  ,  0.00000000     ,  0.00000000     ';
    LStxt{i,1}{53,1}='D,    252,UZ  ,  0.00000000     ,  0.00000000     ';
    LStxt{i,1}{54,1}='D,    252,ROTX,  0.00000000     ,  0.00000000     ';
    LStxt{i,1}{55,1}='D,    252,ROTY,  0.00000000     ,  0.00000000     ';
```

```
        LStxt{i,1}{56,1}='D,    252,ROTZ,  0.00000000    ,  0.00000000    ';
        LStxt{i,1}{57,1}='D,    253,UX  ,  0.00000000    ,  0.00000000    ';
        LStxt{i,1}{58,1}='D,    253,UY  ,  0.00000000    ,  0.00000000    ';
        LStxt{i,1}{59,1}='D,    253,UZ  ,  0.00000000    ,  0.00000000    ';
        LStxt{i,1}{60,1}='D,    253,ROTX,  0.00000000    ,  0.00000000    ';
        LStxt{i,1}{61,1}='D,    253,ROTY,  0.00000000    ,  0.00000000    ';
        LStxt{i,1}{62,1}='D,    253,ROTZ,  0.00000000    ,  0.00000000    ';
        LStxt{i,1}{63,1}='D,    254,UX  ,  0.00000000    ,  0.00000000    ';
        LStxt{i,1}{64,1}='D,    254,UY  ,  0.00000000    ,  0.00000000    ';
        LStxt{i,1}{65,1}='D,    254,UZ  ,  0.00000000    ,  0.00000000    ';
        LStxt{i,1}{66,1}='D,    254,ROTX,  0.00000000    ,  0.00000000    ';
        LStxt{i,1}{67,1}='D,    254,ROTY,  0.00000000    ,  0.00000000    ';
        LStxt{i,1}{68,1}='D,    254,ROTZ,  0.00000000    ,  0.00000000    ';
    LStxt{i,1}{69,1}=strcat('F,',num2str(W1(i,1)),',FY   , -',num2str(W1(i,2)),',  0.00000000'); %Wheel 1
    LStxt{i,1}{70,1}=strcat('F,',num2str(W2(i,1)),',FY   , -',num2str(W2(i,2)),',  0.00000000'); %Wheel 2
    LStxt{i,1}{71,1}=strcat('F,',num2str(W3(i,1)),',FY   , -',num2str(W3(i,2)),',  0.00000000'); %Wheel 3
    LStxt{i,1}{72,1}=strcat('F,',num2str(W4(i,1)),',FY   , -',num2str(W4(i,2)),',  0.00000000'); %Wheel 4
        LStxt{i,1}{73,1}='/GOPR';

        %% Save Load Step
        NameOut=strcat(PathOut,JobName,'.S',num2str(i,'%02.0f')); %path, name and extension
        fid=fopen(NameOut,'w'); %create file
        for j=1:length(LStxt{i,1})
            fprintf(fid,'%s\r\n',LStxt{i,1}{j,1}); %for LSi, print line j
        end
        fclose(fid);
        progressbar(i/N); %update progress
end

%% Save workspace
%save(strcat('C:\Users\Cid\Dropbox\Thesis\ANSYS\LoadSteps\',JobName));
save(strcat('D:\ANSYS\LoadSteps\',JobName));

eltime=toc; %stop timer
disp (['Elapsed time: ' datestr(eltime/24/3600,'DD:HH:MM:SS.FFF')])
disp ([num2str(N),' files have been saved in selected folder'])
disp ' '

clear all
```

G-1-2 Post-process functions

Two functions are used to post-process the output information generated in ANSYS. The output from ANSYS consists of CSV files, one set per project. The MATLAB functions used are:

AnsysPP
: Imports CSV files from a (project) folder into a MAT file. Plots for several variables are generated in time and frequency domain.

AnsysSE
: Compares time and frequency domain response for specific sleeper elements. Plots in both domains are generated for rail displacement, sleeper displacement and sleeper acceleration.

AnsysPP

```
function AnsysPP
%AnsysPP
%  Imports CSV files generated in ANSYS, reads the file and stores each
%  column into a variable. Generates a plot for each variable in time and
%  frequency domain.
%
%  Variables are saved in a MAT file in a folder named
%  ...\[JOBNAME]\[ELEMENT] where JOBNAME and ELEMENT are extracted from the
%  input information.
%
%  Name: A. Ortega García
%  Date: November 2013
%  Last revision: April 2013

%% Opening
clear all
clc

disp 'Imports and postprocess .CSV results from ANSYS.'
disp ' '

% In and Out folders
PathIn=strcat(uigetdir('','Select project folder'),'\');
files=dir(strcat(PathIn,'*.csv'));
temp=strfind(PathIn,'\'); % find folder separations
JobName=PathIn(temp(end-1)+1:temp(end)-1); % name of project (jobname)
PathOut=strcat(uigetdir('','Select folder to save results'),'\');
L=length(files);

disp 'Microsmurfs working, please wait'
disp ' '

```

```
tic
progressbar

%% Extract all .CSV files in folder
for k=1:L
    clearvars -except PathIn PathOut JobName files k L elem

    % File to import
    FileIn=files(k).name; %file name
    NameIn=strcat(PathIn,FileIn); % complete name of file
    fid=fopen(NameIn); % open file

    % Create folder to save results
    [~,Element]=fileparts(NameIn); % single name
    NameOut=strcat(PathOut,'Projects\',JobName,'\',Element);
    mkdir(NameOut); % create folder to save results

    %% Create variables
    tline=fgetl(fid); %read line
    col=regexp(tline,'\, ','split'); %column headers
    n=length(col); %number of variables
    for j=1:n
        vars.(col{1,j})=0; %creates variable in vars structure
        if strcmpi(col{1,j},'TIME')
            col{2,j}='[s]'; %time units
        elseif strcmpi(col{1,j},'RUY') || strcmpi(col{1,j},'SUY')
            col{2,j}='[m]'; %displacement units
        elseif strcmpi(col{1,j},'RAY') || strcmpi(col{1,j},'SAY')
            col{2,j}='[m/s^{2}]'; %acceleration units
        elseif strcmpi(col{1,j},'RFY') || strcmpi(col{1,j},'SFY')...
                || strcmpi(col{1,j},'BFY') || strcmpi(col{1,j},'UFY')
            col{2,j}='[kN]'; %force units
        end
    end

    %% Read and sort per variable
    i=0; %line counter
    while i~=-1
        tline=fgetl(fid); %next text line
        if tline==-1 %end of .csv file
            i=-1;
        else
            i=i+1; %increase counter
            dline=str2num(tline); %convert to decimal
            for j=1:n
                vars.(col{1,j})(i,1)=dline(1,j); %sort into variable
            end
        end
    end

    %% Write element per variable into big table
    for j=2:n
        if k==1; elem.(col{1,j})(:,1)=vars.(col{1,1}); end %Time (once)
```

```
        elem.(col{1,j})(:,k+1)=vars.(col{1,j}); %Variable
    end

    %% Distance vector X
    if k==1
        elem.X(1,1)=0; %blank space
        elem.X(1,k+1)=17.10; %first x-coordinate, insert manually
    else
        elem.X(1,k+1)=elem.X(1,k)+0.6; %distance between sleepers
    end

    %% Generate Data in Frequency Domain (DFD)
    N=length(vars.(col{1,1})); %length of data [points]
    N2=ceil(N/2); %half data length
    dt=vars.(col{1,1})(1,1); %time step [s]
    Fs=1/dt; %frequency [Hz]
    f=transpose(Fs*linspace(0,1,N)); %frequency vector [Hz]
    vars.(col{1,1})(:,2)=f;

    % Save DFD in 2nd column for each variable
    for j=2:n
        DTD=vars.(col{1,j}); %Data in Time Domain
        DFD=fft(DTD); %Data in Frequency Domain
        vars.(col{1,j})(:,2)=abs(DFD); %Save DFD
    end

    %% Plot variables
    for j=2:n
        % Time domain
        f1=figure();
        plot(vars.(col{1,1})(:,1),vars.(col{1,j})(:,1),'LineWidth',1.0);
        grid on
        xlabel('T [s]')
        ylabel(strcat(col{1,j},32,col{2,j}))
        title(strcat(JobName,32,Element))

        % Save plot with name output
        PNGImgLarge=strcat(NameOut,'\Large',Element,'_',col{1,j},...
            'time.png');
        saveas(f1,PNGImgLarge);
        MatFig=strcat(NameOut,'\',Element,'_',col{1,j},'time.fig');
        saveas(f1,MatFig);
        PNGImg=strcat(NameOut,'\',Element,'_',col{1,j},'time.png');
        set(f1,'PaperUnits','inches','PaperPosition',[0 0 4 3])
        print('-dpng',PNGImg,'-r100')

        % Frequency domain
        f2=figure;
        semilogx(vars.(col{1,1})(1:N2,2),vars.(col{1,j})(1:N2,2),...
            'LineWidth',1.0);
        grid on
        xlabel('f [Hz]')
        ylabel(strcat(col{1,j},32,col{2,j}))
```

```
        title(strcat(JobName,32,Element))

        % Save plot with name output
        PNGImgLarge=strcat(NameOut,'\Large',Element,'_',col{1,j},...
            'freq.png');
        saveas(f2,PNGImgLarge);
        MatFig=strcat(NameOut,'\',Element,'_',col{1,j},'freq.fig');
        saveas(f2,MatFig);
        PNGImg=strcat(NameOut,'\',Element,'_',col{1,j},'freq.png');
        set(f2,'PaperUnits','inches','PaperPosition',[0 0 4 3])
        print('-dpng',PNGImg,'-r100')
    end

    %% Save variables
    save(strcat(NameOut,'\',Element), '-struct', 'vars');
    progressbar(k/L);
end
close all

%% Envelope per variable
% If 2 or more elements are imported then Envelope and Animation are
% performed
if L~=1
    for j=2:n
        elem.(strcat(col{1,j},'Env'))(1,:)=max(elem.(col{1,j}));
        elem.(strcat(col{1,j},'Env'))(2,:)=min(elem.(col{1,j}));
    end
    save(strcat(PathOut,'Projects\',JobName,'\',JobName), '-struct',...
        'elem');

    %% Animation
    % Generate plot per time step for now only RUY

    dt=elem.RUY(1,1);
    fps=round(1/dt);
    for i=1:N
        plot(elem.X(1,2:end),elem.RUY(i,2:end));
        grid on
        axis([elem.X(1,2) elem.X(1,end) min(elem.RUYEnv(2,2:end))...
            max(elem.RUYEnv(1,2:end))])
        xlabel('x [m]')
        ylabel('\delta_{rail} [m]')
        title(JobName)
        M(i)=getframe(gca);
    end

    % Save animation
    moviename=strcat(PathOut,'Projects\',JobName,'\',JobName,'.avi');
    movie2avi(M,moviename,'fps',fps,'compression','None');
    close all
end

%% Closing
```

```
disp (['Elapsed time: ' datestr(toc/24/3600,'DD:HH:MM:SS.FFF')])
disp 'Files have been saved in selected folder'
disp ' '

clear all
```

AnsysSE

```
function AnsysSE
%AnsysSE
%  Compares the frequency response of rail displacement, sleeper
%  displacement and sleeper acceleration of different projects. The user
%  specifies the sleeper element number and the function returns the plots
%  in time and frequency domain.
%
%  Name: A. Ortega García
%  Date: January 2014
%  Last revision: April 2014

%% Opening
clear all
clc

disp 'Compare frequency response for specific Sleeper element.'
disp ' '
temp=input('Please type sleeper element to be compared [default=253]: ','s');
disp ' '

if isempty(temp); ElemNum='SE253'; else ElemNum=strcat('SE',temp); end
FileIn=strcat(ElemNum,'.mat');

%% In and Out folders
PathIn=strcat(uigetdir('','Select parent folder'),'\');
d=dir(PathIn); %project subfolders
isub=[d(:).isdir]; %returns logical vector
ProjFold={d(isub).name}'; %cell with name of subfolders
ProjFold(ismember(ProjFold,{'.','..'}))=[]; %delete '.' and '..'
PathOut=strcat(uigetdir('','Select folder to save results'),'\');
NameOut=strcat(PathOut,'Elements\',ElemNum);
mkdir(NameOut); % create folder to save results
L=length(ProjFold);
E=struct(); %General structure with all projects
disp 'Microsmurfs working, please wait'
disp ' '
tic

%% Extract .MAT from Projects
for k=1:L
    clearvars -except ElemNum PathIn FileIn PathOut NameOut ProjFold...
        k L E Case

    %% Load projects
    JobName=ProjFold{k};
    NameIn=strcat(PathIn,JobName,'\',ElemNum,'\',FileIn);
    E.(ProjFold{k})=load(NameIn);
    vars=fieldnames(E.(ProjFold{k}));

```

```
    %% Create cases legend
    E.(ProjFold{k}).Weld=str2num(ProjFold{k}(end-1));
    E.(ProjFold{k}).Void=str2num(ProjFold{k}(end));
    if E.(ProjFold{k}).Weld==0 && E.(ProjFold{k}).Void==0
        Case{k}='Case 1';
    elseif E.(ProjFold{k}).Weld==1 && E.(ProjFold{k}).Void==0
        Case{k}='Case 2';
    elseif E.(ProjFold{k}).Weld==1 && E.(ProjFold{k}).Void==1
        Case{k}='Case 3';
    else
        Case{k}='Case 4';
    end
end

%% Create vars units
lvars=length(vars);
for j=1:lvars
    if strcmpi(vars{j,1},'TIME')
        vars{j,2}='[s]';
    elseif strcmpi(vars{j,1},'RUY') || strcmpi(vars{j,1},'SUY')
        vars{j,2}='[m]';
    elseif strcmpi(vars{j,1},'RAY') || strcmpi(vars{j,1},'SAY')
        vars{j,2}='[m/s^{2}]';
    elseif strcmpi(vars{j,1},'RFY') || strcmpi(vars{j,1},'SFY')...
            || strcmpi(vars{j,1},'BFY')
        vars{j,2}='[kN]';
    end
end

%% Plot vars by cases
lcase=length(Case);
N1=1;
N2=1500;
for j=2:lvars
    for k=2:lcase
        %% Time domain
        f1=figure();
        grid on
        xlabel('t [s]')
        ylabel(strcat(vars{j,1},32,vars{j,2}))
        hold all
        plot(E.(ProjFold{1}).TIME(:,1),E.(ProjFold{1}).(vars{j})(:,1),...
            'LineWidth',1.0);
        plot(E.(ProjFold{k}).TIME(:,1),E.(ProjFold{k}).(vars{j})(:,1),...
            'LineWidth',1.0);
        xlim([0 N1])
        legend({Case{1},Case{k}},'Location','Best');

        PNGImgLarge=strcat(NameOut,'\Large',ElemNum,'_',vars{j},...
            Case{k}(end),'time.png');
        saveas(f1,PNGImgLarge);

        PNGImg=strcat(NameOut,'\',ElemNum,'_',vars{j},Case{k}(end),...
```

```
                'time.png');
            set(f1,'PaperUnits','inches','PaperPosition',[0 0 4 3])
            print('-dpng',PNGImg,'-r100')

            MatFig=strcat(NameOut,'\',ElemNum,'_',vars{j},Case{k}(end),...
                'time.fig');
            saveas(f1,MatFig);

            %% Frequency domain
            f2=figure();
            semilogx(E.(ProjFold{1}).TIME(:,2),...
                E.(ProjFold{1}).(vars{j})(:,2),'LineWidth',1.0);
            hold all
            semilogx(E.(ProjFold{k}).TIME(:,2),...
                E.(ProjFold{k}).(vars{j})(:,2),'LineWidth',1.0);
            grid on
            xlabel('f [Hz]')
            ylabel(strcat(vars{j,1},32,vars{j,2}))
            xlim([1 N2])
            legend({Case{1},Case{k}},'Location','Best');

            PNGImgLarge=strcat(NameOut,'\Large',ElemNum,'_',vars{j},...
                Case{k}(end),'freq.png');
            saveas(f2,PNGImgLarge);

            PNGImg=strcat(NameOut,'\',ElemNum,'_',vars{j},Case{k}(end),...
                'freq.png');
            set(f2,'PaperUnits','inches','PaperPosition',[0 0 4 3])
            print('-dpng',PNGImg,'-r100')

            MatFig=strcat(NameOut,'\',ElemNum,'_',vars{j},Case{k}(end),...
                'freq.fig');
            saveas(f2,MatFig);
        end
end
close all

%% Save structure
save(strcat(NameOut,'\',ElemNum), '-struct', 'E');

%% Closing
eltime=toc; %stop timer
disp (['Elapsed time: ' datestr(eltime/24/3600,'DD:HH:MM:SS.FFF')])
disp 'Files have been saved in selected folder'
disp ' '

clear all
```

G-2 ESAH-M

G-2-1 Post-process functions

The Matlab function post-processes the output files generated by the ESAH-M system. The files (DAT extension) are a combination of ASCII and Binary information heavily packed. The *ESAHMdat2mat* function recognises the nature of the data, processes it and delivers a MAT file along with a series of plots.

ESAHMdat2mat

```
function ESAHMdat2mat
%ESAHMdat2mat
%  Imports ESAHM DAT files from the selected folder. Reads the ASCII and
%  the Binary parts and sorts the data into a structure with the next
%  variables:
%
%  1. ASCII
%  - Name
%  - ASCII text, 27 lines
%  - Column text, 1 line
%  - ASCII data 1, 100 lines (Table per axle)
%  - ASCII data 2, 40 lines (Crossing contact point)
%
%  2. Binary
%  - X, x acceleration
%  - Y, y acceleration
%  - Z, z acceleration
%  - HOH, sleeper voltage
%  - BERO, speed sensor inductive
%
%  Variables are saved in a MAT file with the original DAT filename. The
%  file is saved in the PROJECT folder extracted from the input
%  information. Figures for time and frequency domain are also saved.
%
%  Name: A. Ortega García
%  Date: October 2012
%  Last revision: April 2014

%% Main menu
clear all
close all
clc

disp 'Import .DAT files into .MAT file to be read in Matlab'
disp ' '
disp '(1) Select single file'
disp '(2) Import all files in a folder'
disp ' '
op = input('Please select an option: ', 's');
disp ' '
```

```
disp 'Microsmurfs working, please wait'
disp ' '

%% Switch between options
switch op

    case '1'
        %% Import single .DAT file
        % Select file to import
        [FileIn,PathIn]=uigetfile('.dat'); % file name and path
        NameIn=strcat(PathIn,FileIn); % complete name of file
        fid=fopen(NameIn); % open file

        % Folder to save results
        [~,Name]=fileparts(NameIn); % single name
        temp=strfind(PathIn,'\'); % find folder separations
        Proj=PathIn(temp(end-1)+1:temp(end)-1); % name of the project
        PathOut=strcat(uigetdir('','Select folder to save results'),'\'); % path for results
        NameOut=strcat(PathOut,Proj,'\',Name,'\',Name); %location and name of save file
        mkdir(strcat(PathOut,Proj),Name); %create folder NAME inside PROJ

        % General structure with all variables
        vars=struct;
        vars.Name=Name;
        vars.Project=Proj;
        tic

        %% Step 1: ASCII part
        % 28 lines of ASCII text
        for i=1:27
            vars.ASCIItxt{i,1}=fgetl(fid);
        end

        % 1 line of Column text
        vars.ColHead=regexp(fgetl(fid),'\t','split');

        % 100 lines of ASCII data 1 (Table per axle)
        for i=1:100
            fila=fgetl(fid); % extract line
            if isempty(str2num(fila)) % a letter was found in the line
                temp=regexp(fila,'\t','split'); % separate by tab
                for ii=1:length(temp) %move through the line
                    if temp{1,ii}=='P';
                        vars.ASCIId1(i,ii)=1; % positive contact
                    elseif temp{1,ii}=='N'
                        vars.ASCIId1(i,ii)=-1; % negative contact
                    else
                        vars.ASCIId1(i,ii)=str2num(temp{1,ii}); % normal contact
                    end
                end
```

```
            else % no letters found, only numbers
                vars.ASCIId1(i,:)=str2num(fila);
            end
        end

        % 40 lines of ASCII data 2 (Crossing contact point)
        for i=1:40
            vars.ASCIId2(i,:)=str2num(fgetl(fid));
        end

        %% Step 2: Binary part
        % Retrieve all binary part into TotBin
        TotBin=fread(fid);
        L=length(TotBin);

        % Variables to store converted binary data
        X=zeros(1,1);
        Y=zeros(1,1);
        Z=zeros(1,1);
        HOH=zeros(1,1);
        BERO=zeros(1,1);

        % Read binary data
        k=1; % postion in TotBin to be read
        n=1; % position in new variable
        progressbar % call figure of progress and set starting time

        while k<L
            % Retrieve 7 numbers (decimal)
            D=[TotBin(k,1)
                TotBin(k+1,1)
                TotBin(k+2,1)
                TotBin(k+3,1)
                TotBin(k+4,1)
                TotBin(k+5,1)
                TotBin(k+6,1)];

            % Convert decimal (D) to binary (B)
            B=de2bi(D,8,'left-msb'); %read from left

            % Separate every 1.5 bytes into known variables (binary)
            xbin=[B(1,:),B(2,1:4)]; %x-acc
            ybin=[B(2,5:8),B(3,:)]; %y-acc
            zbin=[B(4,:),B(5,1:4)]; %z-acc
            hohbin=[B(5,5:8),B(6,:)]; %sleeper-disp
            berobin=B(7,:); %speed sensor inductive

            % Binary to decimal
            % Factor and Offset obtained from DIADEM script
            xdec=0.305176*(-2020.0+bi2de(xbin,'left-msb'));
            ydec=0.305176*(-2020.0+bi2de(ybin,'left-msb'));
            zdec=0.305176*(-2020.0+bi2de(zbin,'left-msb'));
            hohdec=(305/90112)*(bi2de(hohbin,'left-msb'));
```

```
        berodec=bi2de(berobin,'left-msb');

        % Store decimal values
        X(n,1)=xdec;
        Y(n,1)=ydec;
        Z(n,1)=zdec;
        HOH(n,1)=hohdec;
        BERO(n,1)=berodec;

        % Increase counters
        k=k+7;
        n=n+1;
        progressbar(k/L); %update figure
    end

    % Save variables in structure
    vars.X=X;
    vars.Y=Y;
    vars.Z=Z;
    vars.HOHuTDr=HOH;
    vars.BERO=BERO;

    %% Step 3: Filter signal
    %From this point and on, only HOH will be processed; I'm not
    %interested in X, Y or Z anymore.

    Fs=10000;                               %frequency of data [Hz]
    dT=1/Fs;                                %time step (\delta t) [s]
    Nu=length(vars.HOHuTDr);                %length of data [points]
    vars.FreqU=transpose(Fs*(linspace(0,1,Nu)));  %Frequency vector [Hz]
    vars.Time=transpose((0:Nu-1)*dT);                   %Time vector [s]

    % Shift graph
    vars.HOHuFDr=fft(vars.HOHuTDr);         %Data in Frequency Domain raw
    vars.HOHuFD=vars.HOHuFDr;
    vars.HOHuFD(1,1)=0;                     %remove first freq to shift graph to origin
    vars.HOHuTD=real(ifft(vars.HOHuFD));    %return to Time Domain shifted
    vars.HOHuTD(1)=vars.HOHuTD(2);
    vars.HOHuTD(end)=vars.HOHuTD(end-1);

    % Filter signal
    smoothtimes=20;
    smoothspan=10;
    for i=1:smoothtimes
        vars.HOHuTD=smooth(vars.HOHuTD,smoothspan);
    end

    %% Step 4: Convert displacement to acceleration
    % Double derivative
```

```
        vars.HOHvTD=diff(vars.HOHuTD)./dT;      %Sleeper velocity in Time
             Domain
        vars.HOHvTD(end+1)=vars.HOHvTD(end);  %Repeat last value to keep
            vector dimensions
        vars.HOHaTD=diff(vars.HOHvTD)./dT;      %Sleeper acceleration in
            Time Domain
        vars.HOHaTD(end+1)=vars.HOHaTD(end);  %Repeat last value to keep
            vector dimensions

        % Convert to frequency domain
        vars.HOHuFD=abs(fft(vars.HOHuTD));      %Sleeper displacement in
            Frequency Domain
        vars.HOHvFD=abs(fft(vars.HOHvTD));      %Sleeper velocity in
            Frequency Domain
        vars.HOHaFD=abs(fft(vars.HOHaTD(50:end-50))); %Sleeper
            acceleration in Frequency Domain

        Na=length(vars.HOHaFD);                 %length of acc data
        vars.FreqA=transpose(Fs*(linspace(0,1,Na)));  %Frequency vector
            for acceleration

        %% Step 5: Plots
        % Time domain
        %Displacement
        f1=figure();
        plot(vars.Time,vars.HOHuTD);
        grid on
        ylabel('\delta [V]')
        xlabel('t [s]')
        set(gca,'LineWidth',1.0)

        PNGImgLarge=strcat(NameOut,'_','LargeHOHutime.png');
        saveas(f1,PNGImgLarge);
        MatFig=strcat(NameOut,'_','HOHutime.fig');
        saveas(f1,MatFig);
        PNGImg=strcat(NameOut,'_','HOHutime.png');
        set(f1,'PaperUnits','inches','PaperPosition',[0 0 4 3])
        print('-dpng',PNGImg,'-r100')

        %Acceleration
        f2=figure();
        plot(vars.Time(50:end-50),vars.HOHaTD(50:end-50));
        grid on
        ylabel('a [V]')
        xlabel('t [s]')
        set(gca,'LineWidth',1.0)

        PNGImgLarge=strcat(NameOut,'_','LargeHOHatime.png');
        saveas(f2,PNGImgLarge);
        MatFig=strcat(NameOut,'_','HOHatime.fig');
        saveas(f2,MatFig);
        PNGImg=strcat(NameOut,'_','HOHatime.png');
        set(f2,'PaperUnits','inches','PaperPosition',[0 0 4 3])
```

```
        print('-dpng',PNGImg,'-r100')

        % Frequency domain
        %Displacement
        N2=1000;
        f3=figure();
        semilogx(vars.FreqU,vars.HOHuFD);
        grid on
        ylabel('\delta [V]')
        xlabel('f [Hz]')
        xlim([1 N2])
        set(gca,'LineWidth',1.0)

        PNGImgLarge=strcat(NameOut,'_','LargeHOHufreq.png');
        saveas(f3,PNGImgLarge);
        MatFig=strcat(NameOut,'_','HOHufreq.fig');
        saveas(f3,MatFig);
        PNGImg=strcat(NameOut,'_','HOHufreq.png');
        set(f3,'PaperUnits','inches','PaperPosition',[0 0 4 3])
        print('-dpng',PNGImg,'-r100')

        %Acceleration
        f4=figure();
        semilogx(vars.FreqA,vars.HOHaFD);
        grid on
        ylabel('a [V]')
        xlabel('f [Hz]')
        xlim([1 N2])
        set(gca,'LineWidth',1.0)

        PNGImgLarge=strcat(NameOut,'_','LargeHOHafreq.png');
        saveas(f4,PNGImgLarge);
        MatFig=strcat(NameOut,'_','HOHafreq.fig');
        saveas(f4,MatFig);
        PNGImg=strcat(NameOut,'_','HOHafreq.png');
        set(f4,'PaperUnits','inches','PaperPosition',[0 0 4 3])
        print('-dpng',PNGImg,'-r100')

        close all

        %% Step 6: Save structure
        save(NameOut, '-struct', 'vars');

        eltime=toc; %stop timer
        disp (['Elapsed time: ' datestr(eltime/24/3600,'DD:HH:MM:SS.FFF')
            ])
        disp 'File has been imported into selected folder'
        disp ' '


    case '2'
        %% Import all .DAT files
        % In and Out folders
```

```
        PathIn=strcat(uigetdir('','Select project folder'),'\'); %folder with all the files to import
        files=dir(strcat(PathIn,'*.dat')); % select all the .DAT files in project folder
        temp=strfind(PathIn,'\'); % find folder separations
        Proj=PathIn(temp(end-1)+1:temp(end)-1); % name of the project
        PathOut=strcat(uigetdir('','Select folder to save results'),'\'); % path for results
        tic

        for j=1:length(files)
            clearvars -except op PathIn PathOut Proj files j

            % File to import
            FileIn=files(j).name;
            NameIn=strcat(PathIn,FileIn); % complete name of file
            fid=fopen(NameIn); % open file

            % Folder to save results
            [~,Name]=fileparts(NameIn); % single name
            NameOut=strcat(PathOut,Proj,'\',Name,'\',Name); %location and name of save file
            mkdir(strcat(PathOut,Proj),Name); %create folder NAME inside PROJ

            % General structure with all variables
            vars=struct;
            vars.Name=Name;
            vars.Project=Proj;

            %% Step 1: ASCII part
            % 28 lines of ASCII text
            for i=1:27
                vars.ASCIItxt{i,1}=fgetl(fid);
            end

            % 1 line of Column text
            vars.ColHead=regexp(fgetl(fid),'\t','split');

            % 100 lines of ASCII data 1 (Table per axle)
            for i=1:100
                fila=fgetl(fid); % extract line
                if isempty(str2num(fila)) % a letter was found in the line
                    temp=regexp(fila,'\t','split'); % separate by tab
                    for ii=1:length(temp) %move through the line
                        if temp{1,ii}=='P';
                            vars.ASCIId1(i,ii)=1; % positive contact
                        elseif temp{1,ii}=='N'
                            vars.ASCIId1(i,ii)=-1; % negative contact
                        else
                            vars.ASCIId1(i,ii)=str2num(temp{1,ii}); % normal contact
```

```
                    end
                end
            else % no letters found, only numbers
                vars.ASCIId1(i,:)=str2num(fila);
            end
        end

        % 40 lines of ASCII data 2 (Crossing contact point)
        for i=1:40
            vars.ASCIId2(i,:)=str2num(fgetl(fid));
        end

        %% Step 2: Binary part
        % Retrieve all binary part into TotBin
        TotBin=fread(fid);
        L=length(TotBin);

        % Variables to store converted binary data
        X=zeros(1,1);
        Y=zeros(1,1);
        Z=zeros(1,1);
        HOH=zeros(1,1);
        BERO=zeros(1,1);

        % Read binary data
        k=1; % postion in TotBin to be read
        n=1; % position in new variable
        progressbar % call figure of progress and set starting time

        while k<L
            % Retrieve 7 numbers (decimal)
            D=[TotBin(k,1)
                TotBin(k+1,1)
                TotBin(k+2,1)
                TotBin(k+3,1)
                TotBin(k+4,1)
                TotBin(k+5,1)
                TotBin(k+6,1)];

            % Convert decimal (D) to binary (B)
            B=de2bi(D,8,'left-msb'); %read from left

            % Separate every 1.5 bytes into known variables (binary)
            xbin=[B(1,:),B(2,1:4)]; %x-acc
            ybin=[B(2,5:8),B(3,:)]; %y-acc
            zbin=[B(4,:),B(5,1:4)]; %z-acc
            hohbin=[B(5,5:8),B(6,:)]; %sleeper-disp
            berobin=B(7,:); %speed sensor inductive

            % Binary to decimal
            % Factor and Offset obtained from DIADEM script
            xdec=0.305176*(-2020.0+bi2de(xbin,'left-msb'));
            ydec=0.305176*(-2020.0+bi2de(ybin,'left-msb'));
```

```
            zdec=0.305176*(-2020.0+bi2de(zbin,'left-msb'));
            hohdec=(305/90112)*(bi2de(hohbin,'left-msb'));
            berodec=bi2de(berobin,'left-msb');

            % Store decimal values
            X(n,1)=xdec;
            Y(n,1)=ydec;
            Z(n,1)=zdec;
            HOH(n,1)=hohdec;
            BERO(n,1)=berodec;

            % Increase counters
            k=k+7;
            n=n+1;
            progressbar(k/L); %update figure
        end

        % Save variables in structure
        vars.X=X;
        vars.Y=Y;
        vars.Z=Z;
        vars.HOHuTDr=HOH(1:end-10);
        vars.BERO=BERO;

        %% Step 3: Filter signal
        %From this point and on, only HOH will be processed; I'm not
        %interested in X, Y or Z anymore.

        Fs=10000;                           %frequency of data [Hz]
        dT=1/Fs;                            %time step (\delta t) [s]
        Nu=length(vars.HOHuTDr);            %length of data [points]
        vars.FreqU=transpose(Fs*(linspace(0,1,Nu)));  %Frequency vector [Hz]
        vars.Time=transpose((0:Nu-1)*dT);             %Time vector [s]

        % Shift graph
        vars.HOHuFDr=fft(vars.HOHuTDr);         %Data in Frequency Domain raw
        vars.HOHuFD=vars.HOHuFDr;
        vars.HOHuFD(1,1)=0;                     %remove first freq to shift graph to origin
        vars.HOHuTD=real(ifft(vars.HOHuFD));    %return to Time Domain shifted
        vars.HOHuTD(1)=vars.HOHuTD(2);
        vars.HOHuTD(end)=vars.HOHuTD(end-1);

        % Filter signal
        smoothtimes=20;
        smoothspan=10;
        for i=1:smoothtimes
            vars.HOHuTD=smooth(vars.HOHuTD,smoothspan);
        end
```

```matlab

%% Step 4: Convert displacement to acceleration
% Double derivative
vars.HOHvTD=diff(vars.HOHuTD)./dT;       %Sleeper velocity in Time Domain
vars.HOHvTD(end+1)=vars.HOHvTD(end);  %Repeat last value to keep vector dimensions
vars.HOHaTD=diff(vars.HOHvTD)./dT;       %Sleeper acceleration in Time Domain
vars.HOHaTD(end+1)=vars.HOHaTD(end);  %Repeat last value to keep vector dimensions

% Convert to frequency domain
vars.HOHuFD=abs(fft(vars.HOHuTD));       %Sleeper displacement in Frequency Domain
vars.HOHvFD=abs(fft(vars.HOHvTD));       %Sleeper velocity in Frequency Domain
vars.HOHaFD=abs(fft(vars.HOHaTD(50:end-50))); %Sleeper acceleration in Frequency Domain

Na=length(vars.HOHaFD);                  %length of acc data
vars.FreqA=transpose(Fs*(linspace(0,1,Na)));  %Frequency vector for acceleration

%% Step 5: Plots
% Time domain
%Displacement
f1=figure();
plot(vars.Time,vars.HOHuTD);
grid on
ylabel('\delta [V]')
xlabel('t [s]')
set(gca,'LineWidth',1.0)

PNGImgLarge=strcat(NameOut,'_','LargeHOHutime.png');
saveas(f1,PNGImgLarge);
MatFig=strcat(NameOut,'_','HOHutime.fig');
saveas(f1,MatFig);
PNGImg=strcat(NameOut,'_','HOHutime.png');
set(f1,'PaperUnits','inches','PaperPosition',[0 0 4 3])
print('-dpng',PNGImg,'-r100')

%Acceleration
f2=figure();
plot(vars.Time(50:end-50),vars.HOHaTD(50:end-50));
grid on
ylabel('a [V]')
xlabel('t [s]')
set(gca,'LineWidth',1.0)

PNGImgLarge=strcat(NameOut,'_','LargeHOHatime.png');
saveas(f2,PNGImgLarge);
MatFig=strcat(NameOut,'_','HOHatime.fig');
```

```
            saveas(f2,MatFig);
            PNGImg=strcat(NameOut,'_','HOHatime.png');
            set(f2,'PaperUnits','inches','PaperPosition',[0 0 4 3])
            print('-dpng',PNGImg,'-r100')

            % Frequency domain
            %Displacement
            N2=1000;
            f3=figure();
            semilogx(vars.FreqU,vars.HOHuFD);
            grid on
            ylabel('\delta [V]')
            xlabel('f [Hz]')
            xlim([1 N2])
            set(gca,'LineWidth',1.0)

            PNGImgLarge=strcat(NameOut,'_','LargeHOHufreq.png');
            saveas(f3,PNGImgLarge);
            MatFig=strcat(NameOut,'_','HOHufreq.fig');
            saveas(f3,MatFig);
            PNGImg=strcat(NameOut,'_','HOHufreq.png');
            set(f3,'PaperUnits','inches','PaperPosition',[0 0 4 3])
            print('-dpng',PNGImg,'-r100')

            %Acceleration
            f4=figure();
            semilogx(vars.FreqA,vars.HOHaFD);
            grid on
            ylabel('a [V]')
            xlabel('f [Hz]')
            xlim([1 N2])
            set(gca,'LineWidth',1.0)

            PNGImgLarge=strcat(NameOut,'_','LargeHOHafreq.png');
            saveas(f4,PNGImgLarge);
            MatFig=strcat(NameOut,'_','HOHafreq.fig');
            saveas(f4,MatFig);
            PNGImg=strcat(NameOut,'_','HOHafreq.png');
            set(f4,'PaperUnits','inches','PaperPosition',[0 0 4 3])
            print('-dpng',PNGImg,'-r100')

            close all

            %% Step 6: Save structure
            save(NameOut, '-struct', 'vars');
        end

        eltime=toc; %stop timer
        disp ' '
        disp (['Elapsed time: ' datestr(eltime/24/3600,'DD:HH:MM:SS.FFF')
            ])
        disp 'Files have been imported into selected folder'
        disp ' '
```

```
end

clear all
```

Bibliography

[1] A. Aikawa. Application of a special sensing sleeper for dynamic interaction within the boundary layer between a sleeper and ballasts. Technical report, Railway Technical Research Institute, 2012.

[2] A. Ambardar. *Digital Signal Processing: A Modern Introduction.* Thompson Learning, 2007.

[3] W. Anderson and A. Key. Model testing of two-layer railway track ballast. *Geotechnical and Geoenvironmental Engineering*, 126(4):317–323, April 2000.

[4] S. Braun. *Discover Signal Processing.* John Wiley & Sons Ltd., 2008.

[5] C. Calla. *Two layered ballast system for improved performance of railway track.* PhD thesis, Coventry University, 2003.

[6] A. de Man. *DYNATRACK, A survey of dynamic railway track properties and their qualities.* PhD thesis, Technische Universiteit Delft, 2002.

[7] ECM. *The Dynamic Analysis of Railway Track Systems.*

[8] C. Esveld. *Modern Railway Track.* MRT-Productions, 2001.

[9] J. Gere. *Mechanics of materials.* Brooks/Cole-Thomson Learning, 6th edition, 2004.

[10] G. Hildebrand and S. Rasmussen. Report 117 development of a high speed deflectograph. Technical report, Danish Road Institute, 2002.

[11] H. Jenkins, J. Stephenson, G. Clayton, G. Morlan, and D. Lyon. The effect of track and vehicle parameters on wheel/rail vertical dynamic forces. *Railway Engineering Journal*, 1974.

[12] A. Johanssona, J. Nielsena, R. Bolmsvikc, A. Karlstromd, and R. Lundena. Under sleeper pads, influence on dynamic train track interaction. *Wear*, 2008.

[13] S. Lobo-Guerrero and L. Vallejo. Discrete element method analysis of railtrack ballast degradation during cyclic loading. *Granular Matter*, 8(3-4):195–204, August 2006.

[14] S. Lu, R. Arnold, S. Farritor, M. Fateh, and G. Carr. On the relationship between load and deflection in railroad track substructure. Technical report, University of Nebraska Lincoln, 2004.

[15] V. Markine and I. Shevtsov. An experimental study on crossing nose damage of railway turnouts in the netherlands. In B. Topping and P. Iványi, editors, *Proceedings of the Fourteenth International Conference on Civil, Structural and Environmental Engineering Computing*, Kippen, Stirlingshire, United Kingdom, 2013. Civil-Comp Press.

[16] MATLAB. *version 7.09.0.529 (R2009b)*. The MathWorks Inc., Natick, Massachusetts, 2009.

[17] C. D. Norman. Measurement of track modulus. Master's thesis, University of Nebraska, 2004.

[18] T. O'Haver. A pragmatic introduction to signal processing. Technical report, University of Maryland at College Park, 2013.

[19] M. Owen. *Practical Signal Processing*. Cambridge University Press, 2007.

[20] P. Pütz. *User manual ESAH-M V2.2*.

[21] R. Sanudo-Ortega. *Optimising track transitions on high speed lines using numerical models*. PhD thesis, Universidad de Cantabria, 2013.

[22] M. Steenbergen. *Wheel-Rail interaction at short-wave irregularities*. PhD thesis, Technische Universiteit Delft, 2008.

[23] M. Steenbergen and C. Esveld. Rail weld geometry and assessment concepts. *Proceding of the Institution of Mechanical Engineers, Part F: Journal of Rail and Rapid Transit*, 2006.

[24] M. Steenbergen and C. Esveld. Relation between the geometry of rail welds and the dynamic wheel-rail response: numerical simulations for measured welds. *Proceding of the Institution of Mechanical Engineers, Part F: Journal of Rail and Rapid Transit*, 2006.

[25] A. S. J. Suiker. *The Mechanical Behaviour of Ballasted Railway Tracks*. PhD thesis, Technische Universiteit Delft, 2002.

[26] U. U. P. Team. Under sleeper pads. Technical report, UIC, 2009.

[27] H. Wang and X. Liu. Measurement report of video gauge system. Technical report, Technische Universiteit Delft, 2013.

[28] W. Zhai, K. Wang, and J. Lin. Modelling and experiment of railway ballast vibrations. *Journal of Sound and Vibrations*, 2004.

[29] S. Zhang, X. Xiao, Z. Wen, and X. Jin. Effect of unsupported sleepers on wheel/rail normal load. Technical report, Southwest Jiaotong University, 2007.

Glossary

List of Acronyms

ANSYS	Analysis System
APDL	ANSYS Parametric Design Language
ASCII	American Standard Code for Information Interchange
AutoCAD	Automatic Computer Aided Design
BPF	Band-Pass Filter
BW	Bodemwaarde
CAE	Computer Aided Engineering
CSV	Coma Separated Variable
CWR	Continuous Welded Rail
DARTS	Dynamic Analysis of Rail Track Systems
DAT	Data
DSP	Digital Signal Processing
ESAH-M	Elektronische SystemAnalyse Herzstijckbereich - Mobil
FEM	Finite Element Method
FFT	Fast Fourier Transform
FIR	Finite Impulse Response
FRF	Frequency Response Function
GUI	Graphical User Interface
IFFT	Inverse Fast Fourier Transform

IGES	Initial Graphics Exchange Specification
IRJ	Insulated Rail Joint
MAF	Moving Average Filter
MAT	Matlab Formatted Data
Matlab	Matrix Laboratory
SLS	Service Limit State
SNR	Signal to Noise Ratio
TXT	Text
UBM	Under-Ballast Mat
UIC	International Union of Railways
ULS	Ultimate Limit State
USP	Under-Sleeper Pad
VW	Veilighedswaarde

List of Symbols

F_{dyn}	Dynamic force amplification $[kN]$
P_0	Static wheel-rail contact force $[kN]$
P_1	First dynamic amplification $[kN]$
P_2	Second dynamic amplification $[kN]$
α	Total dip angle at joint $[rad]$
v	Velocity $[m/s]$
k_H	Linearised Hertzian contact stiffness $[N/m]$
m_u	Unsprung mass $[kg]$
m_{T1}	Equivalent track mass for P_1 calculation $[kg]$
m_{T2}	Equivalent track mass for P_2 calculation $[kg]$
k_{T2}	Equivalent track stiffness for P_2 calculation $[N/m]$
c_{T2}	Equivalent track damping for P_2 calculation $[Ns/m]$
γ	Dimensionless calibration factor
M_{track}	Equivalent track mass $[kg]$
d	Sampling distance in the average and filtered rail geometry signal $[m]$
$\left\lvert \frac{dz}{dx} \right\rvert_{max}$	Standardised gradient of the signal
C	Foundation modulus $[kN/m^3]$

σ	Local compressive stress on the support $[kN/m^2]$
w	Local subsidence of the support $[m]$
k_d	Spring constant of discrete support $[kN/m]$
a	Spacing between discrete supports $[m]$
Q	Vertical wheel load $[kN]$
EI	Bending stiffness of rail $[kNm^2]$
w_{max}	Maximum rail deflection $[m]$
ρ	Density $[ton/m^3]$
E	Young's modulus $[kN/m^2]$
I	Moment of inertia $[m^4]$
ν	Poisson's ratio
m	Mass $[ton]$
k	Stiffness $[kN/m]$
c	Damping $[kNs/m]$
$_p$	Rail pad
$_b$	Ballast
$_u$	Under sleeper pad
f	Frequency $[Hz]$
t	Time $[s]$
l	Axle distance $[m]$